Preparation and characterization of gelatin-tamarind gum / carboxymethyl tamarind gum based phase separated hydrogels and films for tissue engineering applications

Gauri Shankar Shaw

Department of Biotechnology & Medical Engineering
National Institute of Technology Rourkela

PREPARATION AND CHARACTERIZATION OF GELATIN-TAMARIND GUM / CARBOXYMETHYL TAMARIND GUM BASED PHASE-SEPARATED HYDROGELS AND FILMS FOR TISSUE ENGINEERING APPLICATIONS

Dissertation submitted to the

National Institute of Technology Rourkela

in partial fulfillment of the requirements

of the degree of

Master of Technology

(by Research)

in

Biotechnology & Medical Engineering

By

GAURI SHANKAR SHAW

(613BM6012)

under the supervision of

Prof. *Kunal Pal*

and

Prof. *Krishna Pramanik*

April, 2016

Department of Biotechnology & Medical Engineering

National Institute of Technology Rourkela

Biotechnology & Medical Engineering
National Institute of Technology Rourkela

April 12, 2015

Certificate of Examination

Roll Number: 613BM6012
Name: Gauri Shankar Shaw

Title of Dissertation: preparation and characterization of gelatin-tamarind gum/ carboxymethyl tamarind gum based phase-separated hydrogels and films for tissue engineering applications

We the below signed, after checking the dissertation mentioned above and the official record book (s) of the student, hereby state our approval of the dissertation submitted in partial fulfillment of the requirements of the degree of Master in Technology (by research) in Biotechnology and Medical Engineering at National Institute of Technology Rourkela. We are satisfied with the volume, quality, correctness, and originality of the work.

Prof. Krishna Pramanik
Co-Supervisor

Prof. Kunal Pal
Principal Supervisor

Prof. Amit Biswas
Member (DSC)

Prof. Sujit Bhutia
Member (DSC)

Prof. Samit Ari
Member (DSC)

Examiner

Prof. Mukesh Kuma Gupta
Chairman (DSC)

Biotechnology & Medical Engineering
National Institute of Technology Rourkela

Prof. /Dr. Kunal Pal
Assistant Professor

April 12, 2016

Supervisor's Certificate

This is to certify that the work presented in this dissertation entitled *"Preparation and characterization of gelatin-tamarind gum / carboxymethyl tamarind gum based phase-separated hydrogels and films for tissue engineering applications"* by "*Gauri Shankar Shaw*", Roll Number 613BM6012, is a record of original research carried out by him/her under my supervision and guidance in partial fulfillment of the requirements of the degree of *Master in Technology (by research)* in *Biotechnology and Medical Engineering*. Neither this dissertation nor any part of it has been submitted for any degree or diploma to any institute or university in India or abroad.

Kunal Pal

Biotechnology & Medical Engineering
National Institute of Technology Rourkela

April 12, 2015

Supervisors' Certificate

This is to certify that the work presented in this dissertation entitled *"**PREPARATION AND CHARACTERIZATION OF GELATIN-TAMARIND GUM / CARBOXYMETHYL TAMARIND GUM BASED PHASE-SEPARATED HYDROGELS AND FILMS FOR TISSUE ENGINEERING APPLICATIONS**"* by "*Gauri Shankar Shaw*", Roll Number 613BM6012, is a record of original research carried out by him/her under our supervision and guidance in partial fulfillment of the requirements of the degree of M. Tech (R) in *Department of Biotechnology and Medical Engineering*. Neither this dissertation nor any part of it has been submitted for any degree or diploma to any institute or university in India or abroad.

Krishna Pramanik
Co-Supervisor

Kunal Pal
Principal Supervisor

Declaration of Originality

I, Gauri Shankar Shaw, Roll Number 613BM6012 *hereby* declare that this dissertation entitled *" Preparation and characterization of gelatin-tamarind gum / carboxymethyl tamarind gum based phase-separated hydrogels and films for tissue engineering applications"* represents my original work carried out as a postgraduate student of NIT Rourkela and, to the best of my knowledge, it contains no material previously published or written by another person, nor any material presented for the award of any other degree or diploma of NIT Rourkela or any other institution. Any contribution made to this research by others, with whom I have worked at NIT Rourkela or elsewhere, is explicitly acknowledged in the dissertation. Works of other authors cited in this dissertation have been duly acknowledged under the section "Bibliography". I have also submitted my original research records to the scrutiny committee for evaluation of my dissertation.

I am fully aware that in case of any non-compliance detected in future, the Senate of NIT Rourkela may withdraw the degree awarded to me on the basis of the present dissertation.

April 12, 2016
NIT Rourkela

Gauri Shankar Shaw

Acknowledgment

Successful completion of this project is the outcome of consistent guidance and assistance from many people, faculty and friends and I am extremely fortunate to have got this all along the completion of the project.

I owe my profound gratitude and respect to my project guide Dr. Kunal Pal and Dr. Krishna Pramanik, Department of Biotechnology and Medical Engineering, NIT Rourkela for their invaluable academic support and professional guidance, regular encouragement and motivation at various stages of this project. Special thanks to Dr. Indranil Banerjee for giving beautiful ideas and co-operation for the work. I am very much grateful to them for allowing me to follow my own ideas.

I would like to extend my heartfelt gratitude to research scholars Mr. Biswajeet Champaty, Mr Vinay Singh, Mr. Sai Satish, Ms. Beauty Behera, Ms. Dibyajyoti Biswal, Ms. Preeti Madhuri Pandey, Ms. Indu Yadav and Mr. Suraj kumar Nayak whose ever helping nature and suggestions have made my work easier by many folds. I would like to thank all my friends and classmates for their constant moral support, suggestions, advices and ideas. I have enjoyed their presence so much during my stay at NIT, Rourkela.

I will never forget the support provided by Mr. Haldhar Behera for providing valuable help.

April 12, 2016
NIT Rourkela

Gauri Shankar Shaw
Roll Number: 613BM6012

Abstract

The purpose of this research was to synthesize and characterize gelatin and tamarind gum/carboxymethyl tamarind gum based phase-separated hydrogels and films for tissue engineering applications. The polymeric constructs were thoroughly characterized using bright-field microscope, FTIR spectroscope, differential scanning calorimeter (DSC), mechanical tester and impedance analyzer. The biocompatibility and swelling property also evaluated. The antimicrobial efficiency of ciprofloxacin (model antimicrobial drug) loaded hydrogels and films were studied against *E. coli*. The *in vitro* drug release was carried out in pH 7.4. Microstuctural analysis suggested the formation of phase-separated formulations. FTIR studies suggested that carboxymethyl tamarind gum altered the secondary structure of the gelatin molecules. Presence of the polysaccharides within the formulations resulted in the increase in the enthalpy and entropy for evaporation of the moisture from the hydrogels and films. The mechanical studies indicated viscoelastic nature of the polymeric constructs. Electrical analysis suggested an increase in the impedance of the formulations in the presence of the tamarind gum. The presence of carboxymethyl tamarind gum resulted in the decrease in the impedance of the formulations. The hydrogels and films exhibited good biocompatibility, and pH dependent swelling behavior. The drug loaded samples showed good antimicrobial activity and the drug release was pH dependent and diffusion mediated.

Keywords: hydrogels; films; phase-separated; tamarind gum; microstructure; swelling; hydrophobic; ciprofloxacin; Antimicrobial

Contents

List of Figures

List of Tables

Chapter 1

Introduction

Organ transplantation is still the main medical procedure to cure a patient with damaged tissues and organs [1]. In the recent past, tissue engineering has attracted the attention of the researchers and the surgeons. Tissue engineering is a field of science, which involves fabricating of tissues and organs for replacing damaged parts of the human body [2]. This field has opened up a new area in medicine and has provided new treatment modalities for many disease conditions, where conventional treatment has failed. In the last two decades, the field of tissue engineering has gained tremendous importance in the field of medicine due to the enormous advantageous potentialities it has offered to the surgeons [3]. The advances in tissue engineering have allowed the scientists in regenerating organs and tissues [4]. This has allowed the reducing demand for organs and tissues to a great extent, thereby, resulting in overcoming the shortage of organ donors to a certain extent. The field of tissue engineering is multi-disciplinary in nature requiring the expertise of cell biology, materials science and medicine (diseased organ and biomolecule delivery) [5]. In recent days, the advances in imaging modalities (e.g. fluorescent microscopy, confocal microscopy, environmental scanning electron microscopy, field emission scanning electron microscopy) have played an important role in understanding the interaction between the cells and the materials [6]. The major challenge in tissue engineering is the designing of the artificial extracellular matrix (ECM) component, which can promote cell proliferation onto itself [7]. The architectures used as artificial ECM are often regarded as scaffolds. A scaffold is defined as the porous architecture which has the capability to support cell growth and allow deposition of the natural ECM proteins over it during the initial stages [8]. The deposition of the ECM proteins over the scaffolds elicits specific cellular activity, which promotes functional integration of the cell-scaffold constructs

with the body tissues [9]. The deposition of the proteins over the scaffolds is mainly due to the non-specific adsorption [10]. The scaffolds may be designed using materials which undergo biodegradation/ bioresorption during the integration process [11]. Such scaffolds lose their existence once they have completed their tasks. The desired properties (physical or chemical) of the scaffolds are different for different tissues and are mainly dependent on the functionality of the organ and the specific application which is expected to be met by the scaffold [12]. Scaffolds may be designed to induce the regeneration of the tissues and the organs, which do not possess regeneration capability [13]. Such scaffolds have been regarded as regeneration templates. In short, the process of regeneration using the tissue engineering protocol includes initial isolation of specific cells from the biopsies of the patients [14]. The isolated cells are then cultured over the scaffolds *in vitro* and subsequently transplanted into the patient. The transplanted cell-scaffold constructs help in the regeneration of the tissues or organs *in vivo* [15]. If the isolated cells are stem cells, the cells have to be differentiated into the specific cells before the cell-scaffold constructs are transplanted.

The properties of the materials used for the fabrication of the scaffold play a significant role in the success of the tissue engineering procedure [16]. The scaffolds are expected to be highly biocompatible with negligible antigenicity and excellent thromboresistant behavior [17]. Scaffolds can be designed using biomaterials, namely, polymers, ceramics and metals [18]. Of the different types of biomaterials, polymeric biomaterials have gained much importance [19]. This is due to the fact that the polymers are more versatile materials than the other types of biomaterials. Polymers are available with different chemistries. This allows easy modification of the surface properties of the polymeric architectures, which might be necessary to improve the cell proliferation [20]. Additionally, the physical properties of the scaffolds may be easily altered by designing the polymeric architectures using polymer blends and composites [21]. This can allow the scientists to develop scaffolds using materials which can promote biomolecular recognition based interactions of the scaffolds and the surrounding tissues [22]. Further, modulating the properties of the polymeric architectures allow scientists in studying the interactions between the cells and the developed constructs under *in vitro* conditions [23]. The research on the biomaterials has provided information on a group of polymeric materials, which can help restoring the functionality of the diseased/ traumatized tissues or organs in a relatively quick time. Polymeric materials have been successfully used to design sutures, bone plates and screws, acetabular cup, vascular grafts, heart valves, intraocular lens, ligaments, skin grafts, wound dressings and so on [24].

The polymeric biomaterials used for scaffold fabrication are broadly categorized into two groups, namely, synthetic polymers and natural polymers [25]. Though many of the

synthetic polymers are known to have better mechanical properties, controlled biodegradability and biocompatibility, the high cost of these polymers restricts their use to design commercially viable scaffolds [26]. On the other hand, natural polymers are much cheaper due to their abundance in nature [27]. The natural polymers are further categorized into two broad categories as per their source of origin, namely, animal derived natural polymers and plant derived natural polymers [28]. The commonly used animal derived natural polymers include collagen, gelatin, hyaluronic acid, elastin, chondroitin sulphate, and fibrin [29]. On the other hand, plant derived natural polymers include agarose, alginate, chitosan and tamarind gum [30]. These polymers are crosslinked to form hydrogels [31]. The crosslinking may either be due to covalent bonding, physical entanglements, associative interactions due to hydrogen bonding and van der Waals interactions and crystallite interactions [32]. Hydrogels are 3-D polymeric constructs, which can hold large amount of water into their architecture [33]. They are reported to be highly biocompatible in nature. The inherent biocompatibility of the hydrogels has been explained by the presence of water in high quantity. In addition to the presence of water in high quantity, hydrogels are soft and flexible, thereby, mimicking the properties of the tissues. The afore-mentioned properties along with the ability of the hydrogels to deliver drugs at controlled rate make them suitable candidates for tissue engineering applications, where there is a need to deliver growth factors and stem cell differentiation factors for proper regeneration of the tissues and the organs [34].

In recent years, phase-separated hydrogels have received special attention of the researchers. Phase-separated hydrogels are the hydrogels having two distinct phases where a polysaccharide-rich phase is homogeneously dispersed in a protein-rich phase [35]. These are also regarded as water-in-water emulsions due to the existence of two separate aqueous phases having distinct interfaces [36]. The phase separation occurs due to thermodynamic instability of the molecules in the hydrogel [37]. Phase-separated hydrogels have been proposed by various researchers for various tissue engineering and drug delivery applications [38]. Usually, gelatin has been used as continuous polymeric phase. On the other hand, different polysaccharides have been experimented as the dispersed aqueous phase. A thorough literature survey suggested that though tamarind gum and its carboxymethylated derivatives have been used for animal cell culture and tissue engineering applications, no reports on applications on tamarind gum/ carboxymethyl tamarind gum based phase-separated polymeric constructs could be located [39].

Taking a note of the afore-mentioned facts, the current study proposes the development of gelatin and tamarind gum/carboxymethyl tamarind gum based phase-separated hydrogels and films for bone and skin tissue engineering applications. The

hydrogels and films were characterized thoroughly using bright-field microscope, FTIR spectroscope, differential scanning calorimeter (DSC), mechanical tester and impedance analyzer. The swelling and the biocompatibility properties were also evaluated under *in vitro* conditions. The antimicrobial efficiency of ciprofloxacin (model antimicrobial drug) loaded hydrogels and films were studied against *E. coli*. The *in vitro* drug release was carried out in both gastric and intestinal pHs.

Chapter 2

Review of literature

In this section, a thorough review of the literature on various natural biopolymers and their applications in the field of tissue engineering has been done. As previously discussed, the natural polymers can be categorized into two broad categories as per their source of origin, namely, animal derived natural polymers and plant derived natural polymers.

2.1 Animal Derived Natural Polymers

In this section, different applications of animal derived natural polymers in the field of tissue engineering in the last five years have been discussed. The commonly used animal derived natural polymers include collagen, gelatin, hyaluronic acid, elastin, chondroitin sulphate, and fibrin.

2.1.1 Collagen

Collagen is the most abundant protein available in the extracellular matrices (ECMs) of the living tissues [40]. It provides structural support and strength to the tissues along with a degree of elasticity. Collagen is extracted from different animal sources like skin, bones and connective tissues of cow, pig, horse, chicken and fish [41]. The purification of commercial collagen meshwork or sponge is done through enzymatic processes and salt/ acid extraction. Collagen requires proper processing before use to reduce its antigenicity [42]. It has found numerous applications in tissue engineering due to its permeability, *in vivo* stability, porosity and hydrophilic nature.

In the recent years, researchers have also investigated the applicability of collagen based composite polymeric scaffolds (e.g. demineralized bone power homogeneously mixed with type I collagen) for bone tissue engineering applications along with the pure collagen scaffolds. It is found that the collagen based composite polymeric scaffolds exhibit better osteoinductive potential than the pure collagen scaffolds [43]. Lomas *et al.* (2013) reported the use of PHBHHx (poly (3-hydroxybutyrate-co-3-hydroxyhexanoate))/ collagen composite scaffolds in combination with human embryonic stem cells (hESCs) and messenchymal stem cells (MSCs) as a biocompatible approach for replacement of damaged tissues. The PHBHHx/collagen composite scaffolds were prepared through syringe injection of collagen/cell mixtures into PHBHHx porous tubes (generated using a dipping method followed by salt leaching) [44]. Although various properties and structures of natural ECMs are mimicked by collagen, collagen hydrogels often don't exhibit the suitable three-dimensional (3D) and mechanical properties essential for various types of tissues [45]. Han *et al.* (2013) have reported a new microribbon-like scaffold made of type I collagen having adjustable stiffness, 3D structure and microporous nature desirable for cell migration [46]. Cao *et al.* (2015) have reported the development of fish collagen-based scaffolds containing PLGA microspheres for controlled growth factor delivery in skin tissue engineering, where the fish collagen-based scaffolds were prepared by freeze dying method and integrated with bFGF-loaded PLGA microspheres (MPs). These scaffolds exhibited a very good biocompatible nature and the ability to stimulate skin tissue regeneration and fibroblast cell growth [47].

2.1.2 Gelatin

Gelatin is a partial hydrolysis derivative of collagen. It preserves several signaling sequences of collagen like the Arg-Gly-Asp (RGD) sequence that encourages the adhesion, differentiation and growth of cells. Gelatin exhibits much lesser antigenicity than collagen. However, the poor mechanical strength of pure gelatin reduces its direct use in various tissue engineering applications like in cartilage tissue engineering. In general, gelatin based formulations are mechanically stable and function as suitable space filling materials in bone tissue engineering applications [22].

In the recent years, gelatin has received much attention of the researchers because of its natural origin and its capability to suspend cells in a gel at low temperatures [48]. Various researchers have proposed the manual fabrication of liver tissue constructs prepared from gelatin and chitosan mixed with hepatocytes prior to fixation of glutaraldehyde [49].

Billiet et al. (2014) have suggested the 3D printing of gelatin methacrylamide cell-laden tissue-engineered constructs for liver tissue engineering, which have high cell viability [50]. Yazdimamaghani et al. (2014) have synthesized hybrid microporous gelatin/ bioactive-glass/ nanosilver scaffolds having controlled degradation and antimicrobial properties for bone tissue engineering applications. These macroporous scaffolds were prepared from an aqueous solution of gelatin using freeze-drying method and crosslinking was achieved using genipin at ambient temperature. These scaffolds can be used as antibacterial scaffolds as evident from the viability of the hESCs on these scaffolds [51]. Surface topography of the scaffolds has been found to affect the stem cells and is considered as a physical stimulus to alter the cellular activities (e.g. adhesion, growth and differentiation) on two-dimensional (2D) surfaces. Therefore, the incorporation of suitable topography to 3D scaffolds can be helpful to direct the cell fate for various tissue engineering applications. Nadeem et al. (2015) have reported a new fabrication method, based on computer controlled machining and lamination, to produce 3D calcium phosphate/ gelatin scaffolds having surface micropatterns (created by embossing before machining) to promote bone tissue regeneration [52]. Bareil *et al.* (2010) has reported that collagen based biomaterials are the better materials for tissue engineering applications and regenerative medicine due to their superior biocompatibility and low immunogenicity [53]. Gelatin is the denatured form of collagen protein where the natural triple-helix structure of collagen breaks in to single-stand molecules by hydrolysis process. Zhu et al. has proposed that gelatin is less immunogenic than collagen and it retains the signals like Arg-Gly-Asp (RGD) sequence. Due its less immunogenic nature, it promotes the cell adhesion, differentiation, migration and proliferation [54]. Chen *et al.* (2013) has reported that gelatin is potential for in situ applications as it is non-immunogenic in nature [55]. Tan *et al.* (2010) has also proposed that gelatin is a superior material for tissue engineering applications as it is less immunogenic in nature [56].

2.1.3 Hyaluronic acid

Hyaluronic acid is a linear polysaccharide found in all types of connective, epithelial and neural tissues of animals [57]. It is energetically stable and has high molecular weight [58]. Hyaluronic acid is a major component in animal extracellular matrix. It consists of repeated disaccharides made of N-acetylglucosamine and glucuronic acid [59]. It is synthesized by the class of proteins named as hyaluronan synthases.

Collins *et al.* (2013) have reported the fabrication of hyaluronic acid based chemically crosslinked hydrogels for use as space filling and bulking materials to cure urinary incontinence and to maintain alveolar spaces [60]. Nath *et al.* (2015) have synthesized hyaluronic acid/chitosan based scaffolds (crosslinked with genipin), for use in bone tissue engineering, that promotes the regeneration of defective and damaged bones. This can be attributed to the immobilization and controlled release of bone morphogenic protein-2

(BMP-2) from the scaffolds [61]. Hyaluronic acid/tyramine based covalently crosslinked hydrogels are capable of regenerating of cartilage tissues. Skop *et al.* (2014) have reported the application of hyaluronic acid/gelatin based scaffolds in nervous tissues (as cell delivery systems in translational therapy) for stroke recovery [62]. Hyaluronic acid based hydrogels are used as drug delivery vehicles due to their controlled degradation process. High biocompatibility nature of hyaluronic acid doesn't allow scar formation. Park *et al.* (2012) have suggested that hyaluronic acid based scaffolds can induce angiogenesis [63]. Due to its high viscoelastic nature, it has great potential in the field of dermal filling. Liu *et al.* (2013) have reported the development of collagen-gelatin-hyaluronic acid based biomimetic films for cornea tissue engineering applications using 1-ethyl-3-(3-dimethyl aminopropyl) carbodiimide (EDC) and N-hydroxysuccinimide (NHS) as the crosslinkers. These films are highly biocompatible in nature and promote adhesion and proliferation of human corneal epithelial cells [64]. Ivan *et al.* (2014) have reported the synthesis of calcium phosphate-chitosan-hyaluronic acid based biodegradable scaffolds using a biomimetic co-precipitation method for application in the field of bone tissue engineering. These scaffolds exhibit a slow degeneration and limited swelling in simulated body fluids [65].

2.1.4 Elastin

Elastin is a protein based biopolymer, present in various connective tissues. It has an amorphous structure, wavy appearance (when viewed under the light microscope) and highly refractive nature [66]. Although, it constitutes a small fraction of a tissue, its role is highly important. It provides elasticity to tissues and organs [66]. Elastin plays an important role for the flow of blood in the arteries by acting as a medium for pressure wave transmission.

Rnjak *et al.* (2013) have reported the importance of elastin in the healing of wounds and in the designing of dermal substitute [67]. Girrotti *et al.* (2015) have reported the development of recombinant protein-based biomaterials obtained from elastin and their applications for the repairing of soft tissue [68]. Grover *et al.* (2012) have investigated various properties (e.g. structural, mechanical and degradation) of scaffolds synthesized from collagen, gelatin and elastin and have suggested that the use of gelatin (instead of collagen) with incorporation of elastin can be considered as a low cost design strategy of scaffolds for potential applications in soft tissue engineering [69]. Machado *et al.* (2012) have reported the synthesis of elastin based nanoparticles for the delivery of bone morphogenic proteins [70]. Dunphy *et al.* (2014) have proposed that elastin-collagen based hydrogels are suitable materials for application in lung tissue engineering [71].

2.1.5 Chondroitin sulphate

Chondroitin sulfate is an abundant biopolymer, which is commonly derived from the cartilages of shark, pig and cow. It is a sulfated glycosaminoglycan (GAG), which consists of sugars of N-acetylgalactosamine and glucuronic acid. It is the major structural constituent of animal cartilage and provides resistance to the tissues and the organs during compression. Chondroitin sulphate based drugs are commonly used for heart diseases, heart attacks, breast cancer and several bone diseases. It is also used to prepare veterinary medicines to cure wounds, burns and scrapes in animals.

Chondroitin sulphate has useful applications in the cartilage tissues as it the major structural component of cartilage. Silva *et al.* (2013) have reported the fabrication of chitosan- chondroitin sulphate based nanostructured 3D scaffolds, which supported the adhesion and growth of bovine chondrocytes [72]. These scaffolds were highly porous and viscoelastic in nature, which made them a better asset in the area of cartilage tissue engineering. Levett *et al.* (2014) have also reported the preparation of gelatin-chondroitin sulphate based hydrogels for application in field of cartilage tissue engineering. The prepared hydrogels behaved as an extracellular matrix and enhanced the chondrogenesis process [73]. In general, mechanical strength of many polymeric constructs is increased by adding some ceramics for utilizing them as load bearing scaffolds. Venkatesan *et al.* (2012) have fabricated chitosan-hydroxyapatite-chondroitin sulphate based freeze dried scaffolds for bone tissue engineering applications. Due to addition of hydroxyapatite, the mechanical strength of the scaffolds was enhanced. The proliferation of MG-63 cells was improved on the surface of the scaffold and no cytotoxicity was found. So the fabricated scaffolds can be considered as a suitable component in the area of bone tissue engineering [74]. As chondroitin sulphate is highly biodegradable and biocompatible, it has no toxic effect to the living body systems. Deepthi *et al.* (2014) have developed chitin-poly (butylenes succinate) - chondroitin sulphate based hydrogels for skin tissue applications. The presence of chondroitin sulphate in the devloped hydrogels enhanced the cell adhesion process. Proliferation of fibroblasts was better on the hydrogel surface. The above results demonstrated the capability of chondroitin sulphate to be used in skin tissue engineering [75]. Yan *et al.* (2013) have prepared silk fibroin-chondroitin sulphate-hyaluronic acid based scaffolds for the reconstruction of the dermal tissues. In their study, dermis regeneration and collagen deposition was achieved on the scaffold surface [76].

2.1.6 Fibrin

Fibrin is a biopolymer, composed of blood proteins like fibrinogen and thrombin. It is a major ECM component. Fibrin based scaffolds are one of the most useful assets in the field of tissue engineering due to their high biocompatibility, non-toxicity and degradability nature. The physical and chemical properties of the fibrin based scaffolds can be altered as per the requirement. Fibrin is commonly used to prepare scaffolds for skin tissue engineering applications (e.g. wound healing). Fibrin is capable of inducing angiogenesis and can promote the proliferation of cells in an appropriate manner. Martin *et al.* (2013) have reported the influence of fibrin and fibrin-agarose on the ECM profile of bioengineered oral mucosa [77]. Puente *et al.* (2014) have reported the possible cell culture applications of autologous fibrin scaffolds [78].

2.2 Plant Derived Natural Polymers

As discussed in the previous section, the commonly used plant derived natural polymers include agarose, alginate, chitosan, tamarind gum and carboxymethyl tamarind gum. In this section, different applications of plant derived natural polymers in the field of tissue engineering in the last five years have been discussed.

2.2.1 Agarose

Agarose is a linear biopolymer, commonly derived from seaweed. It is a white powder which gets dissolved in hot water and forms gel after cooling. Agarobiose disaccharide is the main structural component of agarose. Agarose is commonly used for gel electrophoresis. Due to low mechanical strength, it is added with other polymers to fabricate polymeric constructs for tissue engineering applications. It is highly biocompatible and degradable in nature.

Miguel *et al.* (2014) have developed chitosan–agarose based hydrogels for skin tissue engineering application. In their study, a better attachment and viability of cells on the hydrogel surface was observed during *in vitro* cell study. The *in vivo* study showed complete healing of the wounds after 21 days. So, the agarose based biomaterials have great potential in the field of skin tissue engineering [79]. Bhatt *et al.* (2012) have fabricated chitosan-gelatin-agarose based cryogels [80]. In their study, different cell lines (cardiac and fibroblast) were cultured on the gel surface and the proliferation was found to be very good. This study also suggested the promising nature of agarose based materials in skin tissue engineering applications. Jebahi *et al.* (2014) have developed

agarose-chitosan based scaffolds as bone grafts for bone tissue engineering applications [81]. The graft was implanted for 30 days in a rabbit. It was found that angiogenesis was increased and formation of new tissue occurred on the site. These results suggest that agarose-chitosan based biomaterials can be used for the regeneration of bones.

2.2.2 Alginate

Alginate is an anionic polymer derived from the cell walls of brown algae. This is a linear polymer with high molecular mass. It has high water absorption property, which makes it useful for thickening of foods in different food industries. It is used as a gelling agent in pharmaceutical industries. Due to high biocompatibility, it acts as an excellent biomaterial for numerous applications.

Venkatesan *et al.* (2015) have developed alginate-chitosan-gelatin based hydrogels which can be used as skin substitutes for skin tissue engineering applications [82]. In recent years, alginate based injectable hydrogels have been prepared to induce tissue regeneration. Kirdponpattara *et al.* (2015) have fabricated freeze dried cellulose-alginate scaffolds for tissue engineering applications. These scaffolds were analyzed by cell study using fibroblast cells. The proliferation and the attachment of the fibroblast cells was quite good on the scaffold surface, which suggested the potential of alginate based scaffolds to be used for tissue engineering applications [83]. Castilho *et al.* (2015) have developed alginate-tri calcium phosphate (TCP) based scaffolds for regeneration of bone tissue. The mechanical strength of the developed hydrogels was high and they promoted proliferation of osteoblast cells. These results suggested the suitability of the alginate-TCP based scaffolds for bone tissue engineering applications [84]. Sowjanya *et al*. (2013) have prepared alginate-chitosan-nano silica based scaffolds for bone tissue engineering applications. These scaffolds showed better proliferation of osteoblasts (during cell study) and no toxic effect was found. These results suggested that alginate can be used for bone tissue applications [85].

2.2.3 Chitosan

Chitosan is a semi-crystalline biopolymer, commonly found in the exoskeleton of marine animals (e.g. shrimps, crabs and lobsters). It is commercially produced by deacetylation of chitin. Shalumon *et al.* (2012) have developed poly(lactic acid)-Chitosan based nanofibers using electrospun method for skin tissue engineering applications [86]. The cell study of the developed nano-fibres with human dermal fibroblasts suggested the orientation of cells along the direction of fiber alignments. These nanofibers have been

proposed for potential use as skin tissue substitutes. Han *et al.* (2014) have fabricated gelatin-chitosan based sponges for potential application as skin substitutes [87]. All the characterizations of the fabricated sponges were done thoroughly and biocompatibility was tested by MTT assay method. Proliferation and adhesion of the cells on the sponge surface was found to be better. Based on these results, the fabricated sponges have been proposed as suitable material for skin tissue engineering applications like wound healing [87]. Rahman *et al.* (2013) have reported the fabrication of gelatin-chitosan porous scaffold films [88]. The microscopic analysis of these films indicated a smooth and homogeneous surface. *In vivo* cell study on a rat model suggested very good healing process. Therefore, gelatin-chitosan porous scaffold films have been proposed as a promising biomaterial for skin tissue applications. Frohbergh *et al.* (2012) have prepared hydroxyapatite-chitosan based nanofibers prepared by electrospinning method [89]. The osteoblast cell proliferation on these nanofibers was found to be very good and they showed expression of mRNA. These results suggested that hydroxyapatite-chitosan based nanofibers can be considered as a potential material for bone tissue engineering. Niranjan *et al.* (2013) have reported the fabrication of zinc doped chitosan/β-glycerophosphate hydrogels. The differentiation and proliferation of osteoblasts were found to be enhanced by these hydrogels which suggested that these hydrogels can be used as materials for bone tissue engineering applications.

2.2.4 Tamarind gum (TG)

Tamarind gum is extracted from the endosperm of the seeds of the tamarind tree (*Tamarindus indica*) [90]. It is also termed as tamarind kernel powder. The seeds are collected initially and put in dry places. Several steps are properly followed to prepare the tamarind gum powder like seed collection, seed coat removal, milling, grinding and sieving. Chemical structure of tamarind gum consists of β-(1,4)-d-glucan back bone substituted with side chains of α-(1,4)-d-xylopyranosy and (1,6) linked(β-d-galactopyranosyl-(1,2)-α-d-xylopyranosyl) to glucose residues [91]. In its chemical composition, glucose, xylose and galactose units are available in the proportions of 2.8:2.25:1.0 as the monomer units. Tamarind gum has common applications as stabilizing, thickening, emulsifying and gelling agent in different food and pharmaceutical industries. It is highly biocompatible, non-toxic, non-carcinogenic, biodegradable and hydrophobic in nature and has high drug loading capacity. These basic characteristics of tamarind gum make it a promising material in the field of tissue engineering. Generally, it forms gel at high temperature, which having viscoelastic nature.

In recent years, researchers have developed tamarind gum based tablets that exhibit very good drug release property [92]. So, tamarind gum has the potential to be used as drug delivery vehicle for tissue engineering applications. Nayak *et al.* (2014) have studied the release of metfomin HCl from tamarind gum polysaccharide-gellan gum based beads [93]. The release was excellent and pH dependent. But, no reports have been found where tamarind gum is used for application of skin and bone tissue engineering. Manchanda *et al.* (2014) has reported that tamarind gum polysaccharide has several applications in the field of pharmaceuticals as it is non-toxic and non-irritant in nature. Due to its high drug holding capacity, it has several applications as controlled drug delivery systems [94]. Sahoo *et al.* (2010) has also proposed that due to high muco-adhesive and non-toxic nature, TG has several applications as biomaterials in tissue engineering applications [95].

2.2.5 Carboxymethyl tamarind gum (CMT)

In some cases, quick degradation and unpleasant odour of tamarind gum reduce its application. So, some chemical modification of tamarind gum has been proposed to make it a better material for tissue engineering application. Carboxymethyl tamarind gum (CMT) is the modification of tamarind gum [96]. The CMT powder solution is more viscous than tamarind gum solution. CMT is hydrophilic in nature and capable of absorbing more water. The carboxymethyl group enhances the viscosity and makes the molecule resistant toward enzymatic attack. Due to above characteristic phenomena, both TG and CMT are commonly used as drug delivery systems and emulsifying agents [97]. CMT has been used to develop novel drug delivery systems for pharmaceutical applications. Sanyasi *et al.* (2014) have developed CMT-HEMA (2-Hydroxyethylmethcrylate) hydrogels, which were capable of inducing osteogenesis [39]. The proliferation and attachment of bone precursor cells were better on their surface. So, CMT can be a useful asset for bone tissue engineering applications.

2.3 Objectives

Taking a note from the literature review, gelatin-tamarind gum and gelatin-carboxymethyl tamarind gum based phase-separated hydrogels and films were developed and analyzed for tissue engineering applications. The following objectives were set:

i. Development of gelatin-tamarind gum and gelatin-carboxymethyl tamarind gum based hydrogels and films for tissue engineering applications.

ii. To study the physicochemical and mechanical properties of the polymeric structures.

iii. Mathematical modelling of the experimental data obtained from the physical and experiments.

Chapter 3

Development and Characterization of Gelatin-Tamarind Gum/Carboxymethyl Tamarind Gum Based Phase-Separated Hydrogels: A Comparative Study

3.1 Introduction

Polysaccharides are generally obtained from plant sources and are usually biocompatible [98]. Due to their inherent biocompatibility, polysaccharides have been explored to design polymeric constructs of biomedical importance (pharmaceutical, cosmetic and tissue engineering applications) [99]. The mechanical properties of the polysaccharide based polymeric constructs are usually poor. Scientists have applied various methodologies to improve the mechanical properties of the polysaccharide constructs [100]. Among the various methodologies, the commonly used techniques include blending the polysaccharides with other polymers (e.g. gelatin, PVA etc.) and crosslinking (chemical and physical) of the polymeric constructs [101]. The commonly studied polysaccharides include starch, carboxymethyl cellulose, methyl cellulose, chitosan, alginate, carboxymethyl chitosan and carboxymethyl starch. In recent years, tamarind gum (TG), due to its thickening property, has been explored as a natural polysaccharide for the development of pharmaceutical formulations [102] and food products [103]. The thickening property of TG helps stabilizing emulsions and induce gelation of the aqueous phase [104]. TG is extracted from the seeds of the plant, *Tamarindus indica [94]*. The backbone of TG consists of β -(1,4)-D-glucan substituted with side chains of α-(1,4)-D-xylopyranose and (1,6) linked [β-D-galactopyranosyl-(1,2)-α-D-xylopyranosyl] to

glucose residues [94, 105]. TG has been reported to be non-carcinogenic and non-toxic (biocompatible) in nature [106]. The addition of TG improves the mucoadhesive property of the pharmaceutical formulations. The main disadvantages of TG include unpleasant odour and quick microbial degradation. To overcome these disadvantages, the derivatization of TG by chemical treatment has been explored. Carboxymethylation is one such chemical modification. Introduction of carboxymethyl group in TG makes the polymer anionic [96]. This improves the hydration of the polysaccharide, thereby, resulting in the higher viscosity of the carboxymethylated product. It has been reported that the increase in the viscosity lowers the biodegradation of the polysaccharide [107]. Though TG has been extensively studied for developing delivery vehicles for neutraceutical and pharmaceutical agents, carboxymethyl tamarind gum (CMT) has not been explored to that extent, even though it holds a great promise in developing controlled release systems. The difference in the chemical structure of TG and CMT has been shown in Figure 3.1.

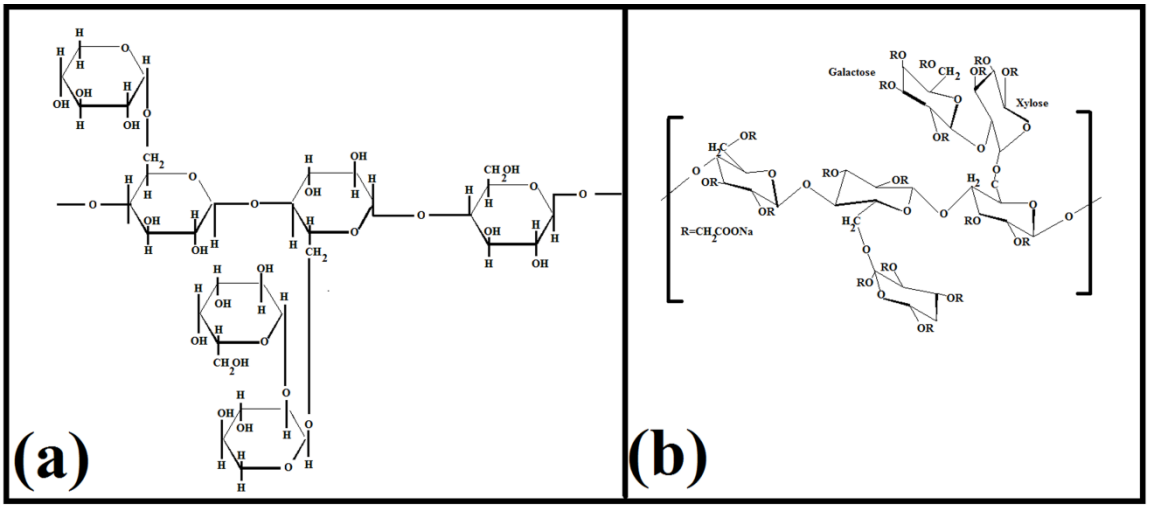

Figure 3.1: Chemical structures of TG and CMT

As mentioned earlier, polysaccharides are seldom used alone for devising polymeric constructs. In this regard, gelatin-polysaccharide based composite hydrogels have been well explored [108]. Gelatin-polysaccharide based hydrogels usually forms phase-separated hydrogels [109]. This may be explained by the thermodynamic incompatibility of the polymer mixture during gelation. This, in turn, results in the formation of two phases: (a) polysaccharide rich phase, and (b) gelatin rich phase. Since both the phases are aqueous in nature, the formed composite hydrogels are often regarded as water-in-water emulsions [110]. The commonly used polysaccharides for developing such systems

include (but not limited to) starch, soluble starch, hydrated starch, carboxymethyl starch, carboxymethyl cellulose dextran and maltodextan. No reports were found to study the properties of gelatin- TG and gelatin- CMT phase-separated hydrogels.

In the current study, an in-depth analysis was done to optimize the gelatin concentration and it was found that gelatin concentration more than 20% is difficult to handle due to higher viscosity [111]. So, the gelatin concentration was fixed to 20% for all the formulations. As per the literature study, 3 % carboxymethyl tamarind gum was used (Sanyasi et al. 2013) to develop the hydrogels, which showed a better proliferation of osteo-precursor cells [39]. Mishra et al. (2011) has reported that tamarind gum is a suitable material for grafting process. In their study, concentration of TG was fixed to 1% and a greater thermal stability was observed in the developed formulations [112]. So, the polysaccharide solution was prepared with two different concentrations (1% and 2 %) to develop the hydrogels. Further, different proportions of gelatin and TG/CMT (5:0, 4:1, 3:2, 2:3 and 1:4) were taken to develop the hydrogels and films. From all the compositions, the best compositions were selected out as per their stability. The formulation 1:4 was not formed due to lower proportion of gelatin. So, all the hydrogels and films were selected by verifying their mechanical strength and stability. Optimization process facilitated choosing the best compositions for the hydrogels and films for their tissue engineering application. Taking a note from the above, we have developed the hydrogels and films by altering both the concentrations and proportions of the polymer and polysaccharides.

Taking inspiration from the above, we have tried to develop gelatin-TG and gelatin-CMT based phase-separated hydrogels. The physicochemical, thermal and electrochemical properties of the hydrogels were thoroughly characterized using FTIR spectroscopy, differential scanning calorimetry, static mechanical tester and impedance analyzer. The biological activity of the hydrogels were studied by mucoadhesive and biocompatibility (hemocompatibility and cell viability assay) studies. To understand the ability of the developed hydrogels as vehicles for controlled release, the hydrogels were loaded with ciprofloxacin (fluroquinolone antibiotic). The drug release kinetics and the antimicrobial activity of the drug loaded hydrogels were also studied in-depth.

3.2 Materials and Methods

3.2.1 Materials

TG and CMT (degree of carboxylation of CMT is 0.372) were procured from Maruti hydrocolloids, India. Gelatin was procured from Himedia, Mumbai, India. Ciprofloxacin

(CF) was procured from Fluka Biochemical, China. Ethanol was obtained from Honyon International Inc., Hong Yang Chemical Corporation, China. Glutaraldehyde (25%, for synthesis; GA) and hydrochloric acid (35% pure) were obtained from Merck Specialities Private Limited Mumbai, India. Goat intestine and blood were collected from the local butcher shop. Double distilled water (DW) was used throughout the study.

3.2.2 Preparation of the formulations

Stock solution of gelatin (20% w/w) and polysaccharides (2% w/w) were freshly prepared. The stock solutions were maintained at 50 ^{o}C. The gelatin and polysaccharide solutions were mixed together (100 rpm, 10 min) in varying proportions (Table 3.1) followed by addition of crosslinking reagent (0.5 ml of GA, 0.5 ml of ethanol, and 0.01 ml of 0.1N HCl). The mixture was mixed for 10 sec and subsequently poured into petri-plates/cylindrical moulds. The petri-plates/moulds were incubated at room temperature (25 ^{o}C) for 1 h to induce gelation.

Drug loaded hydrogels were prepared by dispersing 0.1 g of ciprofloxacin in gelatin solution. Ciprofloxacin containing gelatin solution was used for the preparation of the hydrogels. Rest of the process remained same. The final concentration of the drug in the hydrogels was 0.5 % w/w. The hydrogels were washed thoroughly using PBS buffer and double distilled water before all the experiments. Further, glycine solution (1% w/v) was used to inhibit the chemical reactions of glutaraldehyde after the said incubation period.

Table 3.1: Composition of the hydrogels

Formulations	Gelatin solution (g)	TG Solution (g)	CMT Solution (g)	Crosslinker (ml)	Ciproflaxacin (g)
T1	16	4	--	1	--
T2	12	8	--	1	--
T3	8	12	--	1	--
C1	16	--	4	1	--
C2	12	--	8	1	--
C3	8	--	12	1	--
T1C	15.9	4	--	1	0.1
T2C	11.9	8	--	1	0.1
T3C	7.9	12	--	1	0.1
C1C	15.9	--	4	1	0.1
C2C	11.9	--	8	1	0.1
C3C	7.9	--	12	1	0.1

3.2.3 Microscopy studies

The microstructures of the uncrosslinked physical formulations were visualized under bright field microscope (LEICA-DM 750 equipped with ICC 50-HD camera, Germany). The formulations were converted into thin smears over glass slides before visualization.

3.2.4 Infrared spectroscopy

The raw materials and the hydrogels were analyzed using FTIR spectrophotometer ((Alpha-E, Bruker, USA). The analysis was done in the wavenumber range of 4500 cm^{-1} to 450 cm^{-1}. The spectrophotometer was being operated in the ATR mode.

3.2.5 Thermal analysis

The thermal profiles of the raw materials and the dried hydrogels were tested using differential scanning calorimeter (DSC 200 F3 Maia, Netzsch, Germany) in the temperature range of 40 ^{o}C to 400 ^{o}C under nitrogen atmosphere. The rate of thermal scanning was 5 ^{o}C/min.

3.2.6 Mechanical Analysis

The mechanical properties of the hydrogels were tested using a static mechanical tester (Stable Microsystems, TA-HD plus, U.K). The hydrogels were prepared in cylindrical moulds. The height and diameter of the hydrogels was 20 mm and 15 mm, respectively. This resulted in the L/D ratio of 1.33. The hydrogels were subjected to cyclic compression and cyclic stress relaxation studies to understand the viscoelastic properties of the hydrogels [113].

3.2.7 Impedance analysis

The electrical properties of the hydrogels were tested using an in-house built impedance analyzer in the frequency range of 200 Hz - 20 KHz. The setup was used to determine the V-I characteristic by altering the amplitude of the sinusoidal voltage signals. The frequency of the sinusoidal signal was kept constant at 10 KHz.

3.2.8 Biological Characterization

The mucoadhesive property of the hydrogels was determined using static mechanical tester (Stable Microsystems, TA-HD plus, U.K). Goat intestine was used as the representative mucosal layer for the study. The goat intestine was collected in cold saline from the local slaughter house. The intestines were longitudinally cut open and were further cut into pieces of 1 cm x 1 cm. The intestinal pieces were attached onto the base of the mechanical tester. Subsequently, the hydrogels (5 mm x 5 mm) were attached on the 30 mm flat probe using double sided acrylate tape. Thereafter, the flat probe was lowered at a speed of 0.5 mm/sec and a force of 20 g was applied on mucosal surface for 10 sec to promote adhesion between the hydrogels and the mucosal layer. The probe was then retracted back at the same speed. The force required to separate the hydrogel from the intestinal mucosal surface was noted as mucoadhesive force. The work of mucoadhesion was calculated from the area under the curve of the force-time profile.

The biocompatibility of the hydrogels were estimated by hemocompatibility and cell viability test. The hemocompatibility test dealt with the incubation of the hydrogels in diluted goat blood. The percentage hemolysis of the goat blood was calculated from the absorbance of the supernatant fluid obtained after centrifuging the goat blood containing the hydrogel pieces.

$$\%\,Hemolysis = \left(\frac{OD_{sample} - OD_{-ve}}{OD_{+ve} - OD_{-ve}} \right) \times 100 \qquad (3.1)$$

where, OD_{sample} = Absorbance of sample
OD_{-ve} = Absorbance of –ve control
OD_{+ve} = Absorbance of + ve control

The cytocompatibility of the hydrogels were determined using MG63 cells. The cells were seeded in 96 well plates. $1x10^4$ cells were added in each well. 20 µl of leachants (of hydrogels) was added in each well to understand the toxic effect of the leachants. The cell viability was determined using MTT assay.

The qualitative drug release study was conducted by performing antimicrobial test using disc diffusion method. *E. coli* was used as the test microorganism. Hydrogel samples of 9 mm diameter were used for the analysis. The antimicrobial activity was correlated with the zone of inhibition of the microbial growth.

3.2.9 Swelling studies

The swelling profile of the hydrogel was determined at pH 7.4 (phosphate buffer). The weights of the hydrogels, immersed in the swelling media, were determined after an interval of 15 min for the first 1 h and 30 min for the next 9 h. The study was conducted at room temperature. The swelling index was calculated as per the following equation:

$$Swelling\ Index\ (SI) = \frac{W_T - W_0}{W_T} \quad (3.2)$$

where, W_T = Weight of sample at time T, and W_0 = Dry weight of the sample before the start of the study.

3.2.10 Drug release studies

The drug release studies were carried out using accurately weighed hydrogel samples (~350 mg). The hydrogels were put in dialysis tube containing 1 ml of dissolution media. Both ends of the dialysis membrane were sealed using dialysis tube clips. The setup was lowered in a beaker containing 50 ml of dissolution media, kept under stirring at 100 rpm. The temperature of the dissolution media was maintained at 37 ^{o}C. At regular intervals of time, the dissolution media was replaced with fresh dissolution media for 12 h. The replaced media was analyzed for the drug content using UV-visible spectrophotometer (Systronics, Double beam spectrophotometer (2203), India). The study was conducted using phosphate buffer (pH 7.4).

3.3 Result and Discussion

3.3.1 Preparation of hydrogels

Phase-separated hydrogels are a special class of mix polymer systems. In these hydrogels, the polymers separate out (concentrate) as individual polymeric phases. The phase-separation may happen in different ways due to inter- and intra- polymeric interactions. Based on the interactions, the mix biopolymer system may form three types of molecular architectures, namely, segregative phase-separation, associative phase-separation and bicontinuous phase separation [105, 114]. Segregative phase-separation happens when the two polymers have negative associative interactions. The affinity of the polymer towards the solvent may also alter the molecular dynamics of the segregative phase-separation process. This results in the formation of two phases which are enriched with either of the polymers. The associative phase-separation has been reported to occur when the interactions among the two polymers are very strong. This result in the separation of the

polymer-polymer composite (dispersed phase) and the solvent forms the continuous phase. The biocontinous phase separated hydrogels are formed when both the polymer phases appear as continuum phase. Quite often, many scientists have regarded this class of phase-separated hydrogels as a specific category of segregative phase-separation [115]. Gelatin-polysaccharides based phase-separated systems have been reported to form hydrogels by segregative phase-separation mechanism. These hydrogels are usually chemically crosslinked to improve the physical stability. This is done because the previous reports suggest that water-in-water type of emulsions have stability issues, similar to the one confronted by the oil-water emulsions [116].

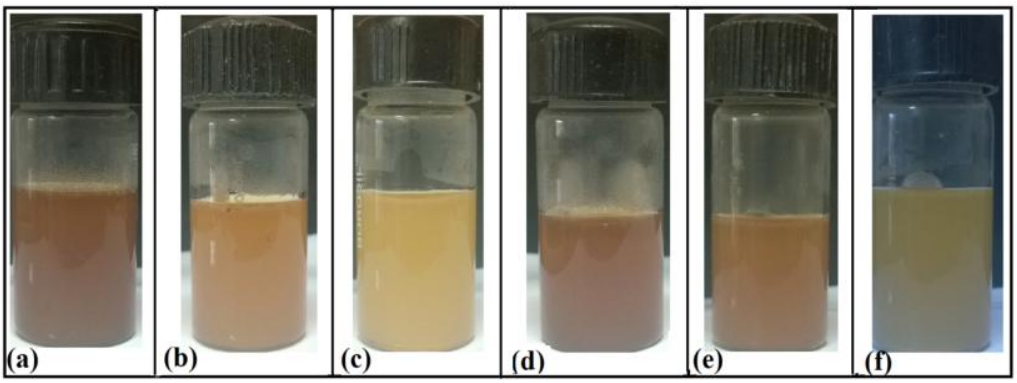

Figure 3.2: Pictographs of the hydrogels. (a) T1, (b) T2, (c) T3, (d) C1, (e) C2, and (f) C3

In this study, it was observed that an increase in the proportion of TG was associated with the increase in the whiteness of the formulation (Figure 3.2). It has been previously reported that the emulsions appears as white in color due to the diffraction of the light from the interface of the internal and the continuum phases. This gives the indication that there was a probability of formation of water-in-water emulsions. Similar observation was also made in the gelatin-CMT hydrogels. The whiteness of the CMT hydrogels was lower than the TG hydrogels. This observation may be explained by the fact that the carboxymethylation of TG resulted in the increased hydrophilicity of the TG backbone. The increase in the hydrophilicity might have improved the interaction amongst gelatin and CMT. Hence, it may be expected that the degree of phase-separation will be lower as compared to the TG hydrogels. Hydrogels were smooth to touch and had a soothing effect.

3.3.2 Microscopy

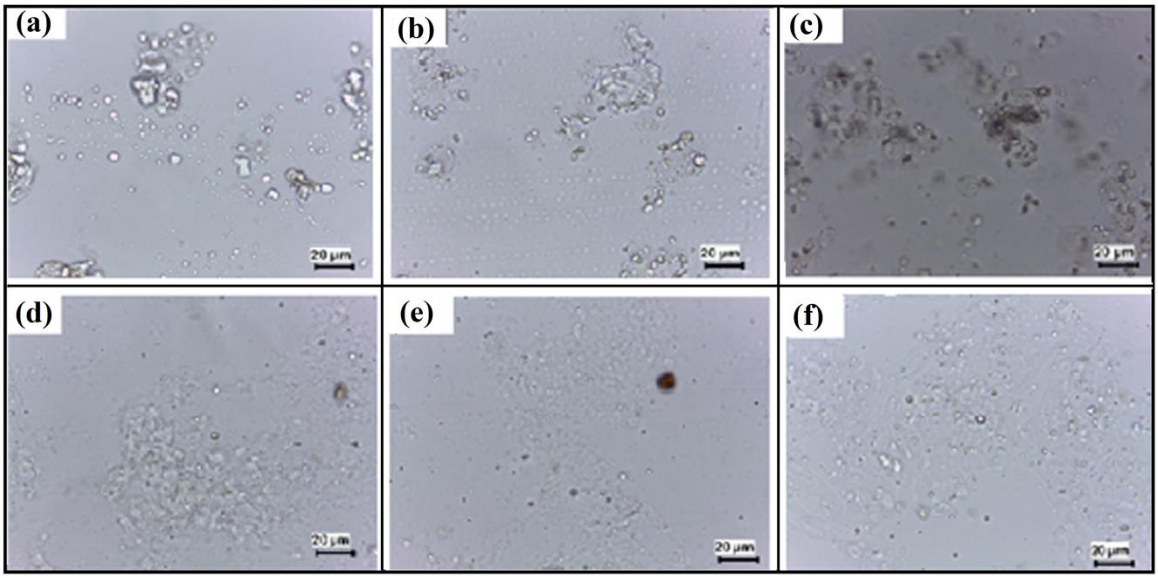

Figure 3.3: Light micrographs of the hydrogels. (a) T1, (b) T2, (c) T3, (d) C1, (e) C2, and (F) C3

The gelatin polysaccharide mixture (50 ^{o}C) was converted into thin smears over a glass slide. The smear was observed under the bright field microscope (Figure 3.3). The micrographs of the formulation show homogeneous distribution of the globular microstructure of polysaccharides within the gelatin continuum phase. The size of the globular microstructures was found to increase as the concentration of the polysaccharides was increased in the formulations. This may be due to the higher intra-polysaccharide interactions during the gelation process. The globular size of the dispersed phase was found to be higher in TG hydrogels. Similar results were expected from the visual observation of the hydrogel matrices. The large globular size of the dispersed phase in the TG hydrogels may be accounted to the higher intra-polysaccharide interactions. Carboxymethylation of tamarind gum resulted in the formation of anionic polyelectrolyte, which in turn, resulted in the increased hydration of the polysaccharides. This resulted in the decrease in the intra-polysaccharide interactions with a subsequent increase in the inter-polymer interactions. The decrease in the intra-polysaccharide interactions may be explained by the ionization of the carboxylic groups of CMT. The ionization of the carboxylic groups resulted in the steric hindrance, which in turn, hindered the process of self-aggregation of CMT [117].

3.3.3 Infrared spectroscopy

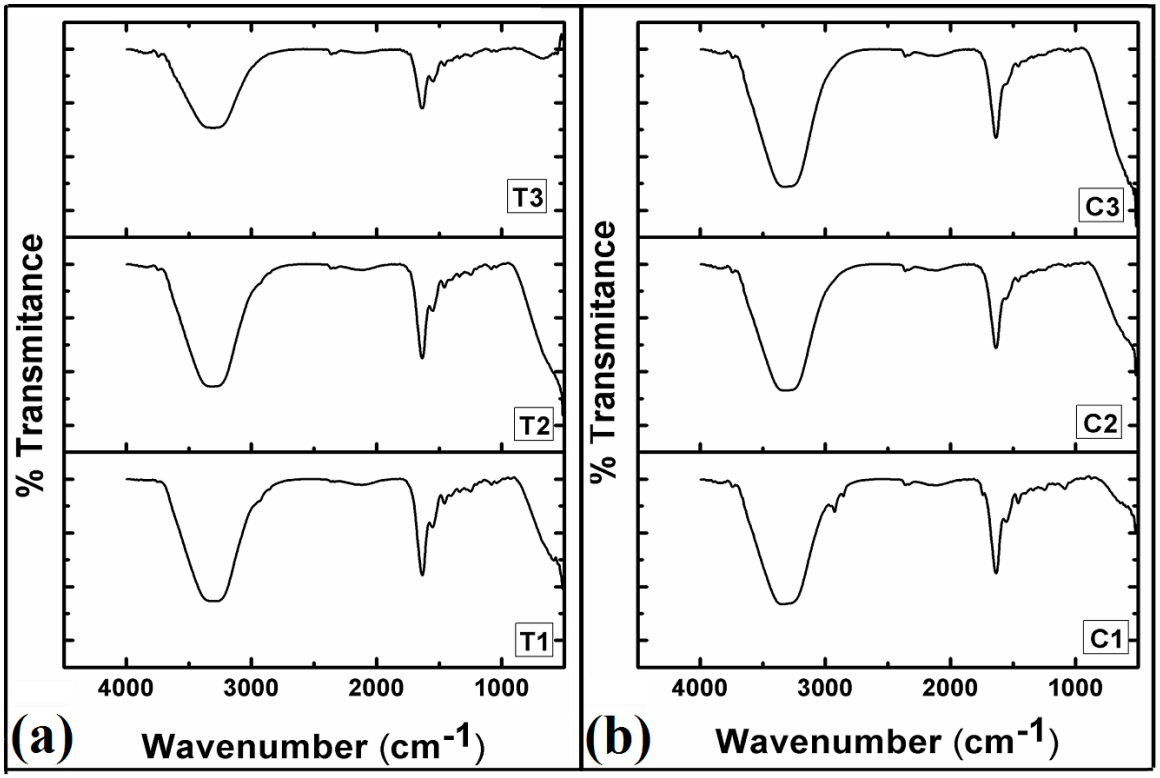

Figure 3.4: FTIR spectra of the hydrogels. (a) TG hydrogels, and (b) CMT hydrogels

The FTIR spectra of hydrogels were acquired in the ATR mode (Figure 3.4, Table 3.2). The spectra of all the hydrogels were found to be similar with that of gelatin alone hydrogel as reported in the literature [118]. Gelatin is a protein molecule. The gelatin hydrogel showed a broad peak at ~3320 cm^{-1}. This peak may be associated with the O-H and N-H stretching vibrations. The peak at ~1650 cm^{-1} can be explained by C-O and C-N stretching of the amide bonds. The peak at ~1550 cm^{1} may be associated with amide –II bonds, whereas, the peak at ~1250 cm^{-1} may be attributed to amide III bonds. It has been reported by various groups that the peak in the region of 1600-1700 cm^{-1} is an important peak for the analysis of the secondary protein structures. Addition of TG to the gelatin hydrogels did not shift the peak position of the gelatin in the hydrogels. This suggested that there were no significant changes in the secondary structure of the gelatin. CMT in lower proportions did not alter the peak position at ~1629 cm^{-1} but at higher concentration of CMT, there was a shift in the amide-I peak towards higher wavenumber. Such shift in the amide-I peak have been previously explained by the interaction of the COO^{-} groups (present in polysaccharides) with the amide-I group of the gelatin [118]. Additionally, the

extent of hydrogen bonding among the polysaccharide containing hydrogels were estimated by determining the area under the curve of the peak present in the region of 3700-2900 cm^{-1}. The area under the curve of the TG hydrogels were found to be in the order of T1>>T2>>T3. On the other hand, the area under the curve for the CMT containing hydrogels was found to be higher for the formulations containing higher amount of CMT. In general, the area under the curve of the CMT hydrogels was higher than the TG hydrogels. The above result may be explained by the relatively hydrophobic nature of TG. An increase in the TG concentration within the formulation resulted in the predominant hydrophobic interaction among the TG molecules. This, in turn, affected the inter-molecular interactions amongst the TG and the gelatin molecules. On the other hand, CMT molecules interacted with the gelatin molecules due to the availability of the free carboxylic groups.

Table 3.2: FTIR peaks of the hydrogels

Formulations	**Amide (I) (cm^{-1})**	**Amide (II) (cm^{-1})**	**Amide (III) (cm^{-1})**	**AUC (Absorbance)**
T1	1657	1562	1260	250.23
T2	1645	1560	1257	223.56
T3	1648	1560	1230	180.65
C1	1656	1563	1264	220.52
C2	1646	1539	1236	232.56
C3	1629	1535	1224	255.85

3.3.4 Thermal analysis

T1, T3, C1 and C3 were taken as the representative hydrogels for the thermal analysis. The thermal profiles and the thermal parameters of the hydrogels have been given in Figure 3.5 and Table 3.3, respectively. A broad peak was observed in the initial part of the thermal profiles. This peak may be explained by the evaporation of the water molecules from the hydrogels. The peak position was at ~100 ^{o}C for T1, whereas, it was at ~78 ^{o}C for T3. The lowering of the endothermic peak temperature suggested that there might be a reduction in the hydrogel-water interactions. This can be explained by the presence of the hydrophobic TG in higher concentration in T3. The enthalpy and entropy of the TG hydrogels were found to be higher when the concentration of the TG was more. This suggested that the energy required to evaporate the water molecules present in the hydrogels was higher when the concentration of polysaccharides was increased.

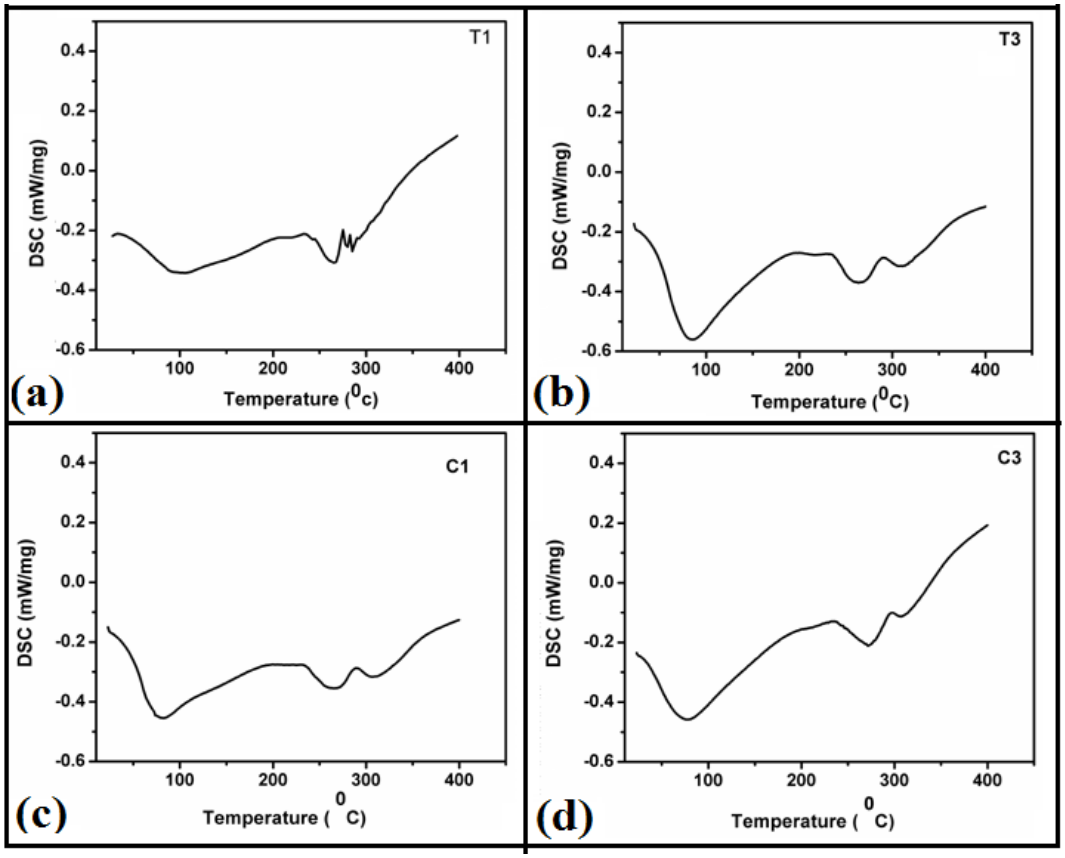

Figure 3.5: Thermal analysis of the hydrogels. (a) T1, (b) T3, (c) C1, and (d) C3

An increase in the endothermic peak temperature was observed when the concentration of the CMT was increased in CMT hydrogels. This can be explained by the relatively hydrophilic nature of CMT (as compared to TG). An increased hydrophilicity increased the interaction of the hydrogel matrices and the water molecules. The enthalpy and the entropy associated with the evaporation of the water molecules was found to be higher in hydrogels containing higher proportions of CMT. Similar changes in enthalpy and entropy was also observed in TG hydrogels. In general, the enthalpy and entropy of the CMT hydrogels were found to be higher as compared to the TG hydrogels of similar composition. This observation can also be explained by the increased hydrophilicity of CMT hydrogels due to the presence of hydrophilic carboxymethylated group. Apart from the broad endothermic peak, associated with the evaporation of the water molecules, two more broad peaks were observed at ~270 ^{o}C and ~315 ^{o}C. These additional peaks may be due to the degradation of the gelatin polymeric structure at higher temperatures. Similar endothermic peaks were also observed in pure gelatin matrices.

Table 3.3: DSC parameters for the hydrogels

Formulations	Endothermic Peaks		
	T_{evap} (°C)	ΔH_{evap} (J/g)	ΔSevap (J/g/K)
T1	100.25	10585.30	105.58
T3	78.12	16523.15	211.50
C1	80.20	12686.20	158.19
C3	83.60	20966.34	250.79

3.3.5 Mechanical Analysis

Cyclic compression test was conducted to understand the variation in the mechanical properties of the hydrogels when repeated stress was applied. In general, the peak force of the hydrogels was found to be lower in the hydrogels with higher proportion of polysaccharides. This suggested that the incorporation of the higher proportion of polysaccharides resulted in the formation of the softer hydrogels. The resilience of the hydrogels was also estimated from the cyclic compression test. Resilience of a particular compressive cycle is defined as the ratio of the area under the curve during the compression to the area under the curve during decompression [119]. The resilience is a measure of the ability of the hydrogels to undergo recovery after compression. In general, the resilience was found to be higher in the hydrogels containing higher proportions of polysaccharides. After cyclic compression for 10 cycles, a non-linear reduction in the resilience was observed. The percentage decrease of resilience after 10 cycles of compression was higher in the hydrogels containing higher proportions of polysaccharides (Figure 3.6a). In general, a higher resilience is observed in softer materials. Our observation suggests that the hydrogels with higher proportion of polysaccharides were softer in nature. Subjecting the hydrogels to repetitive compression resulted in the decrease in the softness. This can be explained by the work hardening phenomenon. Even though the peak force (first cycle) of the TG hydrogels was lower than the CMT hydrogels at lower concentration, the peak forces were found to be nearly equal when the polysaccharide content was increased (Figure 3.6b). After 10 cycles of compression, an increase in the compressive strength of all the hydrogels was observed. The percentage increase in the compressive strength was higher in TG hydrogels. An increase in the compressive strength upon repeated application of the stress indicated that

there was an increase in the elastic component with a corresponding decrease in the viscous component. This kind of phenomenon is often regarded as work hardening.

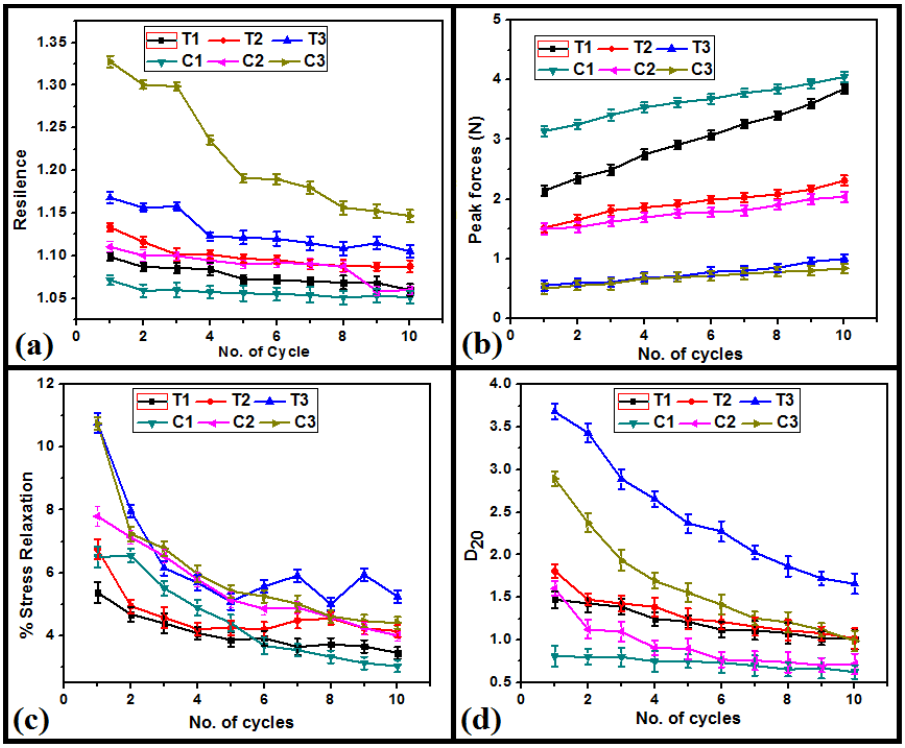

Figure 3.6: Mechanical studies of the hydrogels. (a) Resilience of TG and CMT hydrogels, (b) Peak forces of TG and CMT hydrogels, (c) % Stress relaxation of TG and CMT hydrogels, and (d) D_{20} values of TG and CMT hydrogels

The hydrogels were further subjected to cyclic stress relaxation (SR). The SR was found to be higher in the first cycle. As the hydrogels were subjected to repeated SR studies, a decrease in the SR was observed (Figure 3.6c). This indicated that during the cyclic SR studies, there was an increase in the viscoelastic solid property of the material with the subsequent decrease in the viscoelastic fluid nature. These results are concurrent with the cyclic compression studies which also suggested an increase in the viscoelastic solid component of the hydrogels as they were subjected to cyclic compression.

The firmness of the hydrogels was predicted by calculating the D_{20} values. D_{20} is regarded as the distance travelled by the probe to attain a force of 20g. In general, the D_{20} values are inversely proportional to the firmness of the hydrogels. This is due to the fact that the firm hydrogels will resist the movement of the probe as compared to the softer hydrogels. An increase in the D_{20} values was observed with an increase in the polysaccharide content (Figure 3.6d). Amongst the 2 types of the hydrogels, CMT hydrogels showed a lower D_{20} values as compared to TG hydrogels. This suggested that the CMT hydrogels were

relatively more firm as compared to the TG hydrogels. This result may be correlated to the extent of the H- bonding predicted from the area under the curve of the FTIR peak in the region 3700 cm^{-1}- 2900 cm^{-1}. The FTIR results showed that the AUC were comparatively higher in CMT hydrogels, suggesting a higher degree of hydrogen bonding in CMT hydrogels.

To have a depth analysis on the relaxation processes of the hydrogels, the relaxation profiles obtained from SR studies were fitted with Kohlrausch and Weichart model. Kohlrausch model is a basic mathematical model which is used for the analysis of the relaxation process of the polymeric constructs (Figure 3.7c). The σ_∞/ σ_0 (limiting stress) values are denoted as residual elastic component at the end of the relaxation process (Equation 3.3). The limiting stress values of the TG based hydrogels showed a decrease in limiting stress values with an increase of the polysaccharides contents where CMT based hydrogels showed no significant changes (Table 3.4). In the other hand, σ_1/ σ_0 (transient stress) values of the hydrogels increased with the increase of TG content. The transient stress of CMT based hydrogels has no significant changes like limiting stress values. The relaxation time was same for all the samples.

$$\frac{\sigma_\tau}{\sigma_0} = \frac{\sigma_\infty}{\sigma_0} + \frac{\sigma_1}{\sigma_0} \times e^{\left[-\left(\frac{t}{\tau}\right)\beta\right]} \qquad (3.3)$$

where, $\frac{\sigma_\infty}{\sigma_0}$ =limiting stress, $\frac{\sigma_1}{\sigma_0}$ =transient stress, τ= relaxation time, β=stretching parameter, t= time.

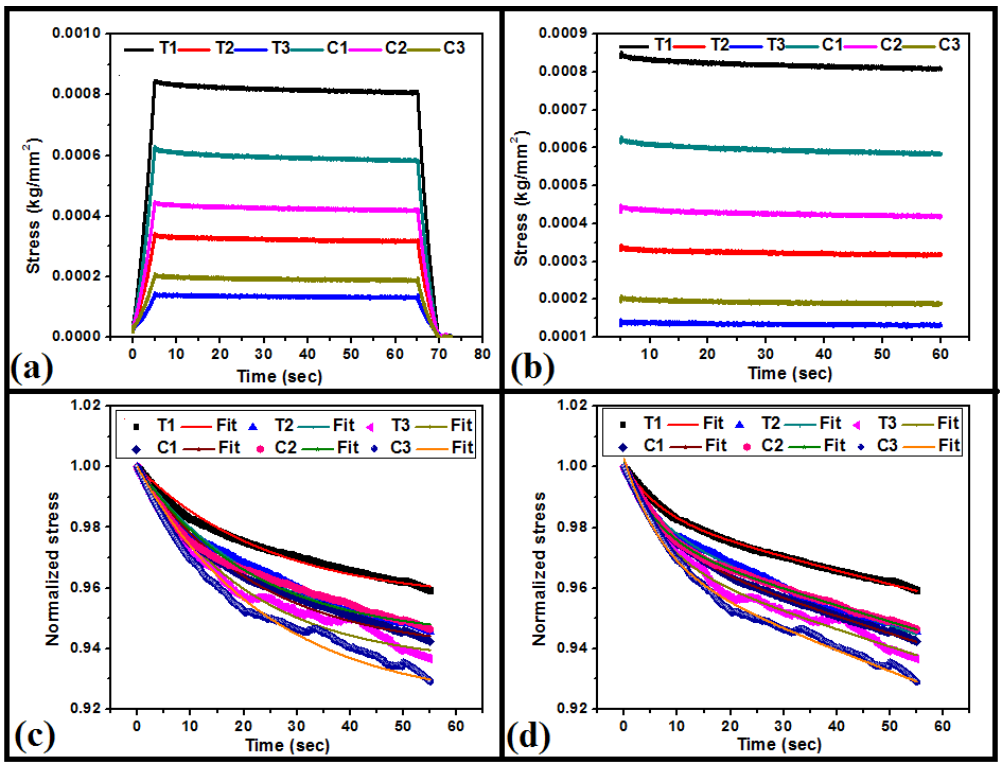

Figure 3.7: Analysis of SR data: (a) Stress relaxation profiles, (b) SR data for modelling, (c) Kohlrausch model fitting of the hydrogels, and (d) Weichart model fitting of the hydrogels

The relaxation data was further fitted to the Weichert model of viscoelasticity (Figure 3.7d, Table 3.4). The time-independent elastic modulus (P_0) was dependent on the composition of the hydrogels which is denoted as the marker of instantaneous elasticity. There was a decrease in the P_0 values with the increase in the polysaccharide content in TG hydrogels. On the contrary, a reverse trend was observed in the CMT hydrogels. Hence, it can be suggested that the viscous component of the hydrogels increased with the increase in the TG content and decreased with the increase in the CMT content, respectively. P_1 values (initial elastic component associated with the Maxwell element of the model) were higher in hydrogels containing higher amount of polysaccharides. P_2 values (delayed elastic component) have no significant changes in both TG and CMT based hydrogels. The relaxation times τ_1 and τ_2 were also calculated from Weichart model (Table 3.4). The initial relaxation times of all the hydrogels remained same whereas the delayed relaxation times of the hydrogels increased initially when polysaccharide content increased in the formulations but again decreased in T3 and C3 (content highest amount of polysaccharides).

$$P(t) = P_0 + P_1 exp(-t / \tau_1) + P_2 exp(-t / \tau_2) \quad (3.4)$$

where, P_0= Instantaneous elasticity, P_1= initial elastic component, P_2= delayed elastic component, τ_1 = initial relaxation time, τ_2 = delayed relaxation time, and t = time.

Table 3.4: Stress relaxation parameters of the hydrogels

Model	Parameters	Formulations					
		T1	**T2**	**T3**	**C1**	**C2**	**C3**
Kohlrausch	σ_∞/σ_0	0.95± 0.005	0.94±0.004	0.93±0.05	0.93±0.006	0.93±0.06	0.93±0.006
	σ_1/σ_0	0.04±0.003	0.05±0.001	0.06±0.02	0.06±0.002	0.05±0.03	0.06±0.003
	β	0.06±0.001	0.07±0.002	0.08±0.01	0.07±0.002	0.07±0.01	0.06±0.001
	τ	1.67±0.04	1.67±0.03	1.67±0.04	1.67±0.03	1.67±0.03	1.67±0.03
	R^2	0.98	0.98	0.98	0.98	0.98	0.98
Weichert	P_0	0.54±0.012	0.38±0.015	0.41±0.07	0.42±0.011	0.45±0.06	0.59±0.016
	P_1	0.43±0.002	0.54±0.001	0.55±0.01	0.54±0.001	0.55±0.03	0.66±0.003
	τ_1 (sec)	935.64±0.1	935.63±0.3	935.6±0.1	935.64±0.1	935.6±0.1	935.6±0.1
	P_2	0.01±0.001	0.02±0.001	0.03±0.02	0.02±0.003	0.02±0.01	0.03±0.001
	τ_2 (sec)	6.71±0.12	7.69±0.21	6.96±0.14	7.69±0.15	6.29±0.10	7.13±0.10
	R^2	0.99	0.97	0.99	0.98	0.98	0.98

3.3.6 Impedance Analysis

The impedance profiles of both the types of hydrogels were found to be similar. An increase in TG content resulted in the increase in the impedance of the hydrogels (Figure 3.8a). This can be explained by the hydrophobic nature of the TG molecules, which promoted the formation of predominant biphasic systems. The TG molecules in the hydrogel system behaved as dielectric material. As the proportion of TG was increased, there was a corresponding increase in the size of the dispersed phase molecules. This, in turn, resulted in the increase in the dielectric behavior of the dispersed phase. In general, higher the proportion of dielectric material, higher is the impedance. An increase in the CMT concentration resulted in the decrease in the impedance of the CMT hydrogels (Figure 3.8b). This observation may be explained by the polyelectrolyte nature of CMT. An increase in the polysaccharide content resulted in the increase in the CMT (polyelectrolyte) content in the hydrogels, which in turn, promoted the flow of current through the hydrogel matrices. The impedance profile of the hydrogels showed higher impedance in lower frequencies. The impedance exponentially degraded to a base level at higher frequencies. This kind of impedance profile is usually associated with the capacitive nature of the materials. The higher impedance at lower frequency may be explained by the electrode polarization effect at lower frequencies. The polarization effect is minimized when the frequency of the injecting current is increased. This is due to the quick reversal of the electrode polarity at higher frequencies. This phenomenon prevents the polarization effect at the electrode-sample interface [120].

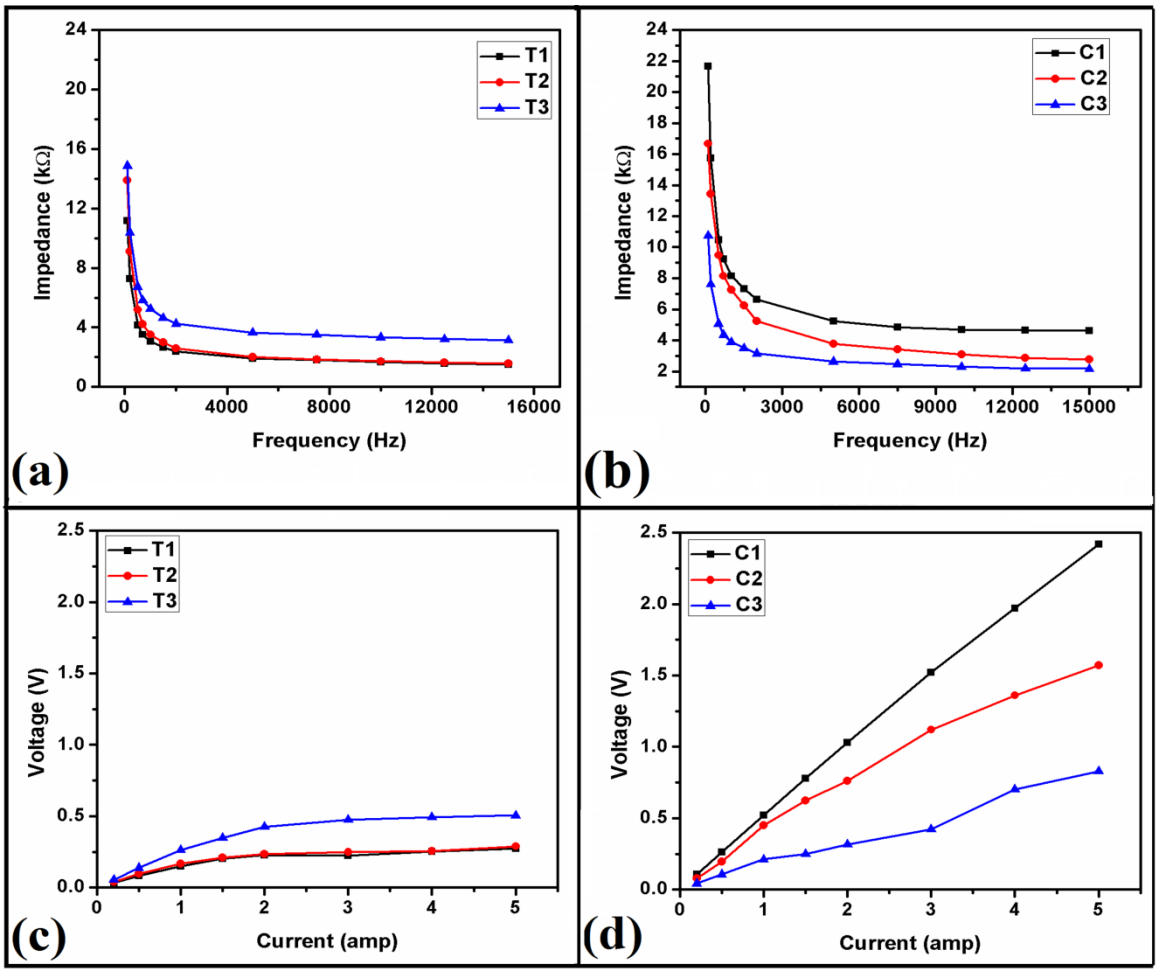

Figure 3.8 Impedance profiles: (a) TG hydrogels, and (b) CMT hydrogels; and V-I characteristics: (c) TG hydrogels, and (d) CMT hydrogels

The V-I characteristics of the hydrogels were measured at 10 KHz. This was done to eliminate the electrode polarization effect of the electrodes. The V-I profile of the TG hydrogels showed an initial linear increase in the voltage when the current was increased (Figure 3.8c). Subsequently, the V-I profiles became saturated as the current was further increased. This may be explained by the internal alteration of the microstructure of the hydrogels when the current was increased beyond a critical value. On the other hand, the V-I profiles of the CMT hydrogels followed a linear profile (Figure 3.8d). This indicated that the CMT hydrogels behaved as pure resistive formulation under the experimental conditions. The slope of the V-I curve gives an indication about the impedance of the material. Similar to the impedance profile, the V-I profile also suggested that an increase in TG resulted in the increased impedance of the TG hydrogels. On the contrary, the impedance of the CMT hydrogels was found to be lower in hydrogels containing higher proportions of CMT.

3.3.7 Biological Characterization

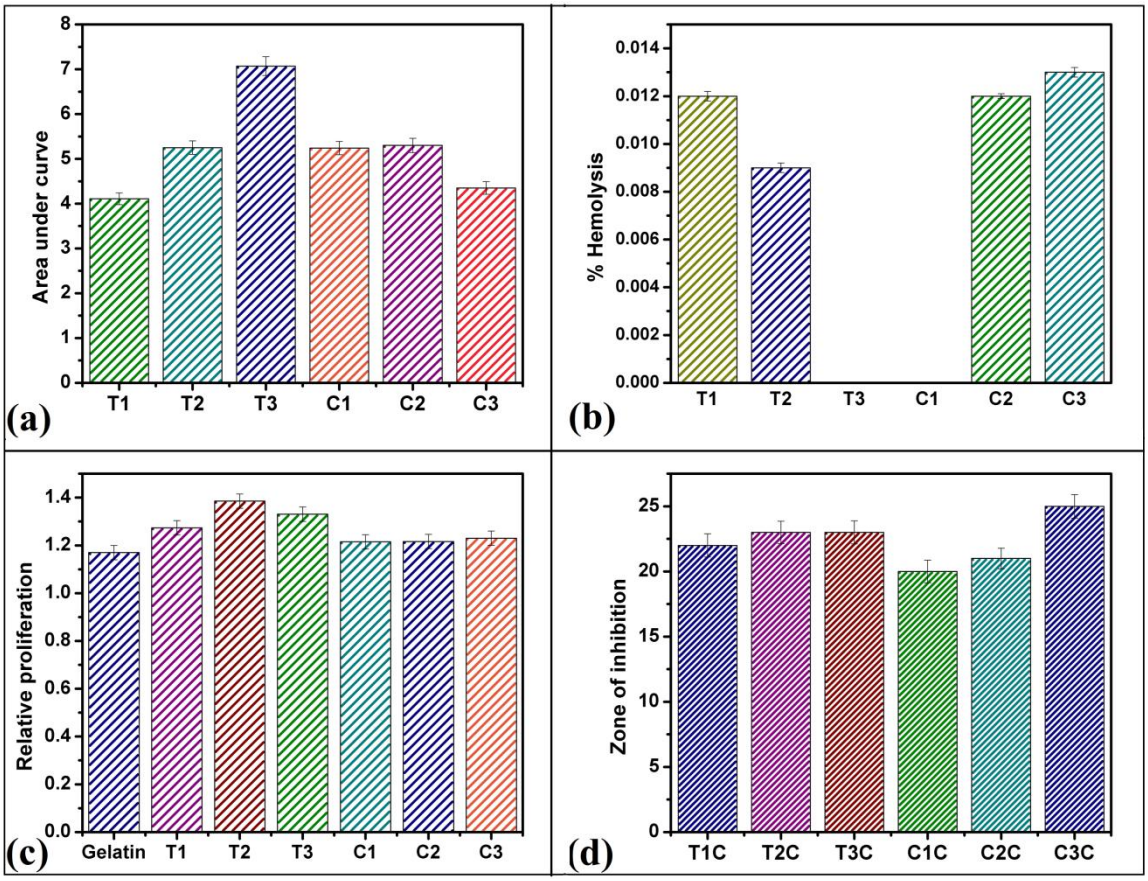

Figure 3.9: Biological characterizations of the hydrogels. (a) Area under the curve of mucoadhesive profiles, (b) % hemolysis of goat blood, (c) Cell proliferation study, and (d) Antimicrobial study.

Both gelatin and polysaccharides have been reported to be excellent materials for designing mucoadhesive systems [121]. Mucoadhesion depends on the type of fictionalization and the method of preparation/extraction of the above biopolymers. In this study, the mucoadhesive property was determined using a static mechanical tester. An increase in the TG content showed an increase in the mucoadhesion of the TG hydrogels (Figure 3.9a). This can be explained by the composition of the hydrogels. In TG hydrogels, incorporation of TG (a non-ionic polysaccharide) resulted in the increase in the number of the hydroxyl groups which have the capability to positively interact with the mucin. On the other hand, an increase in the CMT content resulted in the decrease in the mucoadhesion (Figure 3.9a). This is due to the fact that the mucosal layer mainly consists of mucin (negatively charged polysaccharide) [122]. The negative charge of the mucin resulted in the repulsion of the carboxylic groups present in the CMT hydrogels. This

resulted in a negative interaction between the mucosal layer and the CMT hydrogels. Amongst the hydrogels of similar composition, T1 showed lower mucoadhesive properties than C1, whereas, T2 and C2 showed similar mucoadhesive properties. This observation may be explained by the interaction of the polysaccharides with the gelatin matrix.

The biocompatibility of the hydrogels was determined by hemocompatibility and cytocompatibility tests. The hemocompatibility study is based on the determination of the lysis of RBC in the presence of the hydrogels. The lysis of RBC results in the release of the hemoglobin in the external fluid. The hemoglobin gets solubilized in the external fluid and gives a yellowish color. The suspended unwanted components of the blood are pelletized by centrifugation. The yellowish color of the supernatant fluid is measured using a UV- visible spectrophotometer and is compared with the positive and negative controls to determine the percentage hemolysis of the RBCs in the presence of the hydrogels. All the hydrogel formulations were found to be highly hemocompatible as the percentage hemolysis in the presence of hydrogels was <<5% (Figure 3.9b).

The cytocompatibility of the hydrogels was checked using MG63 cell line (osteoblast cells). Extract of the hydrogels were prepared and were used for the analysis. The experiment was done to test whether the leachants of the hydrogels have any adverse effect on the proliferation of the cells. The relative proliferation of all the hydrogels was > 1, which indicated the cytocompatible nature of the hydrogels (Figure 3.9c). It may also be concluded that the prepared hydrogels supported the growth of MG63 cells to a certain extent as compared to the control. In general, TG hydrogels showed better cell growth as compared to CMT hydrogels.

The antimicrobial activity of the drug loaded hydrogels was estimated against *E. coli*. The blank hydrogels did not show any zone of inhibition but samples loaded with the antimicrobial drug showed a marked zone of inhibitions (Figure 3.9d). This suggested that the blank hydrogels did not contain any antimicrobial activity, whereas, a marked antimicrobial activity of the drug loaded hydrogels was evident. The result suggested that the drug was released from the hydrogels matrices in active form.

3.3.8 Swelling studies

The swelling study was conducted at pH 7.4 (Figure 3.10). The swelling of the all the hydrogels was found to be higher in the formulations containing higher proportion of polysaccharides (TG/CMT). At pH 7.4, the carboxylic and amino groups existed as zwitter ions. This resulted in the existence of the gelatin network as a neutral polymeric architecture. Hence, the swelling of the matrices was dependent mainly on the absorption

of the water molecules by the polysaccharide phase. The above phenomenon resulted in the marked differences in the absorption of the water molecules with the variation in the polysaccharide content.

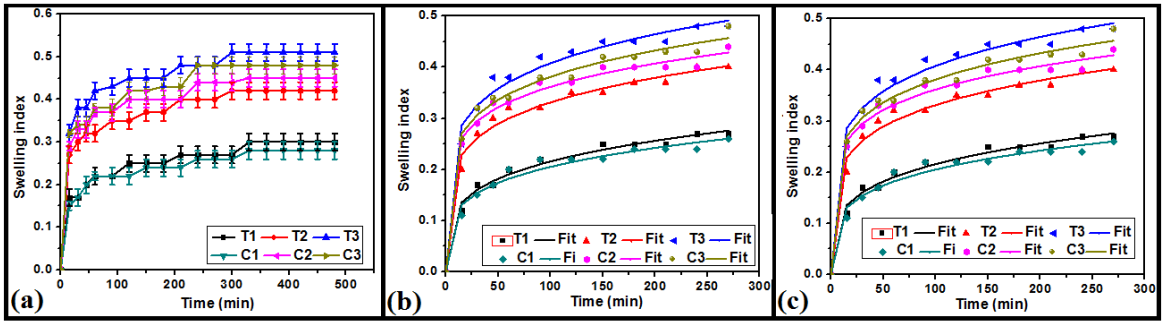

Figure 3.10: Swelling study of the hydrogels. (a) Swelling profiles of the hydrogels (pH 7.4), (b) Weibull model fitting for hydrogels, and (c) Korsmeyer-Peppas model fitting for hydrogels

So, the swelling was found to be higher in the hydrogels, containing higher proportions of polysaccharide. The swelling behavior at pH 7.4 of the CMT hydrogels was found to be lower as that of TG hydrogels.

To have some better analysis about the swelling of the hydrogels, the swelling profiles were fitted with Weibull (Equation 3.5) and Korsmeyer-Peppas model (Equation 3.6). In general, Weibull model explains the nature of the swelling profiles. This mathematical model expresses two basic parameters like scale (a) and shape (b) parameters. The scale parameters denote the positioning of the attainment of the peak on a time scale where a higher scale parameter suggests a delayed swelling process. At pH 7.4, both TG and CMT based hydrogels showed a faster swelling process with increase of the polysaccharide contents in the formulations (Figure 3.10b, Table 3.5). The shape parameter showed a parabolic nature of the profiles. The Korsmeyer-Peppas model was used to calculate the diffusion coefficient (n) of the hydrogels. In general, it explains the diffusion of the water molecules within the matrices. The diffusion coefficient (n) of all the hydrogels were below 0.45 at pH 7.4 which suggested that the diffusion was predominantly Fickian diffusion mediated for all the hydrogels (Figure 3.10c, Table 3.5).

$$m = 1 - exp\left[-\left(\frac{t - T}{a}\right)^{b}\right] \qquad (3.5)$$

where, *m*= fraction of water absorbed, t = time (sec), T= delay time (sec), a = time-scale parameter, and b = shape parameter.

$$m = k \times t^{n} \quad (3.6)$$

where, k= rate constant, n= diffusion exponent

Table 3.5: Swelling parameters of the hydrogels

Model	**Model parameters**	**Formulations**					
		T1	**T2**	**T3**	**C1**	**C2**	**C3**
Weibull	a	524.8±17.41	332.5±5.23	269.8±6.54	549.2±7.23	300.6±7.12	286.9±4.89
	b	0.24±0.001	0.19±0.001	0.18±0.001	0.23±0.001	0.17±0.001	0.18±0.001
	R^2	0.99	0.99	0.99	0.98	0.99	0.99
Korsmeyer- Peppas	K	0.19±0.001	0.29±0.001	0.37±0.001	0.18±0.001	0.33±0.001	0.34±0.001
	n	0.24±0.001	0.19±0.001	0.18±0.001	0.23±0.001	0.17±0.001	0.18±0.001
	R^2	0.99	0.99	0.98	0.98	0.99	0.99

3.3.9 Drug release study

The swelling studies of the hydrogels indicated a possibility of pH dependent drug release from the phase-separated hydrogels. In general, the release of the drug from the hydrogels is dependent on the swelling property of the hydrogels. Hence, to understand the pH sensitive drug release behavior from the hydrogels, the drug release studies were conducted at 7.4 (average intestinal pH) (Figure 3.11a). The release of the drug from the TG hydrogels was higher from the hydrogels with higher TG content, i.e, cumulative percentage of drug release (CPDR) was in the order of T1<T2<T3. The CPDR of the CMT at pH 7.4 was also found to be in the order of C1<C2<C3. The observed result from the phase-separated hydrogels can be correlated and well explained by the swelling studies. In general, the release of the drugs from the hydrogel matrices depends on the rate of diffusion of the dissolution media into the matrices. Higher flow of dissolution media into the hydrogels resulted in the increased dissolution of the drug and consequently increased diffusion of the drug from the polymer matrices.

To make a depth analysis of the drug release process, the drug releases were fitted with Weibull (Equation 3.7), Korsmeyer-Peppas (Equation 3.8) and Peppas-sahlin (Equation 3.9) models. The scale (a) and shape (b) parameters of the Weibull model explain the nature of the release profiles. At ph 7.4, the release was slowest in T1 and C1. But with an increase in the polysaccharide contents, the release became faster in the hydrogels. The shape parameter showed a parabolic nature of the profiles. Subsequently, the diffusion mechanism of the drug from the hydrogels was estimated by calculating the diffusion value (n) using Korsmeyar-Peppas diffusion model (Figure 3.11c). The 'n' values for the TG hydrogels (except T2) were found to be <0.45 at pH 7.4. This suggested that the diffusion was predominantly Fickian Mediated for all the TG hydrogels (except T2) at pH 7.4. Whereas the release of the drugs from the CMT based hydrogels was Fickian diffusion mediated for all the samples (except C1) at pH 7.4. Pappas- Sahlin model was used to predict the contribution of the polymer chain relaxation in the release profile [123]. The constant K_1 is associated with the Fickian diffusion, whereas, the constant K_2 is associated with the diffusion due to the polymer relaxation (Figure 3.11d). At pH 7.4, constant K_1 and K (from Korsmeyer-Peppas model) were of the similar trend. This was quite expected because the Korsmeyer-Peppas model indicated that the diffusion of the drug was predominantly Fickian diffusion mediated. The K_2 values of all the films were much lower. This suggested a least effect of polymer relaxation during the drug release process (Table 3.6).

$$CPDR = 1 - exp\left[-\left(\frac{t - T}{a}\right)^{b}\right] \quad (3.7)$$

where, CPDR= Cumulative percent drug release, t = time (sec), T= delay time (sec), a = time-scale parameter, and b = shape parameter.

$$CPDR = k \times t^{n} \quad (3.8)$$

where, k= release rate constant, n= release constant, t = time (sec).

$$CPDR = k_1 \times t^{m} + k_2 \times t^{2m} \quad (3.9)$$

where, k_1= constant (associated with Fickian diffusion), k_2= constant (associated with diffusion due to polymer relaxation), m = release constant

$$\frac{R}{F} = \frac{k_2}{k_1} \times t^{m} \quad (3.10)$$

where, k_1 and k_2 are rate constants, m is the release constant.

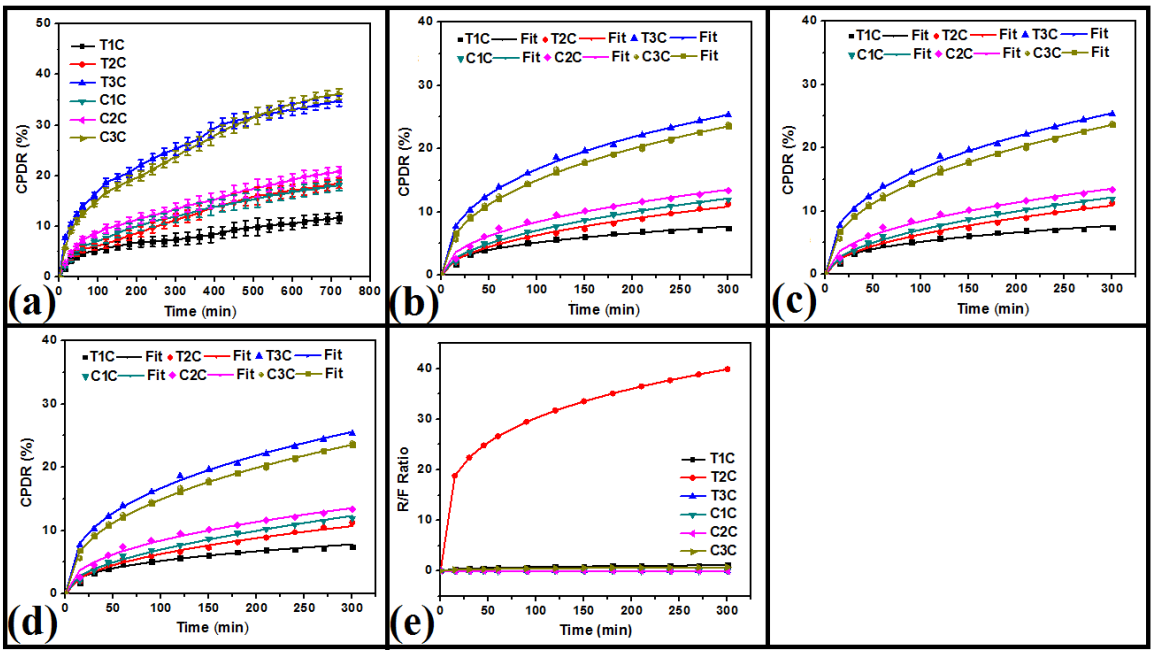

Figure 3.11: Drug release study of the hydrogels at pH 7.4. (a) Drug release profiles of TG and CMT hydrogels, (b) Weibull model fitting for hydrogels, (c) Korsmeyer-Peppas model fitting for hydrogels, (d) Peppas-Sahlin model fitting for hydrogels, and (e) R/F ratio from Peppas-Sahlin model.

Table 3.6: Drug release parameters of the hydrogels

Model	**Parameters**	**Formulations**					
		T1	**T2**	**T3**	**C1**	**C2**	**C3**
Weibull	a	105.25±2.15	62.32±1.01	38.67±1.45	146.32±3.25	92.31±2.35	49.23±2.13
	b	0.37±0.001	0.51±0.01	0.42±0.001	0.51±0.01	0.45±0.01	0.45±0.01
	R^2	0.99	0.98	0.99	0.99	0.99	0.98
Korsmeyer-Peppas	K	0.96±0.03	0.64±0.02	2.84±0.06	0.72±0.01	1.13±0.03	2.20±0.04
	n	0.36±0.001	0.49±0.01	0.38±0.001	0.49±0.01	0.43±0.001	0.41±0.001
	R^2	0.99	0.98	0.99	0.98	0.99	0.99
Peppas- Sahlin	K_1	0.95±0.02	0.68±0.01	2.28±0.05	0.83±0.03	1.14±0.04	2.22±0.05
	K_2	0.01	0.01	0.01	0.04	0.01	0.01
	m	0.36±0.001	0.24±0.001	0.38±0.001	0.39±0.001	0.43±0.001	0.41±0.001
	R^2	0.99	0.99	0.98	0.98	0.99	0.99

3.4 Conclusion

The current study delineates the development of TG and CMT based phase-separated hydrogels. In this study, gelatin was used as the second polymeric phase. An increase in the hydrophilicity of TG by carboxymethylation resulted in the increase in the compatibility of the polysaccharide and the gelatin phase. This resulted in the better mechanical properties of the CMT based hydrogels. A higher proliferation of the MG63 cells was observed in the presence of the extracts of TG hydrogels. The CMT based hydrogels also showed higher proliferation as compared to the controls. Both types of the hydrogels also showed good mucoadhesive properties. Due the presence of the free carboxylic groups in CMT, a pH sensitive swelling and drug release behavior from the CMT hydrogels were observed.

Chapter 4

Preparation, characterization and assessment of the novel gelatin-tamarind gum/ carboxymethyl tamarind gum based phase-separated films for skin tissue engineering applications

4.1 Introduction

Protein and polysaccharide based formulations have been studied extensively for food and pharmaceutical applications [124]. Depending upon the composition of the formulations, there is a drastic change in the structural properties of the protein-polysaccharide formulations. When the aqueous solution of the proteins and the polysaccharides are mixed together, there is a possibility of formation of a liquid water-in-water emulsion, complex coacervates (where both the polymers appears in a single concentrated phase) and soluble complexes due to formation of self-organised formulations at different length scales [125]. The formation of any of the above-mentioned formulations is governed by the thermodynamic compatibility amongst the proteins and polysaccharides [126]. Recently, there has been an increased research on the development of protein-polysaccharide based formulations. Various polysaccharides (starch, cellulose, pectin, chitin, and glycogen) have been used either alone or in different combinations [127]. This has resulted in the development of formulations of different properties.

Gelatin is an animal protein and is used for developing hydrogels for biomedical applications (tissue engineering, drug delivery, wound healing) [128]. It is usually

obtained by controlled hydrolysis of collagen, obtained from the bovine bones (gelatin-B) and porcine skins (gelatin-A) [129]. Gelatin is highly biocompatible, biodegradable and has good mechanical properties which makes it suitable to be used for tissue engineering and wound healing applications [130]. Due to its film-forming ability, gelatin has been used to develop films. Gelatin films have been explored as wound dressing materials [29]. Tamarind gum (TG) is obtained from the outer layer of tamarind seed kernels (*Tamarindus indica*) [131]. TG is a non-anionic branched polysaccharide and is soluble in water. Solubilization of TG in water results in the formulation of a viscous solution [132]. Due to this reason, aqueous solution of TG is commonly used for thickening and gelling purposes [133]. This gum has been approached for food applications in Japan [134]. The main advantage of TG is its easy availability and low cost. The main drawback of TG is its fast biodegradability. Hence, chemical modifications of TG have been proposed. Amongst the various proposed chemical modifications, carboxymethylation of TG is most common [96]. Unfortunately, due to very poor mechanical properties of TG, it has to be blended with another polymer, which will provide better mechanical property.

Taking a note from the above, gelatin- TG/ CMT phase-separated films were prepared. Polyethylene glycol (PEG, 400 molecular weight) was used as the plasticizer [135]. The gelatin-polysaccharide based films were prepared in different concentrations [136]. The films were thoroughly characterized by bright field microscopy, FTIR spectroscopy, differential scanning calorimetry (DSC), mechanical analyzer and impedance analyzer. The swelling properties of the films were tested in different pH conditions (1.2 and 7.4). The biocompatibility of the films was established by hemocompatibility (using goat blood) and cell viability (using HaCaT cells) studies. To study the ability of the films as controlled delivery vehicles, the films were loaded with ciprofloxacin. The release profiles of the drug-loaded films were determined at three different pHs (1.2 and 7.4). The antimicrobial activities of the drug-loaded films were tested against the *E. coli* as the model microorganism [137].

4.2 Materials and method

4.2.1 Materials

TG and CMT (degree of carboxylation is 0.372) were purchased from Maruti Hydrocolloids, India. Gelatin was procured from Himedia, Mumbai, India. Ciprofloxacin (CF) was purchased from Fluka Biochemical, China. Ethanol was obtained from Honyon International Inc., Hong Yang Chemical Corporation, China. Glutaraldehyde (25%, for synthesis; GA) and hydrochloric acid (35% pure) were obtained from Merck Specialities

Private Limited Mumbai, India. Polyethylene glycol (PEG 400 mol. Weight) was purchased from Rankem, Gurgaon, India. Goat blood was collected from the local butcher shop. Double distilled water was used throughout the study.

4.2.2 Preparation of polymeric solutions

100 g of 20% gelatin solution was prepared by dissolving 20 g of gelatin in 70 g of water (50 ^{o}C). The final weight of the solution was made up to100 g using water (50 ^{o}C). The water was continuously stirred at 100 rpm using a magnetic stirrer during the preparation of the gelatin solution. The polysaccharide solutions were prepared by dissolving sufficient amount of polysaccharides (TG and CMT) in water (50 ^{o}C, kept on stirring at 100 rpm). Thereafter, the final weight of the solutions was made up to 100 g using water (50 ^{o}C). The polysaccharides solutions were made at two concentrations (1% and 2% w/w). The polysaccharide solutions, so formed were kept at 5 ^{o}C overnight before use.

Table 4.1: Composition of TG and CMT based films

Formulations	GS-20 (g)	TS-1 (g)	TS- 2 (g)	CS -1 (g)	CS-2 (g)	CL (ml)	CFX (g)	PEG (g)
C	20	--	--	--	--	0.6	--	1.6
T1	8	12	--	--	--	0.6	--	0.64
T2	8	--	12	--	--	0.6	--	0.64
C1	8	--	--	12	--	0.6	--	0.64
C2	8	--	--	--	12	0.6	--	0.64
CC	20	--	--	--	--	0.6	0.1	1.6
T1C	8	12	--	--	--	0.6	0.1	0.64
T2C	8	--	12	--	--	0.6	0.1	0.64
C1C	8	--	--	12	--	0.6	0.1	0.64
C2C	8	--	--	--	12	0.6	0.1	0.64

*GS: Gelatin solution (20% w/w); TS-1: Tamarind gum solution (1% w/w); TS-2: Tamarind gum solution (2% w/w); CS-1: Carboxymethyl tamarind gum solution (1% w/w); CS-2: Carboxymethyl tamarind gum solution (2% w/w); CL: Crosslinking reagent; CFX: Ciprofloxacin; and PEG: Poly ethylene glycol.

4.2.3 Preparation of films

The compositions of the prepared films have been given in Table 4.1. The films were prepared by conventional solution casting method. In brief, 8 g of the gelatin solution (50 ^{o}C) was added to the 12 g of the polysaccharide solutions (50 ^{o}C) with continuous stirring at 100 rpm. PEG was added to the above mixture such that the weight of PEG was 40% of the dry weight of gelatin. The concentration of the PEG was selected as per the previously

reported literature. Thereafter, the crosslinking agent (0.4 ml of ethyl alcohol, 0.1 ml of glutaraldehyde, 0.01 ml of HCl) was added to the above mixture and stirred for 30 secs. The petri plates were then put in an environmental chamber for 48 h at 40 ^{o}C. The dried films were collected from the environmental chamber at the end of 48 h and were kept at 5 ^{o}C in sealed polyethylene packets for the further studies. The drug loaded films were prepared in a similar manner. Ciprofloxacin was added to the mixture of gelatin-polysaccharide and PEG. Rest of the method remained same. The films were washed thoroughly using PBS buffer and double distilled water before all the experiments. Further, glycine solution (1% w/v) was used to inhibit the chemical reactions of glutaraldehyde after the said incubation period.

4.2.4 Microscopy studies

The bright field micrographs of the films were observed under bright field microscope (LEICA-DM 750 equipped with ICC 50-HD camera, Germany). The formulations were converted into thin smears over glass slides before visualization.

4.2.5 Infrared spectroscopy

The IR spectra of the prepared films were measured using a FTIR spectrometer (AlpHa-E, Bruker, USA) working in the ATR mode. The analysis was done in the wavenumber range of 4500 cm^{-1} to 450 cm^{-1}. The ATR module was fitted with the ZnSe.

4.2.6 Thermal analysis

The thermal profiles of the films were analysed using differential scanning calorimeter (DSC 200 F3 Maia, Netzsch, Germany) in the temperature range of 40 ^{o}C to 400 ^{o}C at a scanning rate of 5 ^{o}C/min under inert atmosphere (nitrogen gas). The calibration was done using indium. Nearly 10 mg of the sample was used for the analysis.

4.2.7 Mechanical analysis

The mechanical properties of the films were tested using a static mechanical tester (Stable Microsystems, TA-HD plus, U.K). The samples were cut in rectangular pieces having dimensions of 5 mm x 60 mm. The films were attached to the sample holder, such that the sample length during the study was 50 mm. The tensile strength of the films was determined by stretching the films at a rate of 1 mm/sec till the breaking point was

achieved. The bursting strength of the films was measured using a 5 mm spherical probe. For the test, the samples were cut into 30 mm x 30 mm square pieces and attached to the sample holder. Thereafter, the spherical probe was allowed to penetrate the sample at a rate of 1 mm/sec till the bursting of the films was achieved. Stress relaxation (SR) was done in the tensile mode. For Stress relaxation, the samples were stretched to 10 mm at rate of 1 mm/sec and were subsequently allowed to relax for sixty seconds.

4.2.8 Impedance analysis

The electrical properties of the films were measured using an in-house built impedance analyzer in the frequency range of 100 Hz and 20 KHz. The current-voltage relationship (I-V characteristic) was measured at frequency of 1 KHz.

4.2.9 Biological characterizations

The hemolysis of the RBCs (goat blood) in the presence of the prepared films were studied as per the reported literature [138]. The study provides information about the hemocompatibility of the samples. For this study, fresh goat blood was collected in a round bottom flask which contained tri-sodium citrate. The round bottom flask was immediately transferred to an ice-bath. The collected blood was used within 1 h of collection [139]. 8 ml of the blood was diluted with 10 ml of normal saline. The +ve control of the test was made by adding 0.1 ml of HCl in a 15 ml falcon tube containing 0.5 ml of diluted blood. The volume was made up to 10 ml with normal saline. The -ve control was prepared by diluting 0.5 ml of the dilute blood to 10 ml of normal saline. The test sample was prepared by diluting 0.5 ml of blood to 10 ml using normal saline and adding the pieces of the films (3 mm x 3 mm). Thereafter, all the falcon tubes were incubated for 2 h in an incubator (37 ^{o}C). After the incubation, the falcon tubes were centrifuged at 4000 rpm for 10 min, so as to allow the settling of the blood components. The supernatant was spectrophotometrically analyzed using UV-visible spectrophotometer. Percentage hemolysis was calculated as per equation 4.1.

$$\%\,Hemolysis = \left(\frac{OD_{sample} - OD_{-ve}}{OD_{+ve} - OD_{-ve}} \right) \times 100 \qquad (4.1)$$

where, OD_{sample} = Absorbance of sample

OD_{-ve} = Absorbance of –ve control

OD_{+ve} = Absorbance of + ve control

For antimicrobial study, the films were cut as 9 mm discs. The discs were placed over nutrient agar plates, previously inoculated with 100 µl of *E. coli* suspension [139]. The petri-plates were put in an incubator (37^o C) for a period of 12 h. At the end of the incubation, the zone of inhibition was measured.

The proliferative index of the HaCaT cells in the presence of test samples was studied via MTT assay. The cells were maintained in complete DMEM media (10% FBS and 1% antimycotic-antibiotic solution) at 37°C, 5% CO_2. Wells of a sterile 96-well plate that were pre-treated with solutions were let to set before inoculation of cells. Cells culture flasks upon attaining 80% confluence were trypsinized for cell harvesting and 1 x 10^4 cells were added to each well of the 96 well plate containing either TG or CMT films and incubated for 24 hrs to ensure proper cell adhesion. MTT assay was carried out by adding 100µl of MTT reagent (MTT reagent and DMEM complete media in the ratio 1:10) to each well for 4 h of incubation. After completion of incubation, the formazan crystals formed were dissolved in 100 µl of DMSO. The absorbance of DMSO solution was then measured at 595nm and the cell proliferation was represented in terms of cell proliferation index (CPI).

4.2.10 Swelling studies

The water absorption profile of the films was measured at pH 7.4. For this study, the films were cut into rectangular pieces of 3 mm x 5 mm size (initial weight: W_i) and the films were put into the swelling medium. The films were taken out from the swelling media at regular intervals, wiped using tissue paper to get rid of the free water and weighed accurately (W_f). The swelling index was determined using the formula given in equation 4.2.

$$\textit{Swelling index (SI)} = \frac{W_f - W_i}{W_i} \qquad (4.2)$$

where, W_f = Initial weight of the films

W_i = Final weight of the films

4.2.11 Drug release studies

The drug loaded films were cut into rectangular pieces (3mm x 5mm). The films were put into dissolution media. At predefined intervals of time, the films were taken out from the dissolution media. The previous dissolution media was spectrophotometrically analyzed at 271 nm to determine the amount of the drug released. The experiment was conducted at 37 ^{o}C for 12 h.

4.3 Result and Discussion

4.3.1 Preparation of the films

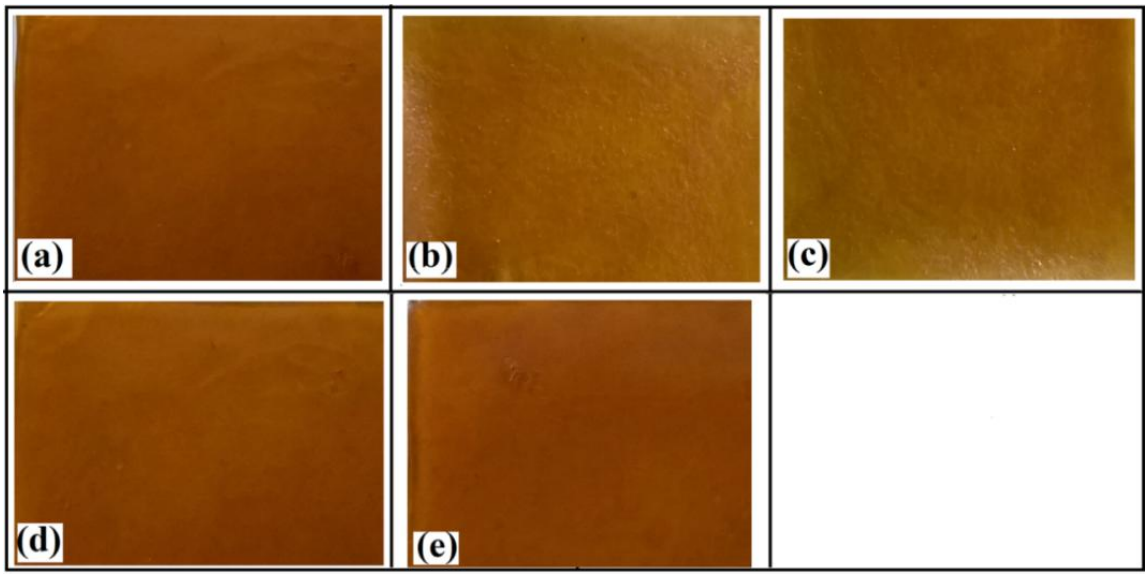

Figure 4.1: Photographs of the films. (a) C, (b) T1, (c) T2, (d) C1, and (e) C2

The prepared films were found to be stretchable and flexible in nature (Figure 4.1). The thickness of the films was in the range of 0.18 mm and 0.20 mm. The gelatin film (C) was slightly dark brown in colour and was transparent in nature (gelatin film was taken as control and denoted as C) (Figure 4.1a). This can be attributed to the transparent nature of the gelatin films [140]. Incorporation of the polysaccharides into the gelatin matrices decreased the apparent transparency of the films. The polysaccharides containing films were whitish-brown in colour. This may be explained by the diffraction of the light from the interface of the polysaccharide rich and gelatin rich phases, which resulted in the formation of water-in-water type of emulsions [141]. The films had a characteristic odour, which can be associated with the odour of the gelatin.

4.3.2 Microscopic analysis

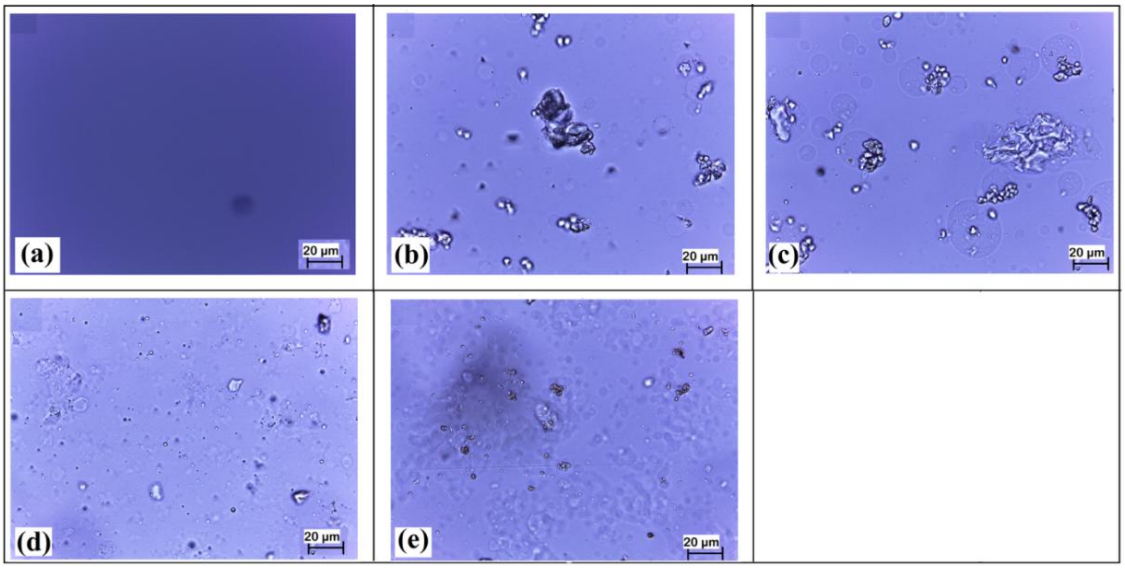

Figure 4.2: Light micrographs of the films. (a) C, (b) T1, (c) T2, (d) C1, and (e) C2

The bright field micrographs of all the films showed presence of globular structures (Figure 4.2). Apart from the globular structures, the TG containing films showed presence of agglomerated gum particles. This can be explained by the higher hydrophobic nature of TG. Due to the hydrophobic nature of TG, some of the TG particles might not have hydrated uniformly in water. The agglomerated particles were also present in the CMT films, but the extent of agglomeration was much lower as compared to the TG films. An increase in the polysaccharide proportion resulted in the formation of phase-separated systems having larger droplet diameter[142]. The diameters of the TG droplets were found to be larger as compared to the CMT droplets. The smaller droplets of the CMT may be explained by the relatively hydrophilic nature of the CMT gum. This might have resulted in the better dispersion of the polysaccharide droplets in the gelatin matrix due to the increase in the CMT-gelatin thermodynamic compatibility [126]. From the pictures of the films, it was found that the polysaccharide containing films were slightly whitish in nature. From this it can be predicted that the whiteness of the films was due to the diffraction of the light from the interface of the polysaccharide-gelatin interface [143]. The microstructures of the films showed the existence of prominent interface amongst the polysaccharide rich and gelatin rich phases.

4.3.3 Infrared spectroscopy

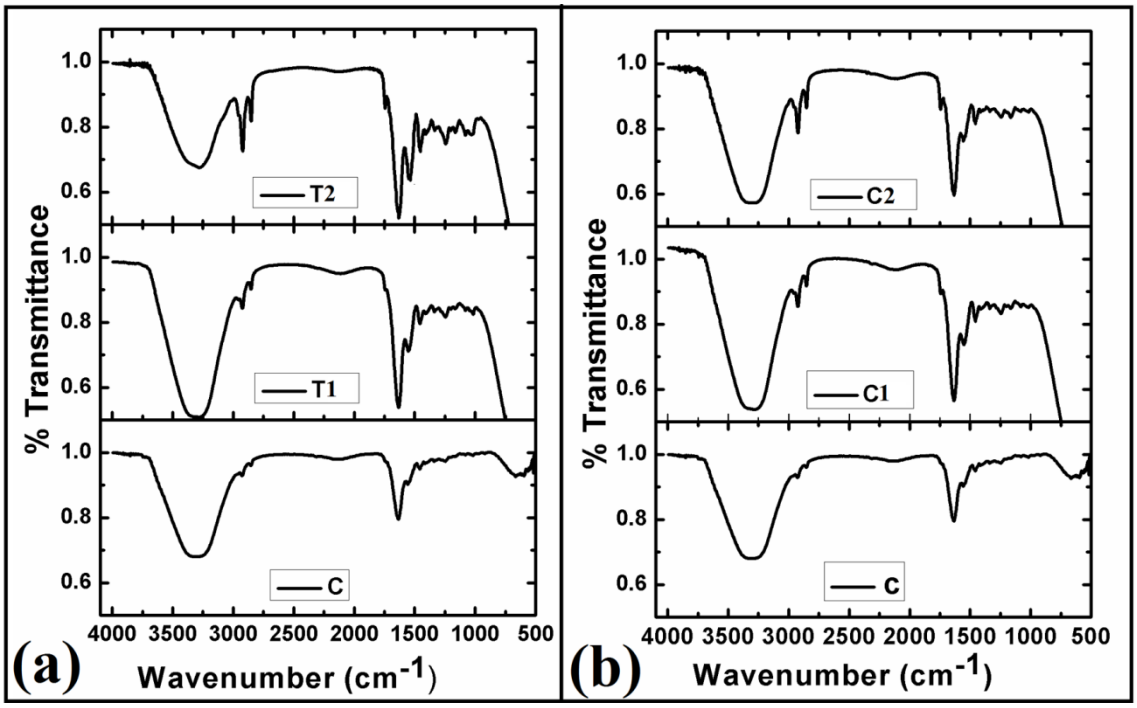

Figure 4.3: FTIR spectra of the films

The gelatin film (C) showed the presence of distinct peaks at 1240 cm^{-1}, 1575 cm^{-1} and 1640 cm^{-1} (Figure 4.3, Table 4.2). The peak at 1240 cm^{-1} can be associated with the amide-III stretching vibrations, whereas, the peaks at 1575 cm^{-1} and 1640 cm^{-1} can be explained by the amide-II and amide-I stretching vibrations, respectively. This suggested that the secondary structure of the gelatin molecules was conserved in the gelatin films. The peaks corresponding to amide-I, II and III were also observed in the polysaccharide containing films. But there were changes in the positioning of the amide peaks. Amide-I peak is due to the C=O and C-N stretching vibrations, whereas, the amide –II and amide-III peaks are mainly due to the N-H bending vibrations and C-H stretching vibrations[144]. When polysaccharide content was lower (1% w/w), no significant changes in the position of the amide-I peak was observed but when the polysaccharide content was increased (2% w/w), there was a significant shift of the amide-I peak towards lower wavenumber. The amide-II peaks were significantly lowered in the polysaccharide containing films. Unlike amide-I peak, the amide –III peak remained at the same position. As per the literature, the amide-I peak is used for the analysis of the secondary protein structure. From the peak positioning of the amide-I peak, it can be predicted that even

though, there were no significant changes in the secondary protein structure of the gelatin protein when polysaccharide content was lower. An increase in the polysaccharide content to 2% has significantly affected the secondary protein structures of the gelatin. The broad peak at around 3400 cm^{-1} can be associated with the stretching vibration of O-H groups bonded with N-H groups [145]. The area under the curve provides information about the extent of interactions. An increase in the TG content resulted in the decrease in the area under the curve of the peak. This was due to the hydrophobic nature of TG which resulted in the decrease in the interaction of the polar groups of the TG and the gelatin molecules. On the contrary, due to presence of the carboxymethyl groups, an increased interaction amongst the CMT and the gelatin molecules were observed (increase in the area under curve with increase in the CMT content). The peak at ~3400 cm^{-1} was also observed in gelatin film (C). This peak can be explained by the intermolecular interactions of the hydroxyl groups and the amino groups of the gelatin molecules and intermolecular interaction amongst the hydroxyl groups of the PEG and the amino groups of the gelatin molecules [146].

Table 4.2: FTIR peaks of the films

Formulations	**Amide (I) (cm^{-1})**	**Amide (II) (cm^{-1})**	**Amide (III) (cm^{-1})**	**AUC (Absorbance)**
C	1640	1575	1240	167.2323
T1	1644	1548	1446	252.226
T2	1624	1531	1244	179.334
C1	1646	1536	1240	201.4654
C2	1626	1546	1242	211.9797

4.3.4 Thermal analysis

All the films showed a broad endothermic peak in the region of 75 ^{o}C and 90 ^{o}C. A careful examination of the peaks suggested that the broad peak is a combination of two endothermic peaks (Figure 4.4). In all the films, the second endothermic peak appeared as a shoulder peak (demarcated by arrow marks). The presence of the dual peaks can be explained by the evaporation of the water molecules from the films. In general, there are two types of water molecules which are present in the biopolymeric films, namely free water and bound water. The first peak is associated with the evaporation of the free water from the films, whereas, the second peak is due to the evaporation of the bound water molecules.

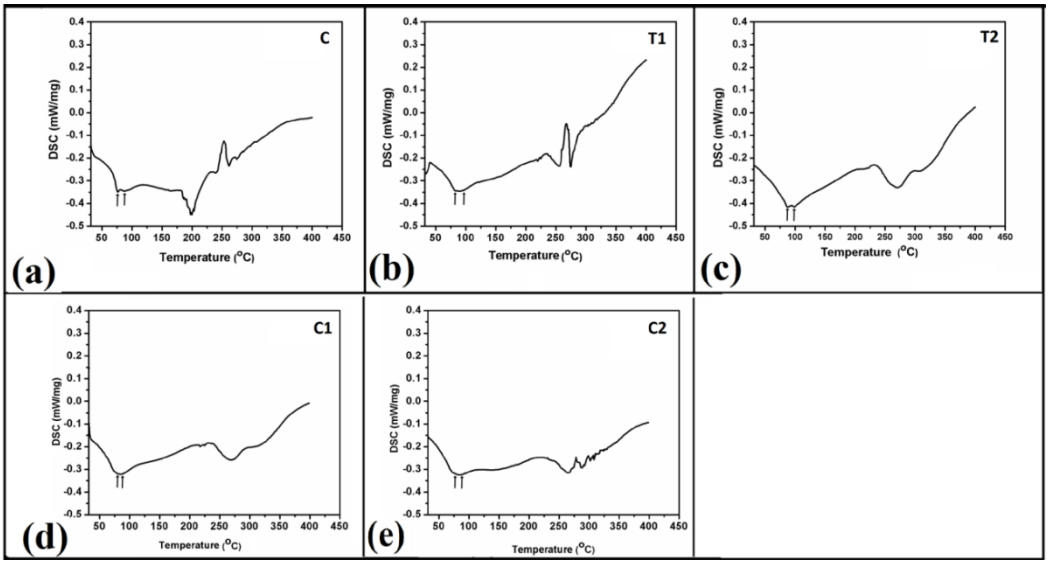

Figure 4.4: Thermal profiles of the films. (a) C, (b) T1, (c) T2, (d) C1, and (e) C2

The enthalpy of water evaporation (free water + bound water) was calculated from the Netzsch proteus software. The enthalpies of the polysaccharide containing films were much higher as compared to the control (Table 4.3). This can be explained by the better water holding capacity of the polysaccharides. An increase in the polysaccharide content correspondingly increased the enthalpy of water evaporation [147]. This indicated that the water holding capacity of the films which contained higher amount of polysaccharides were better as compared to the films, which contained lower amount of polysaccharides. The enthalpy of evaporation of water molecule was slightly higher in C1 as compared to T1 but when polysaccharide content was increased in T2 and C2, the enthalpy of T2 was higher as compared to C2. This may be due to the fact that once the hydrophobic chains of the TG were exposed; there was an interaction between the water molecules and the hydrophobic domains present in the polysaccharide. This interaction resulted in the absorption of more amount of water. The water which is absorbed due to the hydrophobic domains is regarded as secondary bound water. On the contrary, the presence of the carboxylic groups in CMT resulted in relative hydrophilic nature of the polysaccharide. Hence, the interactions of the water molecules with the hydrophobic domains of the polysaccharides were negligible. The above observation may be explained by the significant increase in the enthalpy of the TG films and a minor increase in the CMT films.

Table 4.3: Changes in enthalpy (ΔH) and entropy (ΔS) of the films

Formulations	Endothermic peaks		
	$T_{evap.}$ (°C)	$\Delta H_{evap.}$ (J/g)	$\Delta S_{evap.}$ (J/g/K)
C	76.2	77.76	47.36572
T1	89.8	140.8	100.3082
T2	87.9	176.1	141.056
C1	83.6	144.3	108.1737
C2	85.6	149.4	114.9796

4.3.5 Mechanical studies

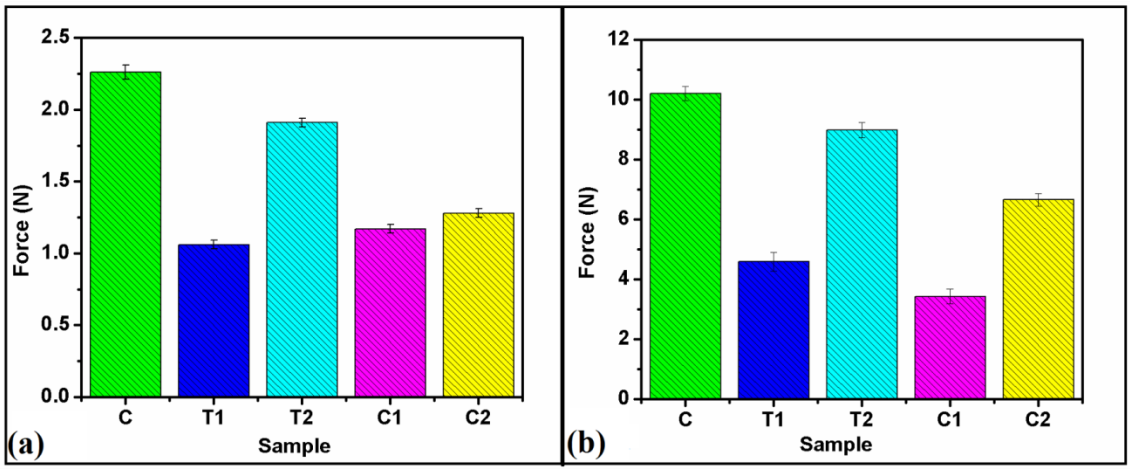

Figure 4.5: Tensile and bursting strength results of the films. (a) Tensile strengths of the films, and (b) Bursting strengths of the films

The tensile strength of the gelatin film was highest (Figure 4.5a). Incorporation of polysaccharides in the gelatin films decreased the tensile strength of the films. This can be explained by the decrease in the gelatin content when the polysaccharide was incorporated. Gelatin forms intermolecular triple helical crosslink points, which is responsible for imparting the mechanical strength of the gelatin based polymeric network [148]. Further, gelatin appears as fine strands. This result in the increased inter-molecular interactions amongst the gelatin fibers [148]. Hence, there was a decrease in the mechanical strength of the films when the gelatin content was reduced. The tensile strength of the films containing lower amount of polysaccharide (T1 and C1) showed lower tensile strength as compared to the polysaccharide containing higher amount of polysaccharides (T2 and C2). The tensile strength of T1 was 1.08 N, which was lowest amongst all the films. This may be explained by the fact that TG particles might have

behaved as defect in the films [149]. An increase in the TG concentration resulted in the drastic increase in the tensile strength which may be explained by the filler effect exerted by the polysaccharide phase [104]. The tensile strengths of C1 and C2 were nearly equal and were slightly higher than T1. Similar to the tensile strength, the bursting strength of the gelatin film was found to be highest (Figure 4.5b). Also, a decrease in the bursting strength was observed when polysaccharide was incorporated within the films. Amongst the same type of the polysaccharides, an increase in the bursting strength was observed with the increase in the polysaccharide content.

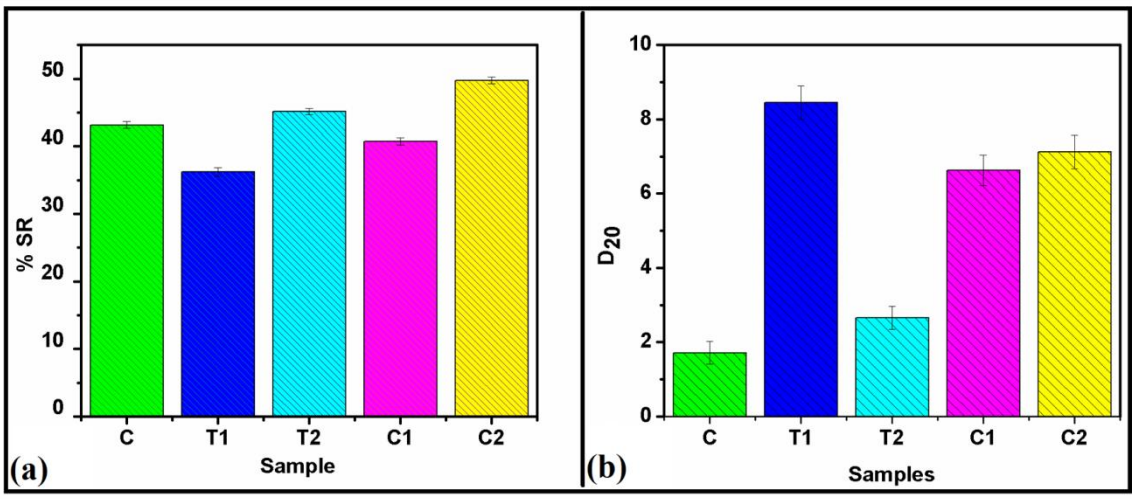

Figure 4.6: Stress relaxation results of the films. (a) % Stress relaxation of the films, and (b) D_{20} values of the films

The stress relaxation (SR) properties of the films were studied in the tensile mode (Figure 4.6a). The peak force obtained during the application of the stress (F_0) was in the same order as obtained in tensile strength studies (Table 4.4). The residual stress (F_r) was highest in the gelatin film. An increase in the TG content resulted in the increase in the residual force. On the contrary, an increase in the CMT content resulted in the decrease in the residual force. % SR was higher in the films containing higher proportions of polysaccharides (Figure 4.6a) (Equation 4.3). This indicated that an increase in the polysaccharide content promoted the relaxation of the films [150]. D_{20} values were calculated from the stress relaxation profiles [151] (Figure 4.6b). D_{20} value is defined as the distance moved by the probe to attain a force of 20 g [152]. It provides information about the ductility of the materials. Higher the D_{20} values, better is the ductility. The results showed that the ductility of the gelatin film was lowest (Figure 4.6b). Incorporation of the polysaccharides in the gelatin films resulted in the increase in the ductility. Amongst the TG containing films, the ductility of T1 was higher. An increase in

the TG content in T2 resulted in a drastic reduction in the ductility of the films. The ductility of the CMT containing films was nearly equal and may be explained by the fact that the compatibility amongst the CMT and the gelatin molecules were much better due to introduction of the carboxymethyl groups in CMT.

$$\%SR = \frac{F_0 - F_r}{F_0} \times 100 \quad (4.3)$$

where, F_0= applied stress, F_r= residual stress.

The relaxation profiles (from SR studies) were fitted with Kohlrausch model (Figure 4.7c) (Equation 4.4), the simplest model used for predicting the relaxation process of the polymeric constructs [153]. It is an empirical relaxation function and is useful in justifying the occurrence of common relaxation processes [154]. The σ_∞/ σ_0 (limiting stress) values are an indicator the residual elastic component at the end of the relaxation process. The limiting stress values suggested that the residual elastic component of gelatin film (control), except C2, was lower than the polysaccharide containing films (Table 4.4). The tamarind gum films showed higher limiting stress values as compared to carboxymethyl tamarind gum films. An increase in the polysaccharide content lowered the limiting stress of the films. This confirmed our prediction that the filler effect was predominant in these films. An increase in the polysaccharide content (in T2 and C2) drastically decreased the limiting stress values thereby confirming our prediction that at higher polysaccharide content defects were incorporated within the films. Additionally, it was observed that the limiting stress was better in the tamarind gum containing films as compared to the carboxymethyl tamarind gum containing films. This observation may be related to the hydrophilic nature of the carboxymethyl tamarind gum. The σ_1/ σ_0 (transient stress) values of the gelatin film was higher (except C2) than the polysaccharide films. In general, the relaxation of the gelatin film was faster as compared to the polysaccharide containing films (except C2). The relaxation time was fastest in C2. This suggested a predominant polymer relaxation process as compared to the polymer chain breakage mediated relaxation process [153]. The stretching parameter (β) had values in the range of 0 and 1 suggesting a stretched decay processed.

$$\frac{\sigma_\tau}{\sigma_0} = \frac{\sigma_\infty}{\sigma_0} + \frac{\sigma_1}{\sigma_0} \times e^{\left[-\left(\frac{t}{\tau}\right)^\beta\right]} \quad (4.4)$$

where, $\frac{\sigma_\infty}{\sigma_0}$ = limiting stress, $\frac{\sigma_1}{\sigma_0}$ = transient stress, τ= relaxation time, β= stretching parameter, t= time.

The normalized relaxation profiles (from SR studies) were further fitted to the Weichert model of viscoelasticity (Figure 4.7d) (Equation 4.5) [153]. P_0 values are a marker of the instantaneous elasticity. The P_0 values were in same order as that of the limiting stress values (calculated from the Kohlrausch model). In general, the P_0 values were higher than P_1 and P_2 values. This suggested predominant elastic nature of the films. P_1 values (initial elastic component associated with the Maxwell element of the model) were higher in the films with higher proportions of polysaccharides. The P_2 (delayed elastic component) values were higher than the P_1 values in gelatin and films containing lower proportions of polysaccharide (T1 and C1). At higher proportions of polysaccharides (T2 and C2), a reverse trend was observed. The relaxation times were also calculated from the Weichert model (Table 3.4). The initial relaxation time (τ_1) was lowest in C2 followed by gelatin film, T1, C1 and T2, respectively. An increase in the tamarind gum content delayed the initial relaxation process. On the contrary, an increase in the carboxylmethyl tamarind gum promoted initial relaxation process. This suggested that tamarind gum in higher proportions delayed molecular rearrangement whereas carboxymethyl tamarind gum promoted molecular rearrangement. Similar trend was also seen in the τ_2 (delayed relaxation time) values for the polysaccharide containing films. Interestingly, the delayed relaxation time value of gelatin film was highest and comparable with T2. The delayed relaxation time provide information about the polymer-polymer interactions and the breakage of the polymer chains, respectively [155]. The result suggested an increased polymer-polymer interaction with a corresponding lower chance of polymer chain breakage when tamarind gum content was increased (in T2). The gelatin film had similar delayed relaxation time as that of T2. The delayed relaxation time of carboxylmethyl tamarind gum films was not significantly different, suggesting that the variation in the proportion of the carboxymethyl tamarind gum (within the experimental compositions) did not affect the polymer-polymer interactions and chances of polymer chain breakage.

$$P(t) = P_0 + P_1 \exp(-t/\tau_1) + P_2 \exp(-t/\tau_2) \quad (4.5)$$

where, P_0= Instantaneous elasticity, P_1= initial elastic component, P_2= delayed elastic component, τ_1= initial relaxation time, τ_2= delayed relaxation time, and t = time

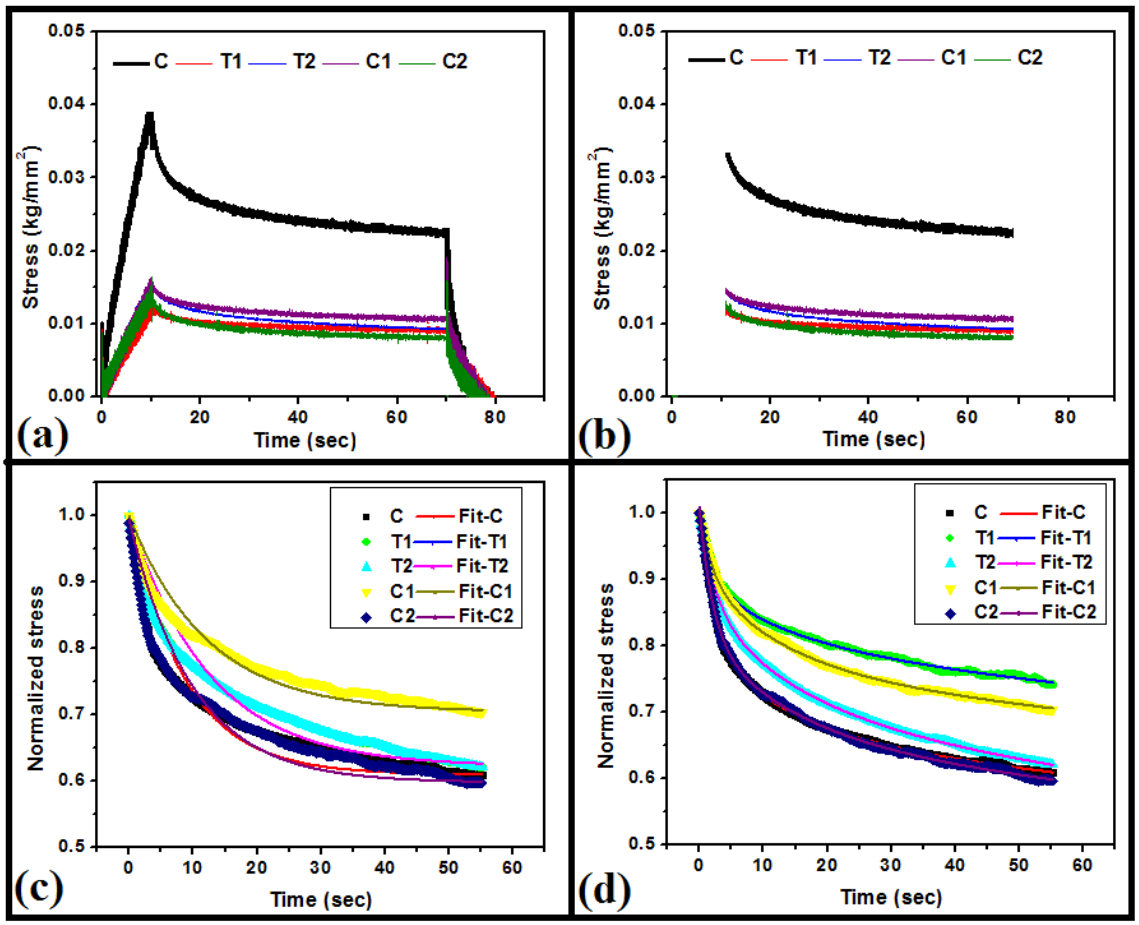

Figure 4.7: Analysis of SR data: (a) Stress relaxation profiles, (b) SR data for modeling, (c), Kohlrausch model fitting of the films, and (d) Weichart model fitting of the films

Table 4.4: Stress relaxation parameters of the films

Model	Parameters	Formulations				
		C	T1	T2	C1	C2
--	F_0 (g)	67.93±0.78	24.54±0.45	58.65±0.56	29.32±0.61	27.20±0.55
	Fr (g)	38.61±0.41	15.65±0.47	31.97±0.39	17.38±0.52	13.66±0.39
	% SR	43.16 ±0.54	36.21±0.61	42.47±0.47	40.72±0.55	49.75 ± 0.5
	D_{20} (mm)	1.71 ± 0.30	8.44 ± 0.45	2.64 ± 0.31	6.62 ± 0.41	7.12 ± 0.45
Kohlrausch	σ_∞/σ_0	0.53±0.005	0.61±0.004	0.55±0.005	0.59±0.006	0.47±0.006
	σ_1/σ_0	0.46±0.003	0.38±0.001	0.44±0.002	0.41±0.002	0.52±0.003
	β	0.19±0.001	0.44±0.002	0.13±0.001	0.21±0.002	0.27±0.001
	τ	1.12±0.04	1.59±0.03	1.29±0.04	1.26±0.03	1.23±0.03
	R^2	0.94	0.91	0.96	0.91	0.91
Weichert	P_0	0.53±0.012	0.60±0.015	0.54±0.017	0.59±0.011	0.47±0.016
	P_1	0.20±0.002	0.14±0.001	0.25±0.001	0.18±0.001	0.20±0.003
	τ_1 (sec)	17.15±0.21	17.55±0.33	21.25±0.21	18.15±0.42	16.06±0.43
	P_2	0.25±0.001	0.24±0.001	0.18±0.002	0.21±0.003	0.16±0.001
	τ_2 (sec)	0.86±0.12	0.35±0.21	0.87±0.14	0.44±0.15	0.42±0.10
	R^2	0.99	0.97	0.99	0.98	0.98

4.3.6 Impedance analysis

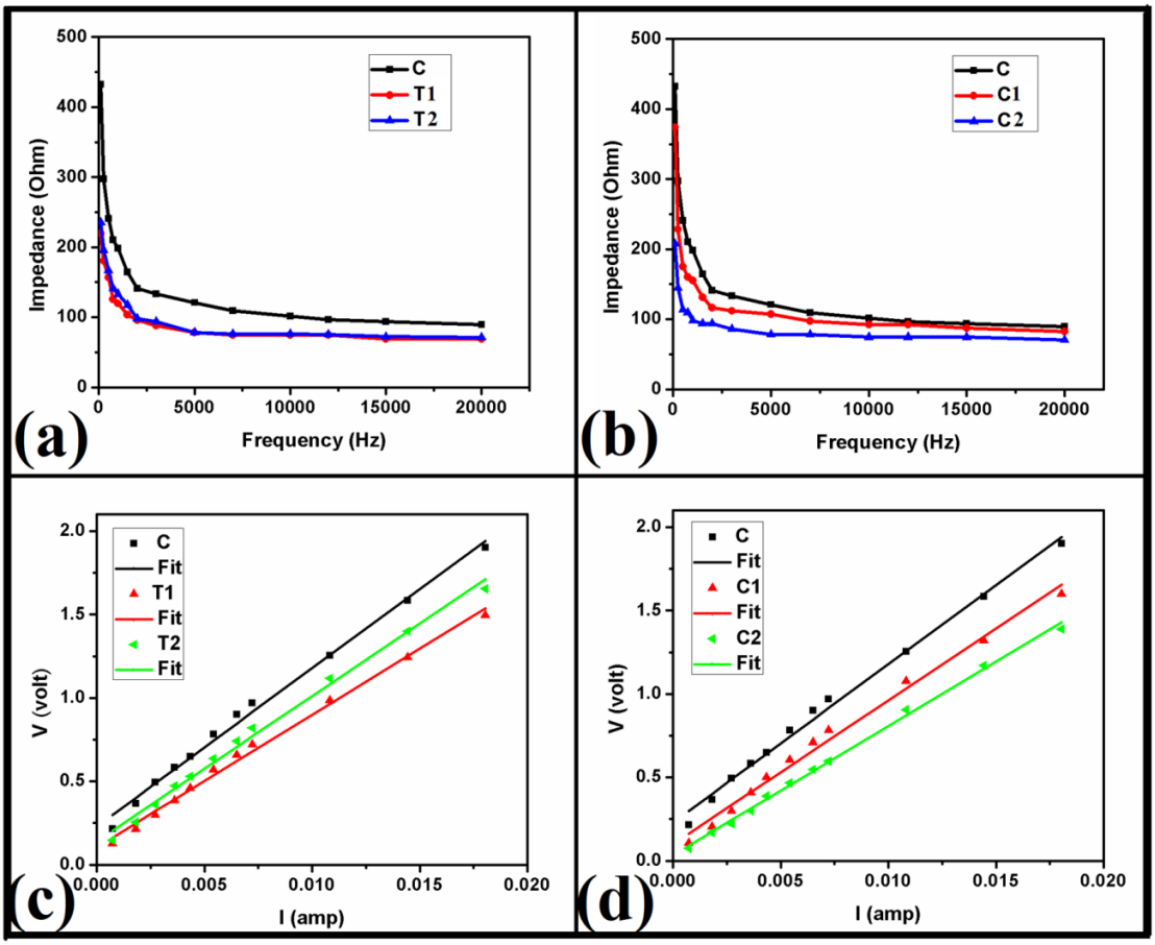

Figure 4.8: Impedance profiles: (a) TG films, and (b) CMT films; and V-I profiles: (c) TG films, and (b) CMT films

The impedance of T1 and T2 were nearly equal and were lower than gelatin film (Figure 4.8a). Whilst the impedance of C1 and C2 had a marked difference (Figure 4.8b). The impedance of C1 was higher as compared to C2. Like the TG containing films, the impedance of CMT containing films were also lower than the gelatin films. This suggested that the inclusion of the polysaccharides increases the conductivity of the films. This can be explored by the ability of the polysaccharides to hold more bound water as compared to the gelatin molecules. The impedance profiles of the all the films were similar; higher impedance at lower frequency which died down quickly to a constant impedance at higher frequencies. This type of profile is usually showed by capacitive dominance formulations.

V-I profiles of all the hydrogels showed linear profiles (Figure 4.8c and Figure 4.8d). For TG based formulations, there was an increase in the voltage when current was

increased with the simultaneous increase of the TG content in the formulations (T2>T1). But both the films have lower values than the gelatin film. The linear profiles suggested the formation of pure resistive formulations under the experimental condition. In case of CMT based formulations, a reverse trend was followed. C1 showed a higher profile than C2. But gelatin film has higher V-I values as compared to the all polysaccharide content films.

4.3.7 Biological characterizations

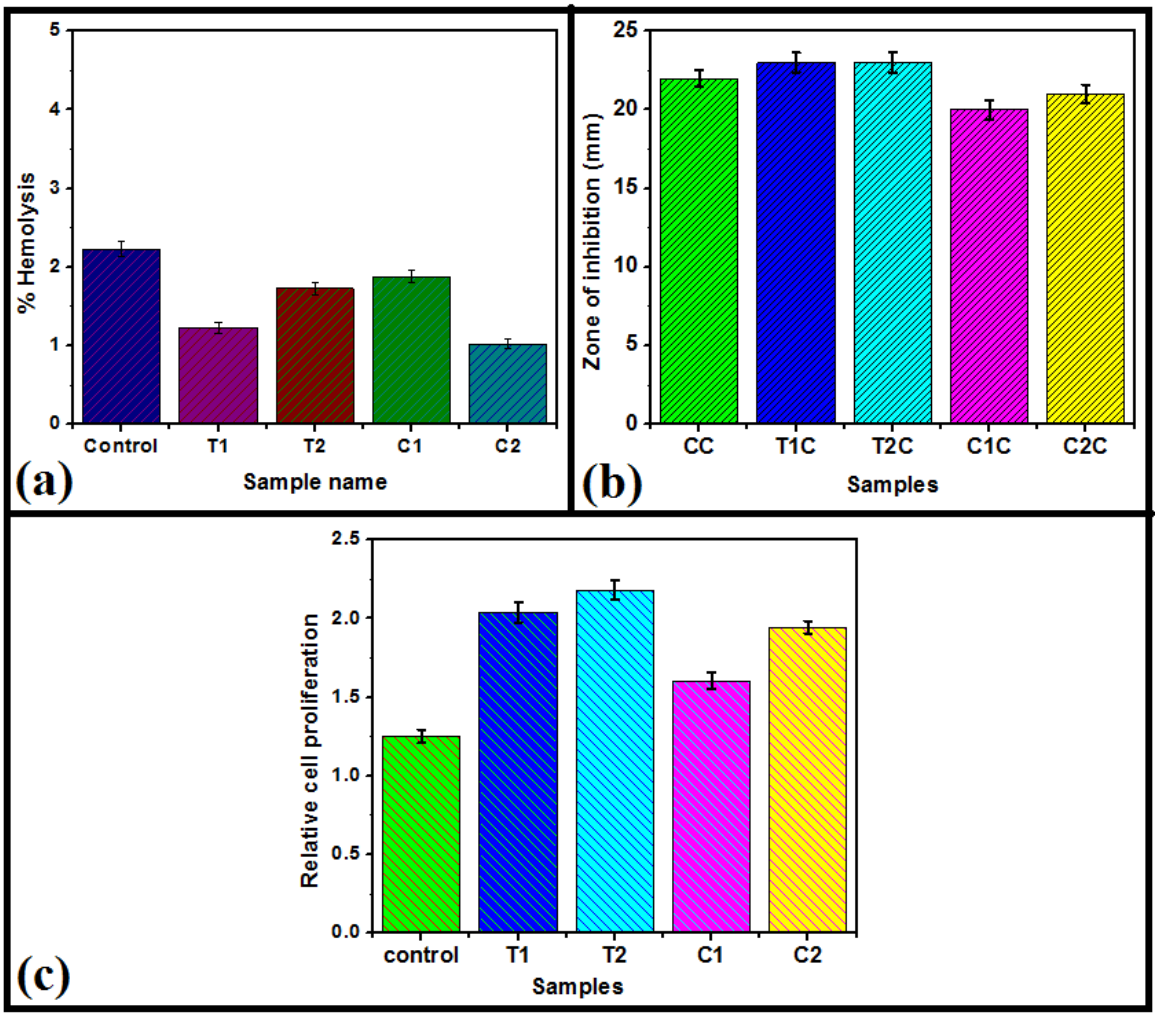

Figure 4.9: Biological characterizations of the films. (a) Hemocompatibility, (b) Antimicrobial study, and (c) Cell proliferation study using osteoblast cells

The study of the hemocompatibility of the wound dressing materials is an important study as the materials are expected to be in contact with the blood cells at wound-site [156]. In this study, the films were incubated in the presence of the goat blood cells and the degree of disruption of the RBCs was determined. All the prepared films showed a hemolysis

percentage of < 5% (Figure 4.9a). This suggested the hemocompatible nature of the films. The introduction of the polysaccharides into the films resulted in the improved hemocompatibility than the gelatin films (C).

The ability of the drug loaded films to inhibit the growth of the microorganisms (*E .coli*) was studied. The results suggested that the antimicrobial activity of T1C and T2C was slightly higher as compared to the gelatin films (Figure 4.9b). The antimicrobial activity of C1C and C2C was almost same. The result suggested that all the films had sufficient antimicrobial property to be used as matrices for control delivery of antimicrobial drugs.

In this present study MTT assay was performed for the HaCaT cells grown on the tamarind and carboxy methyl tamarind gum based films. Pure gelatin was used as the control. Relative proliferation rate of the cells for all the samples were found with respect to TCP (cells grown on normal tissue culture plate). T2 showed the highest proliferation rate of followed by C2, T1 and C1 respectively (Figure 4.9c). Therefore from this experiment, it is evident that all the films support the growth of human keratinocytes cells.

4.3.8 Swelling

The swelling of the films was studied at pH 7.4 (Figure 4 .10). The swelling of the gelatin film was lower than the polysaccharide containing films. An increase in the polysaccharide content resulted in the increase in the swelling proportion. Unlike TG containing films, CMT containing films showed relatively higher swelling at neutral pHs (pH 7.4). This observation can be explained by the anionic nature of CMT, which undergo ionization at neutral and basic pHs. The ionization of the carboxylic groups present in CMT promotes absorption of the water in higher capacity. A pre-examination of the swelling profile indicated that there was a rapid increase in the absorption of the water molecules at the initial stages, which attained a plateau phase at later stages.

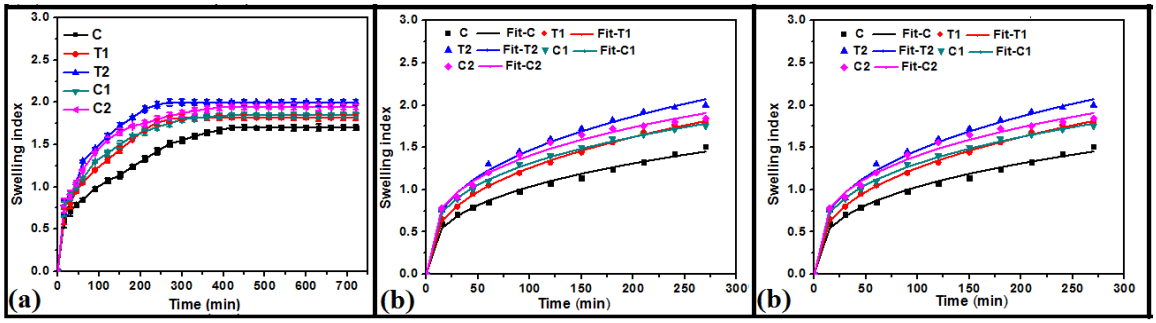

Figure 4.10: Swelling study of the films. (a) Swelling profiles of the films, (b) Weibull model fitting, and (c) Korsmeyer-Peppas model fitting

To have a depth analysis of the swelling kinetics of the films, the experimental data was fitted to Weibull model (Equation 4.6) and Korsmeyer-Peppas (KP) model (Equation 4.7). Weibulll model is a general model which helps in the analysis of the nature of the profiles [157]. Scale (a) and shape (b) parameters of the swelling profiles were calculated from the Weibull model (Table 4.6). The scale parameters indicate the positioning of the attainment of the peak on a time scale. A higher scale parameter suggests a delayed process. From the results, it was observed that the swelling was faster in the films with higher amount of polysaccharides. The scale value of the gelatin film was highest (C) which showed that the swelling was slowest in gelatin films. For both TG and CMT films, the swelling was faster in higher polysaccharide content formulations (T2 and C2). Amongst the polysaccharides containing films, an increase in the polysaccharide content resulted in the increase in the diffusion coefficient (k values from KP model) of the water molecules within the films. This, in turn, resulted in the faster absorption of the water molecules within the film matrices. The shape parameter (b) calculated from the Weibull model indicated a parabolic nature of the profiles. Diffusion exponent (n) value was calculated from the Korsmeyer-Peppas model. The n-value gives an indication about the nature of the diffusion of the water molecules within the matrices. At pH 7.4, the n-value suggested that the diffusion of the water molecules in all the films except gelatin film (C) was governed by anomalous diffusion (n value in the range of 0.45 to 0.89). This suggested that the absorption of the water by films was due to the simultaneous occurrence of diffusion of water molecules and relaxation of the polymeric chains during the swelling process. The n value for C was lower than 0.45, this suggested the swelling process was predominantly Fickian diffusion mediated.

$$m = 1 - exp\left[-\left(\frac{t - T}{a}\right)^{b}\right] \tag{4.6}$$

where, m= fraction of water absorbed, t= time (sec), T= delay time (sec), a= time-scale parameter, and b= shape parameter.

$$m = K \times t^{n} \tag{4.7}$$

where, k= rate constant, n= diffusion exponent.

Table 4.5: Swelling parameters of the films

Model	Model parameters	Formulations				
		C	**T1**	**T2**	**C1**	**C2**
Weibull	a	114.29±2.32	95.32±1.20	80.73±1.11	88.77±1.30	82.80±1.20
	b	0.34±0.002	0.36±0.003	0.34±0.001	0.31±0.002	0.30±0.003
	R^2	0.99	0.97	0.98	0.98	0.97
Korsmeyer- Peppas	K	0.88±0.01	0.44±0.01	0.50±0.01	0.45±0.01	0.48±0.01
	n	0.32±0.001	0.55±0.01	0.49±0.01	0.48±0.01	0.45±0.01
	R^2	0.99	0.98	0.97	0.98	0.98

4.3.9 Drug release

The release of the drug from the films was studied at 7.4 (Figure 4.11). The result showed that the higher polysaccharide content films showed higher release of drugs. Gelatin film (C) has lowest release of drugs as compared to TG and CMT films. At pH 7.4, C2 showed highest release of drugs as compared to all the samples.

The release profiles were modelled by using Weibull model (Equation 4.8), Korsmeyer-Peppas (Equation 4.9) and Peppas–Sahlin (Equation 4.10) models. The scale factor of the gelatin film (C) was highest at pH 7.4 (Table 4.6). This suggested that the release of drug from the gelatin film was slowest. But in the other films, there was a faster drug release with increase of the polysaccharide contents in the films. Amongst the polysaccharides containing films, the scale factors of CMT films were lower as compared to TG films suggesting that the release of drug was faster in CMT films at pH 7.4. The diffusion rate of the drugs within the matrix (calculated from the Korsmeyer-Peppas model) supported the predictions made from the Weibull model where higher polysaccharide content films had higher coefficient values. The exponent values (n) > 0.5. This suggested the diffusion of drug was by anomalous diffusion. In general, the rate of drug diffusion, calculated from the Korsmeyer-Peppas model, is due to the combination of various factors, e.g. Fickian diffusion, polymer chain relaxation and degradation of the matrix. From the swelling studies, it was found that there was no degradation of the films. Hence, there was a probability that the relaxation of the polymer chains might have influenced the release behavior. To predict the contribution of the polymer chain relaxation in the release profile, Pappas- Sahlin model was used [123]. In this model, the constant K_1 is associated with the Fickian diffusion, whereas, the constant K_2 is associated with the diffusion due to the polymer relaxation. The constant K_1 and K (from Korsmeyer-Peppas model) were of the similar trend. The K_2 values of all the films were found to be 0. This suggested the absence of polymer relaxation during the drug release.

$$CPDR = 1 - exp\left[-\left(\frac{t - T}{a}\right)^{b}\right] \tag{4.8}$$

where, CPDR= Cumulative percent drug release, t = time (sec), T= delay time (sec), a = time-scale parameter, and b = shape parameter.

$$CPDR = k \times t^{n} \tag{4.9}$$

where, k= release rate constant, n= release constant, t= time (sec).

$$CPDR = k_1 \times t^m + k_2 \times t^{2m} \tag{4.10}$$

where, K_1= constant (associated with Fickian diffusion), K_2= constant (associated with diffusion due to polymer relaxation), m = release constant.

$$\frac{R}{F} = \frac{k_2}{k_1} \times t^m \tag{4.11}$$

where, K_1 and K_2 are rate constants, m is the release constant.

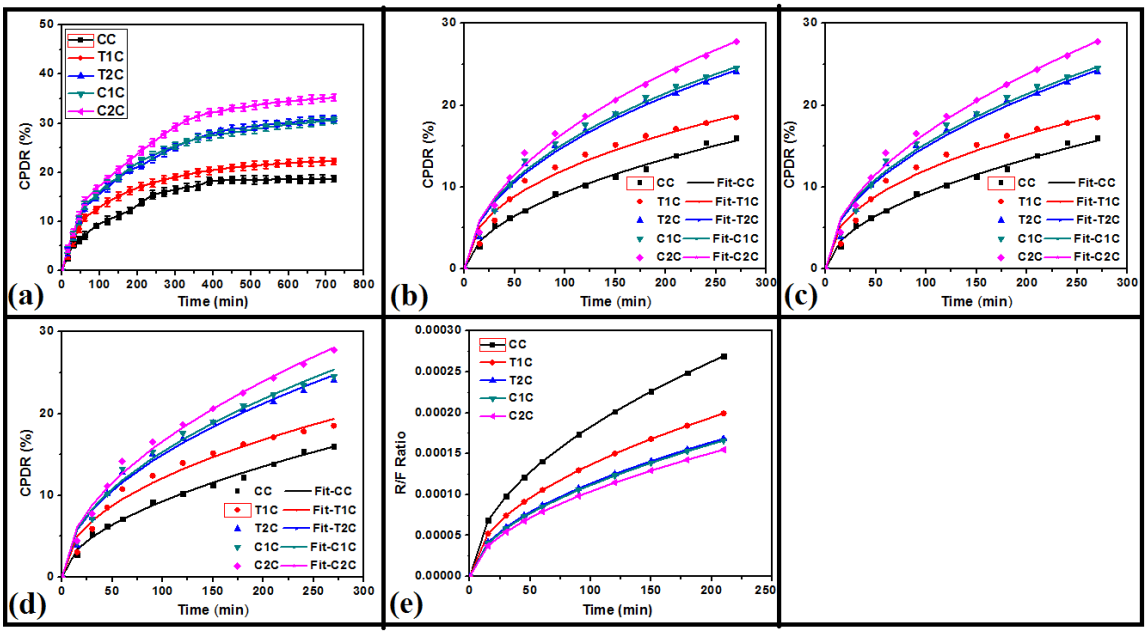

Figure 4.11: Drug release study of the films at pH 7.4. (a) Drug release profiles of TG and CMT films, (b) Weibull model fitting for films, (c) Korsmeyer-Peppas model fitting for films, (d) Peppas-Sahlin model fitting for films, and (e) R/F ratio from Peppas-Sahlin model

Table 4.6: Drug release parameters of the films

Model	Parameters	Formulations				
		C	T1	T2	C1	C2
Weibull	a	13.49±0.15	9.84±0.14	8.06±0.13	7.83±0.12	7.33±0.11
	b	0.55±0.01	0.47±0.01	0.53±0.02	0.53±0.01	0.57±0.02
	R^2	0.97	0.97	0.98	0.98	0.99
Korsmeyer- Peppas	K	7.14±0.12	9.65±0.13	11.66±1.21	11.98±0.20	12.74±0.18
	n	0.52±0.01	0.45±0.01	0.48±0.01	0.48±0.01	0.51±0.01
	R^2	0.97	0.98	0.98	0.97	0.99
Peppas- Sahlin	K_1	6.83±0.15	9.54±0.18	11.586±0.10	11.85±0.11	12.70±0.16
	K_2	0.03	0.00	0.00	0.00	0.00
	m	0.51±0.0	0.46±0.01	0.50±0.01	0.50±0.02	0.52±0.01
	R^2	0.99	0.98	0.99	0.99	0.99

4.4 Conclusion

The current chapter discusses about the development of the gelatin-tamarind gum (TG)/carboxymethyl tamarind gum (CMT) based phase separated films for skin tissue engineering and drug delivery applications. The agglomeration of the polysaccharide phase was higher in the TG containing films as compared to the CMT films. This can be explored by the derivatization of TG molecules with carboxymethyl group which increased the hydrophilicity of the CMT molecules. The FTIR studies suggested that when the polysaccharide was in corporate in higher proportions, the helical structure of the gelatin molecules might have been altered significantly. The thermal profiles of the films suggested that the incorporation of the polysaccharides in the films increased the water containing capacity of the films. The extent of water holding capacity was higher in CMT containing films as compared to the TG films at similar composition. The mechanical properties indicated better mechanical properties of the TG containing films which was attributed to the filler effect exerted by the TG molecules. The stress relaxation studies suggested that CMT containing films showed better relaxation properties as compared to TG containing films. All the films were found to be hemocompatible when tested with goat blood. The drug loaded films (Ciprofloxacin) showed good antimicrobial properties against E. coli. The ability of the films to support HaCaT (human keratinocytes) was examined. Incorporation of polysaccharides within the gelatin films improved the proliferation of the HaCaT cells. Amongst the polysaccharide containing films an increase in the polysaccharide content improved the cell proliferation. Amongst TG and CMT based films, TG films showed better cell viability. The result suggested that the TG and CMT containing films may be tried as matrices for skin tissue engineering. The swelling profiles of the films showed a slight pH dependent behavior. Drug release profiles indicated a pH dependent release profile. From the above result it can be concluded that the development has sufficient properties for exploration as matrices for skin tissue engineering and controlled drug delivery applications.

Chapter 5

Summary

The current research work was focused on the fabrication and characterization of gelatin-tamarind gum (TG)/carboxymethyl tamarind gum based phase-separated architectures for tissue engineering applications. The microscopic analysis of the hydrogels clearly indicated the formation of phase-separated systems by forming both gelatin rich phase and polysaccharide rich phase in a distinct manner. The FTIR spectroscopy of the hydrogels showed an alteration in the secondary structure of the gelatin molecules due to the addition of the carboxymethyl tamarind gum in to the formulations. The swelling and drug release were pH dependent for all the hydrogels. The hydrogels were hemocompatible in nature and had good mucoadhesive property. The *in vitro* cell culture of the hydrogels suggested a better proliferation of osteoblast cells (MG 63) on polysaccharide content formulations. So the hydrogels can be used as non-load bearing substitutes in bone tissue engineering. The films were prepared by conventional solution casting method. Polyethylene glycol was used as the plasticizer to induce a better elasticity in the films. The microscopy showed the formation of phase separated systems. Tamarind gum based films showed the presence of agglomerated gum particles due the hydrophobic nature of the tamarind gum. FTIR spectroscopy suggested the presence of both gelatin and polysaccharides within the films. The water holding capacity and mechanical properties were better in the polysaccharide containing films as was indicated by the thermal and mechanical studies, respectively. Impedance analysis suggested the better dielectric properties of the TG films as compared to the CMT films. The films were hemocompatible in nature and supported the proliferation of human keratinocytes. The drug containing films showed good antimicrobial properties against *E. coli*. The films showed pH dependent swelling and drug release profiles. The analysis of the afore-mentioned results indicated that the pre prepared films may be tried as matrices for skin

tissue engineering and drug release applications. So, the above developed polymeric architectures are can be used for tissue engineering applications.

Future aspects

The toxicity profiles of the prepared polymeric architectures need to be assessed using suitable mammalian models. The prepared polymeric structures need to be assessed for tissue engineering applications in suitable animal models. The *in vivo* studies are further required to analyze the biocompatibility of the developed biomaterials. To have some better understanding about the drug release profiles, different drugs are needed. After all, it's not the end of this research. It's a long path to cover.

Bibliography

[1] G. Rigotti, A. Marchi, M. Galie, G. Baroni, D. Benati, M. Krampera, A. Pasini, and A. Sbarbati, "Clinical treatment of radiotherapy tissue damage by lipoaspirate transplant: a healing process mediated by adipose-derived adult stem cells," *Plastic and reconstructive surgery*, vol. 119, pp. 1409-1422, 2007.

[2] L. G. Griffith and G. Naughton, "Tissue engineering--current challenges and expanding opportunities," *Science*, vol. 295, pp. 1009-1014, 2002.

[3] D. F. Stamatialis, B. J. Papenburg, M. Gironés, S. Saiful, S. N. Bettahalli, S. Schmitmeier, and M. Wessling, "Medical applications of membranes: drug delivery, artificial organs and tissue engineering," *Journal of Membrane Science*, vol. 308, pp. 1-34, 2008.

[4] J. W. Nichol and A. Khademhosseini, "Modular tissue engineering: engineering biological tissues from the bottom up," *Soft matter*, vol. 5, pp. 1312-1319, 2009.

[5] H. F. Tibbals, *Medical nanotechnology and nanomedicine*: CRC Press, 2010.

[6] J. Bergsma, F. Rozema, R. Bos, G. Boering, W. De Bruijn, and A. Pennings, "In vivo degradation and biocompatibility study of in vitro pre-degraded as-polymerized polylactide particles," *Biomaterials*, vol. 16, pp. 267-274, 1995.

[7] B.-S. Kim and D. J. Mooney, "Development of biocompatible synthetic extracellular matrices for tissue engineering," *Trends in biotechnology*, vol. 16, pp. 224-230, 1998.

[8] C. Liu, Z. Xia, and J. Czernuszka, "Design and development of three-dimensional scaffolds for tissue engineering," *Chemical Engineering Research and Design*, vol. 85, pp. 1051-1064, 2007.

[9] H. Shin, S. Jo, and A. G. Mikos, "Biomimetic materials for tissue engineering," *Biomaterials*, vol. 24, pp. 4353-4364, 2003.

[10] E. Brynda, J. Pacherník, M. Houska, Z. Pientka, and P. Dvorák, "Surface immobilized protein multilayers for cell seeding," *Langmuir*, vol. 21, pp. 7877-7883, 2005.

[11] Y. Onuma and P. W. Serruys, "Bioresorbable scaffold the advent of a new era in percutaneous coronary and peripheral revascularization?," *Circulation*, vol. 123, pp. 779-797, 2011.

[12] S. J. Hollister, "Porous scaffold design for tissue engineering," *Nature materials*, vol. 4, pp. 518-524, 2005.

[13] K. Leong, C. Cheah, and C. Chua, "Solid freeform fabrication of three-dimensional scaffolds for engineering replacement tissues and organs," *Biomaterials*, vol. 24, pp. 2363-2378, 2003.

[14] F. Oberpenning, J. Meng, J. J. Yoo, and A. Atala, "De novo reconstitution of a functional mammalian urinary bladder by tissue engineering," *Nature biotechnology*, vol. 17, pp. 149-155, 1999.

[15] T. Shin'oka, Y. Imai, and Y. Ikada, "Transplantation of a tissue-engineered pulmonary artery," *New England Journal of Medicine*, vol. 344, pp. 532-533, 2001.

[16] S. Zhang, "Fabrication of novel biomaterials through molecular self-assembly," *Nature biotechnology*, vol. 21, pp. 1171-1178, 2003.

[17] D. W. Hutmacher, "Scaffold design and fabrication technologies for engineering tissues—state of the art and future perspectives," *Journal of Biomaterials Science, Polymer Edition*, vol. 12, pp. 107-124, 2001.

[18] S. I. Stupp and P. V. Braun, "Molecular manipulation of microstructures: biomaterials, ceramics, and semiconductors," *Science*, vol. 277, pp. 1242-1248, 1997.

[19] C. Agrawal and R. B. Ray, "Biodegradable polymeric scaffolds for musculoskeletal tissue engineering," *Journal of biomedical materials research*, vol. 55, pp. 141-150, 2001.

[20] B. K. Mann, A. S. Gobin, A. T. Tsai, R. H. Schmedlen, and J. L. West, "Smooth muscle cell growth in photopolymerized hydrogels with cell adhesive and proteolytically degradable domains: synthetic ECM analogs for tissue engineering," *Biomaterials*, vol. 22, pp. 3045-3051, 2001.

[21] S. Yang, K.-F. Leong, Z. Du, and C.-K. Chua, "The design of scaffolds for use in tissue engineering. Part I. Traditional factors," *Tissue engineering*, vol. 7, pp. 679-689, 2001.

[22] D. W. Hutmacher, J. T. Schantz, C. X. F. Lam, K. C. Tan, and T. C. Lim, "State of the art and future directions of scaffold-based bone engineering from a biomaterials perspective," *Journal of tissue engineering and regenerative medicine*, vol. 1, pp. 245-260, 2007.
[23] S. H. Cartmell, B. D. Porter, A. J. García, and R. E. Guldberg, "Effects of medium perfusion rate on cell-seeded three-dimensional bone constructs in vitro," *Tissue engineering*, vol. 9, pp. 1197-1203, 2003.
[24] J. B. Park and J. D. Bronzino, *Biomaterials: principles and applications*: crc press, 2002.
[25] A. R. Shrivats, M. C. McDermott, and J. O. Hollinger, "Bone tissue engineering: state of the union," *Drug discovery today*, vol. 19, pp. 781-786, 2014.
[26] J. C. Middleton and A. J. Tipton, "Synthetic biodegradable polymers as orthopedic devices," *Biomaterials*, vol. 21, pp. 2335-2346, 2000.
[27] L. Yu, K. Dean, and L. Li, "Polymer blends and composites from renewable resources," *Progress in Polymer Science*, vol. 31, pp. 576-602, 2006.
[28] D. L. Kaplan, *Introduction to biopolymers from renewable resources*: Springer, 1998.
[29] S. Huang and X. Fu, "Naturally derived materials-based cell and drug delivery systems in skin regeneration," *Journal of Controlled Release*, vol. 142, pp. 149-159, 2010.
[30] R. A. Gross and B. Kalra, "Biodegradable polymers for the environment," *Science*, vol. 297, pp. 803-807, 2002.
[31] A. S. Hoffman, "Hydrogels for biomedical applications," *Advanced drug delivery reviews*, vol. 64, pp. 18-23, 2012.
[32] W. Hennink and C. F. Van Nostrum, "Novel crosslinking methods to design hydrogels," *Advanced drug delivery reviews*, vol. 64, pp. 223-236, 2012.
[33] Q. Wang, J. L. Mynar, M. Yoshida, E. Lee, M. Lee, K. Okuro, K. Kinbara, and T. Aida, "High-water-content mouldable hydrogels by mixing clay and a dendritic molecular binder," *Nature*, vol. 463, pp. 339-343, 2010.
[34] Y. Qiu and K. Park, "Environment-sensitive hydrogels for drug delivery," *Advanced drug delivery reviews*, vol. 64, pp. 49-60, 2012.
[35] V. K. Singh, S. S. Sagiri, K. Pal, S. M. Khade, D. K. Pradhan, and M. K. Bhattacharya, "Gelatin-carbohydrate phase-separated hydrogels as bioactive carriers in vaginal delivery: preparation and physical characterizations," *Journal of Applied Polymer Science*, vol. 131, 2014.
[36] E. Dickinson, "Hydrocolloids at interfaces and the influence on the properties of dispersed systems," *Food Hydrocolloids*, vol. 17, pp. 25-39, 2003.
[37] R. G. Weiss and P. Terech, "Molecular gels," *Materials with Self-Assembled Fibrillar Networks*, 2006.
[38] A. S. Hoffman, "The origins and evolution of "controlled" drug delivery systems," *Journal of controlled release*, vol. 132, pp. 153-163, 2008.
[39] S. Sanyasi, A. Kumar, C. Goswami, A. Bandyopadhyay, and L. Goswami, "A carboxy methyl tamarind polysaccharide matrix for adhesion and growth of osteoclast-precursor cells," *Carbohydrate Polymers*, vol. 101, pp. 1033-1042, 2014.
[40] L. L. Hench and J. M. Polak, "Third-generation biomedical materials," *Science*, vol. 295, pp. 1014-1017, 2002.
[41] K. Jayathilakan, K. Sultana, K. Radhakrishna, and A. Bawa, "Utilization of byproducts and waste materials from meat, poultry and fish processing industries: a review," *Journal of food science and technology*, vol. 49, pp. 278-293, 2012.
[42] W. Zhao, X. Jin, Y. Cong, Y. Liu, and J. Fu, "Degradable natural polymer hydrogels for articular cartilage tissue engineering," *Journal of Chemical Technology and Biotechnology*, vol. 88, pp. 327-339, 2013.
[43] T. Thitiset, S. Damrongsakkul, T. Bunaprasert, W. Leeanansaksiri, and S. Honsawek, "Development of collagen/demineralized bone powder scaffolds and periosteum-derived cells for bone tissue engineering application," *International journal of molecular sciences*, vol. 14, pp. 2056-2071, 2013.
[44] A. J. Lomas, W. R. Webb, J. Han, G.-Q. Chen, X. Sun, Z. Zhang, A. J. El Haj, and N. R. Forsyth, "Poly (3-hydroxybutyrate-co-3-hydroxyhexanoate)/collagen hybrid scaffolds for tissue engineering applications," *Tissue Engineering Part C: Methods*, vol. 19, pp. 577-585, 2013.
[45] S. Ahn, H. Yoon, G. Kim, Y. Kim, S. Lee, and W. Chun, "Designed three-dimensional collagen scaffolds for skin tissue regeneration," *Tissue Engineering Part C: Methods*, vol. 16, pp. 813-820, 2009.

[46] L. H. Han, S. Yu, T. Wang, A. W. Behn, and F. Yang, "Microribbon-Like Elastomers for Fabricating Macroporous and Highly Flexible Scaffolds that Support Cell Proliferation in 3D," *Advanced Functional Materials,* vol. 23, pp. 346-358, 2013.
[47] H. Cao, M.-M. Chen, Y. Liu, Y.-Y. Liu, Y.-Q. Huang, J.-H. Wang, J.-D. Chen, and Q.-Q. Zhang, "Fish collagen-based scaffold containing PLGA microspheres for controlled growth factor delivery in skin tissue engineering," *Colloids and Surfaces B: Biointerfaces,* vol. 136, pp. 1098-1106, 2015.
[48] D. J. Richards, Y. Tan, J. Jia, H. Yao, and Y. Mei, "3D printing for tissue engineering," *Israel Journal of Chemistry,* vol. 53, pp. 805-814, 2013.
[49] Y. Yan, X. Wang, Y. Pan, H. Liu, J. Cheng, Z. Xiong, F. Lin, R. Wu, R. Zhang, and Q. Lu, "Fabrication of viable tissue-engineered constructs with 3D cell-assembly technique," *Biomaterials,* vol. 26, pp. 5864-5871, 2005.
[50] T. Billiet, E. Gevaert, T. De Schryver, M. Cornelissen, and P. Dubruel, "The 3D printing of gelatin methacrylamide cell-laden tissue-engineered constructs with high cell viability," *Biomaterials,* vol. 35, pp. 49-62, 2014.
[51] M. Yazdimamaghani, D. Vashaee, S. Assefa, K. Walker, S. Madihally, G. Köhler, and L. Tayebi, "Hybrid macroporous gelatin/bioactive-glass/nanosilver scaffolds with controlled degradation behavior and antimicrobial activity for bone tissue engineering," *Journal of biomedical nanotechnology,* vol. 10, pp. 911-931, 2014.
[52] D. Nadeem, C.-A. Smith, M. J. Dalby, R. D. Meek, S. Lin, G. Li, and B. Su, "Three-dimensional CaP/gelatin lattice scaffolds with integrated osteoinductive surface topographies for bone tissue engineering," *Biofabrication,* vol. 7, p. 015005, 2015.
[53] R. Parenteau-Bareil, R. Gauvin, and F. Berthod, "Collagen-based biomaterials for tissue engineering applications," *Materials,* vol. 3, pp. 1863-1887, 2010.
[54] J. Zhu and R. E. Marchant, "Design properties of hydrogel tissue-engineering scaffolds," *Expert review of medical devices,* vol. 8, pp. 607-626, 2011.
[55] T. Chen, H. D. Embree, E. M. Brown, M. M. Taylor, and G. F. Payne, "Enzyme-catalyzed gel formation of gelatin and chitosan: potential for in situ applications," *Biomaterials,* vol. 24, pp. 2831-2841, 2003.
[56] H. Tan and K. G. Marra, "Injectable, biodegradable hydrogels for tissue engineering applications," *Materials,* vol. 3, pp. 1746-1767, 2010.
[57] G. Kogan, L. Šoltés, R. Stern, and P. Gemeiner, "Hyaluronic acid: a natural biopolymer with a broad range of biomedical and industrial applications," *Biotechnology letters,* vol. 29, pp. 17-25, 2007.
[58] J. Necas, L. Bartosikova, P. Brauner, and J. Kolar, "Hyaluronic acid (hyaluronan): a review," *Veterinarni medicina,* vol. 53, pp. 397-411, 2008.
[59] A. Fakhari and C. Berkland, "Applications and emerging trends of hyaluronic acid in tissue engineering, as a dermal filler and in osteoarthritis treatment," *Acta biomaterialia,* vol. 9, pp. 7081-7092, 2013.
[60] M. N. Collins and C. Birkinshaw, "Hyaluronic acid based scaffolds for tissue engineering—A review," *Carbohydrate Polymers,* vol. 92, pp. 1262-1279, 2013.
[61] S. D. Nath, C. Abueva, B. Kim, and B. T. Lee, "Chitosan–hyaluronic acid polyelectrolyte complex scaffold crosslinked with genipin for immobilization and controlled release of BMP-2," *Carbohydrate Polymers,* vol. 115, pp. 160-169, 2015.
[62] N. B. Skop, F. Calderon, C. H. Cho, C. D. Gandhi, and S. W. Levison, "Improvements in biomaterial matrices for neural precursor cell transplantation," *Molecular and cellular therapies,* vol. 2, p. 1, 2014.
[63] D. Park, Y. Kim, H. Kim, K. Kim, Y.-S. Lee, J. Choe, J.-H. Hahn, H. Lee, J. Jeon, and C. Choi, "Hyaluronic acid promotes angiogenesis by inducing RHAMM-TGFβ receptor interaction via CD44-PKCδ," *Molecules and cells,* vol. 33, pp. 563-574, 2012.
[64] Y. Liu, L. Ren, and Y. Wang, "Crosslinked collagen–gelatin–hyaluronic acid biomimetic film for cornea tissue engineering applications," *Materials Science and Engineering: C,* vol. 33, pp. 196-201, 2013.
[65] F. D. Ivan, A. Marian, C. E. Tanase, M. Butnaru, and L. Vereştiuc, "Biomimetic composites based on calcium phosphates and chitosan-hyaluronic acid with potential application in bone tissue engineering," in *Key Engineering Materials,* 2014, pp. 191-196.
[66] L. B. Sandberg, N. T. Soskel, and J. G. Leslie, "Elastin structure, biosynthesis, and relation to disease states," *New England Journal of Medicine,* vol. 304, pp. 566-579, 1981.

[67] J. Rnjak-Kovacina and A. S. Weiss, "The role of elastin in wound healing and dermal substitute design," in *Dermal Replacements in General, Burn, and Plastic Surgery*, ed: Springer, 2013, pp. 57-66.

[68] A. Girotti, D. Orbanic, A. Ibáñez-Fonseca, C. Gonzalez-Obeso, and J. C. Rodríguez-Cabello, "Recombinant Technology in the Development of Materials and Systems for Soft-Tissue Repair," *Advanced healthcare materials*, vol. 4, pp. 2423-2455, 2015.

[69] C. N. Grover, R. E. Cameron, and S. M. Best, "Investigating the morphological, mechanical and degradation properties of scaffolds comprising collagen, gelatin and elastin for use in soft tissue engineering," *Journal of the mechanical behavior of biomedical materials*, vol. 10, pp. 62-74, 2012.

[70] R. Machado, P. C. Bessa, R. L. Reis, J. C. Rodriguez-Cabello, and M. Casal, "Elastin-based nanoparticles for delivery of bone morphogenetic proteins," *Nanoparticles in Biology and Medicine: Methods and Protocols*, pp. 353-363, 2012.

[71] S. E. Dunphy, J. A. Bratt, K. M. Akram, N. R. Forsyth, and A. J. El Haj, "Hydrogels for lung tissue engineering: Biomechanical properties of thin collagen–elastin constructs," *Journal of the mechanical behavior of biomedical materials*, vol. 38, pp. 251-259, 2014.

[72] J. M. Silva, N. Georgi, R. Costa, P. Sher, R. L. Reis, C. A. Van Blitterswijk, M. Karperien, and J. F. Mano, "Nanostructured 3D constructs based on chitosan and chondroitin sulphate multilayers for cartilage tissue engineering," *PloS one*, vol. 8, p. e55451, 2013.

[73] P. A. Levett, F. P. Melchels, K. Schrobback, D. W. Hutmacher, J. Malda, and T. J. Klein, "A biomimetic extracellular matrix for cartilage tissue engineering centered on photocurable gelatin, hyaluronic acid and chondroitin sulfate," *Acta biomaterialia*, vol. 10, pp. 214-223, 2014.

[74] J. Venkatesan, R. Pallela, I. Bhatnagar, and S.-K. Kim, "Chitosan–amylopectin/hydroxyapatite and chitosan–chondroitin sulphate/hydroxyapatite composite scaffolds for bone tissue engineering," *International journal of biological macromolecules*, vol. 51, pp. 1033-1042, 2012.

[75] S. Deepthi, C. Viha, C. Thitirat, T. Furuike, H. Tamura, and R. Jayakumar, "Fabrication of chitin/poly (butylene succinate)/chondroitin sulfate nanoparticles ternary composite hydrogel scaffold for skin tissue engineering," *Polymers*, vol. 6, pp. 2974-2984, 2014.

[76] S. Yan, Q. Zhang, J. Wang, Y. Liu, S. Lu, M. Li, and D. L. Kaplan, "Silk fibroin/chondroitin sulfate/hyaluronic acid ternary scaffolds for dermal tissue reconstruction," *Acta biomaterialia*, vol. 9, pp. 6771-6782, 2013.

[77] S. S. Martin, M. Alaminos, T. Zorn, M. Sánchez-Quevedo, I. Garzon, I. Rodriguez, and A. Campos, "The effects of fibrin and fibrin-agarose on the extracellular matrix profile of bioengineered oral mucosa," *Journal of tissue engineering and regenerative medicine*, vol. 7, pp. 10-19, 2013.

[78] P. de la Puente and D. Ludeña, "Cell culture in autologous fibrin scaffolds for applications in tissue engineering," *Experimental cell research*, vol. 322, pp. 1-11, 2014.

[79] S. P. Miguel, M. P. Ribeiro, H. Brancal, P. Coutinho, and I. J. Correia, "Thermoresponsive chitosan–agarose hydrogel for skin regeneration," *Carbohydrate Polymers*, vol. 111, pp. 366-373, 2014.

[80] S. Bhat and A. Kumar, "Cell proliferation on three-dimensional chitosan–agarose–gelatin cryogel scaffolds for tissue engineering applications," *Journal of bioscience and bioengineering*, vol. 114, pp. 663-670, 2012.

[81] S. Jebahi, G. B. Saleh, M. Saoudi, S. Besaleh, H. Oudadesse, M. Mhadbi, T. Rebai, H. Keskes, and A. El Feki, "Genotoxicity effect, antioxidant and biomechanical correlation: experimental study of agarose–chitosan bone graft substitute in New Zealand white rabbit model," *Proceedings of the Institution of Mechanical Engineers, Part H: Journal of Engineering in Medicine*, vol. 228, pp. 800-809, 2014.

[82] J. Venkatesan, R. Jayakumar, S. Anil, E. P. Chalisserry, R. Pallela, and S.-K. Kim, "Development of Alginate-Chitosan-Collagen Based Hydrogels for Tissue Engineering," *Journal of Biomaterials and Tissue Engineering*, vol. 5, pp. 458-464, 2015.

[83] S. Kirdponpattara, A. Khamkeaw, N. Sanchavanakit, P. Pavasant, and M. Phisalaphong, "Structural modification and characterization of bacterial cellulose–alginate composite scaffolds for tissue engineering," *Carbohydrate Polymers*, vol. 132, pp. 146-155, 2015.

[84] M. Castilho, J. Rodrigues, I. Pires, B. Gouveia, M. Pereira, C. Moseke, J. Groll, A. Ewald, and E. Vorndran, "Fabrication of individual alginate-TCP scaffolds for bone tissue engineering by means of powder printing," *Biofabrication*, vol. 7, p. 015004, 2015.

[85] J. Sowjanya, J. Singh, T. Mohita, S. Sarvanan, A. Moorthi, N. Srinivasan, and N. Selvamurugan, "Biocomposite scaffolds containing chitosan/alginate/nano-silica for bone tissue engineering," *Colloids and Surfaces B: Biointerfaces,* vol. 109, pp. 294-300, 2013.

[86] F. Croisier and C. Jérôme, "Chitosan-based biomaterials for tissue engineering," *European Polymer Journal,* vol. 49, pp. 780-792, 2013.

[87] F. Han, Y. Dong, Z. Su, R. Yin, A. Song, and S. Li, "Preparation, characteristics and assessment of a novel gelatin–chitosan sponge scaffold as skin tissue engineering material," *International journal of pharmaceutics,* vol. 476, pp. 124-133, 2014.

[88] M. M. Rahman, S. Pervez, B. Nesa, and M. A. Khan, "Preparation and characterization of porous scaffold composite films by blending chitosan and gelatin solutions for skin tissue engineering," *Polymer International,* vol. 62, pp. 79-86, 2013.

[89] M. E. Frohbergh, A. Katsman, G. P. Botta, P. Lazarovici, C. L. Schauer, U. G. Wegst, and P. I. Lelkes, "Electrospun hydroxyapatite-containing chitosan nanofibers crosslinked with genipin for bone tissue engineering," *Biomaterials,* vol. 33, pp. 9167-9178, 2012.

[90] T. Gerard, "Tamarind Gum in Hand book of water soluble gums and resins," *USA: McGraw-Hill Book Co,* vol. 12, pp. 1-23, 1980.

[91] H. Mirhosseini and B. T. Amid, "A review study on chemical composition and molecular structure of newly plant gum exudates and seed gums," *Food Research International,* vol. 46, pp. 387-398, 2012.

[92] G. Phani Kumar, G. Battu, and L. R. N. Kota, "Preparation and evaluation of sustained release matrix tablets of lornoxicam using tamarind seed polysaccharide," *Int J pharm Res & Dev,* vol. 2, pp. 90-98, 2011.

[93] A. K. Nayak, D. Pal, and K. Santra, "Tamarind seed polysaccharide–gellan mucoadhesive beads for controlled release of metformin HCl," *Carbohydrate Polymers,* vol. 103, pp. 154-163, 2014.

[94] M. Sharma, D. Mondal, C. Mukesh, and K. Prasad, "Preparation of tamarind gum based soft ion gels having thixotropic properties," *Carbohydrate polymers,* vol. 102, pp. 467-471, 2014.

[95] S. Sahoo, R. Sahoo, and P. L. Nayak, "Tamarind Seed Polysachharide: A Versatile Biopolymer For Mucoadhesive Applications," *J. Pharm. Biomed. Sci,* vol. 8, pp. 1-12, 2011.

[96] P. Goyal, V. Kumar, and P. Sharma, "Carboxymethylation of tamarind kernel powder," *Carbohydrate polymers,* vol. 69, pp. 251-255, 2007.

[97] R. Manchanda, S. Arora, and R. Manchanda, "Tamarind seed polysaccharide and its modification-versatile pharmaceutical excipients-a review," *Int J PharmTech Res,* vol. 6, pp. 412-420, 2014.

[98] V. F. Sechriest, Y. J. Miao, C. Niyibizi, A. Westerhausen–Larson, H. W. Matthew, C. H. Evans, F. H. Fu, and J. K. Suh, "GAG-augmented polysaccharide hydrogel: A novel biocompatible and biodegradable material to support chondrogenesis," *Journal of biomedical materials research,* vol. 49, pp. 534-541, 2000.

[99] R. Gref, J. Rodrigues, and P. Couvreur, "Polysaccharides grafted with polyesters: novel amphiphilic copolymers for biomedical applications," *Macromolecules,* vol. 35, pp. 9861-9867, 2002.

[100] A. Dufresne, "Comparing the mechanical properties of high performances polymer nanocomposites from biological sources," *Journal of Nanoscience and Nanotechnology,* vol. 6, pp. 322-330, 2006.

[101] G. Ciardelli, V. Chiono, G. Vozzi, M. Pracella, A. Ahluwalia, N. Barbani, C. Cristallini, and P. Giusti, "Blends of poly-(ε-caprolactone) and polysaccharides in tissue engineering applications," *Biomacromolecules,* vol. 6, pp. 1961-1976, 2005.

[102] G. K. Jani, D. P. Shah, V. D. Prajapati, and V. C. Jain, "Gums and mucilages: versatile excipients for pharmaceutical formulations," *Asian J Pharm Sci,* vol. 4, pp. 309-323, 2009.

[103] R. R. Leakey, "Potential for novel food products from agroforestry trees: a review," *Food chemistry,* vol. 66, pp. 1-14, 1999.

[104] D. R. Picout, S. B. Ross-Murphy, N. Errington, and S. E. Harding, "Pressure cell assisted solubilization of xyloglucans: Tamarind seed polysaccharide and detarium gum," *Biomacromolecules,* vol. 4, pp. 799-807, 2003.

[105] R. V. Kulkarni, S. Mutalik, B. S. Mangond, and U. Y. Nayak, "Novel interpenetrated polymer network microbeads of natural polysaccharides for modified release of water soluble drug: in-vitro and in-vivo evaluation," *Journal of Pharmacy and Pharmacology,* vol. 64, pp. 530-540, 2012.

[106] M. Sano, E. Miyata, S. Tamano, A. Hagiwara, N. Ito, and T. Shirai, "Lack of carcinogenicity of tamarind seed polysaccharide in B6C3F< sub> 1</sub> mice," *Food and chemical toxicology,* vol. 34, pp. 463-467, 1996.
[107] J. Tomlin and N. Read, "The relation between bacterial degradation of viscous polysaccharides and stool output in human beings," *British journal of nutrition,* vol. 60, pp. 467-475, 1988.
[108] K. Ross, L. Pyrak-Nolte, and O. Campanella, "The effect of mixing conditions on the material properties of an agar gel—microstructural and macrostructural considerations," *Food Hydrocolloids,* vol. 20, pp. 79-87, 2006.
[109] J.-L. Doublier, C. Garnier, D. Renard, and C. Sanchez, "Protein–polysaccharide interactions," *Current Opinion in Colloid & Interface Science,* vol. 5, pp. 202-214, 2000.
[110] V. Tolstoguzov, "Compositions and phase diagrams for aqueous systems based on proteins and polysaccharides," *International review of cytology,* vol. 192, pp. 3-31, 1999.
[111] N. J. Einerson, K. R. Stevens, and W. J. Kao, "Synthesis and physicochemical analysis of gelatin-based hydrogels for drug carrier matrices," *Biomaterials,* vol. 24, pp. 509-523, 2003.
[112] A. Mishra and A. V. Malhotra, "Graft copolymers of xyloglucan and methyl methacrylate," *Carbohydrate polymers,* vol. 87, pp. 1899-1904, 2012.
[113] J. M. Cloyd, N. R. Malhotra, L. Weng, W. Chen, R. L. Mauck, and D. M. Elliott, "Material properties in unconfined compression of human nucleus pulposus, injectable hyaluronic acid-based hydrogels and tissue engineering scaffolds," *European Spine Journal,* vol. 16, pp. 1892-1898, 2007.
[114] N. Lorén, M. Langton, and A.-M. Hermansson, "Confocal laser scanning microscopy and image analysis of kinetically trapped phase-separated gelatin/maltodextrin gels," *Food Hydrocolloids,* vol. 13, pp. 185-198, 1999.
[115] F. Jara, O. E. Pérez, and A. M. Pilosof, "Impact of phase separation of whey proteins/hydroxypropylmethylcellulose mixtures on gelation dynamics and gels properties," *Food Hydrocolloids,* vol. 24, pp. 641-651, 2010.
[116] D. Oakenfull, J. Pearce, and R. Burley, "Protein gelation," *FOOD SCIENCE AND TECHNOLOGY-NEW YORK-MARCEL DEKKER-*, pp. 111-142, 1997.
[117] L. Huang, G. Reekmans, D. Saerens, J.-M. Friedt, F. Frederix, L. Francis, S. Muyldermans, A. Campitelli, and C. V. Hoof, "Prostate-specific antigen immunosensing based on mixed self-assembled monolayers, camel antibodies and colloidal gold enhanced sandwich assays," *Biosensors and bioelectronics,* vol. 21, pp. 483-490, 2005.
[118] Y. Pranoto, C. M. Lee, and H. J. Park, "Characterizations of fish gelatin films added with gellan and< i> κ</i>-carrageenan," *LWT-Food Science and Technology,* vol. 40, pp. 766-774, 2007.
[119] M. De La Cochetiere, T. Durand, P. Lepage, A. Bourreille, J. Galmiche, and J. Dore, "Resilience of the dominant human fecal microbiota upon short-course antibiotic challenge," *Journal of clinical microbiology,* vol. 43, pp. 5588-5592, 2005.
[120] L. Bammou, M. Mihit, R. Salghi, A. Bouyanzer, S. Al-Deyab, L. Bazzi, and B. Hammouti, "Inhibition effect of natural Artemisia oils towards tinplate corrosion in HCL solution: chemical characterization and electrochemical study," *Int. J. Electrochem. Sci,* vol. 6, pp. 1454-1467, 2011.
[121] J. Smart, I. Kellaway, and H. Worthington, "An in-vitro investigation of mucosa-adhesive materials for use in controlled drug delivery," *Journal of pharmacy and pharmacology,* vol. 36, pp. 295-299, 1984.
[122] A. Smirnov, E. Tako, P. Ferket, and Z. Uni, "Mucin gene expression and mucin content in the chicken intestinal goblet cells are affected by in ovo feeding of carbohydrates," *Poultry science,* vol. 85, pp. 669-673, 2006.
[123] H. Mohammadi and W. Herzog, "A novel model for diffusion based release kinetics using an inverse numerical method," *Medical engineering & physics,* vol. 33, pp. 893-899, 2011.
[124] L. Chen, G. E. Remondetto, and M. Subirade, "Food protein-based materials as nutraceutical delivery systems," *Trends in Food Science & Technology,* vol. 17, pp. 272-283, 2006.
[125] C. F. Rediguieri, O. de Freitas, M. P. Lettinga, and R. Tuinier, "Thermodynamic incompatibility and complex formation in pectin/caseinate mixtures," *Biomacromolecules,* vol. 8, pp. 3345-3354, 2007.
[126] S. Turgeon, M. Beaulieu, C. Schmitt, and C. Sanchez, "Protein–polysaccharide interactions: phase-ordering kinetics, thermodynamic and structural aspects," *Current opinion in colloid & interface science,* vol. 8, pp. 401-414, 2003.

[127] T. F. Vandamme, A. Lenourry, C. Charrueau, and J. Chaumeil, "The use of polysaccharides to target drugs to the colon," *Carbohydrate polymers*, vol. 48, pp. 219-231, 2002.
[128] J. L. Drury and D. J. Mooney, "Hydrogels for tissue engineering: scaffold design variables and applications," *Biomaterials*, vol. 24, pp. 4337-4351, 2003.
[129] G. Zhang, T. Liu, Q. Wang, L. Chen, J. Lei, J. Luo, G. Ma, and Z. Su, "Mass spectrometric detection of marker peptides in tryptic digests of gelatin: A new method to differentiate between bovine and porcine gelatin," *Food Hydrocolloids*, vol. 23, pp. 2001-2007, 2009.
[130] Y. Ikada and H. Tsuji, "Biodegradable polyesters for medical and ecological applications," *Macromolecular rapid communications*, vol. 21, pp. 117-132, 2000.
[131] M. S. Jangdey, A. Gupta, and A. K. Sah, "Development and Evaluation of Mucoadhesive Sustained Release Tablet using Tamarindus indica Gum," *Asian Journal of Research in Pharmaceutical Science*, vol. 4, pp. 77-82, 2014.
[132] M. F. Saettone, S. Burgalassi, B. Giannaccini, E. Boldrini, P. Bianchini, and G. Luciani, "Ophthalmic solutions viscosified with tamarind seed polysaccharide," ed: Google Patents, 2000.
[133] A. Mishra and A. V. Malhotra, "Tamarind xyloglucan: a polysaccharide with versatile application potential," *Journal of Materials Chemistry*, vol. 19, pp. 8528-8536, 2009.
[134] C. S. Kumar and S. Bhattacharya, "Tamarind seed: properties, processing and utilization," *Critical reviews in food science and nutrition*, vol. 48, pp. 1-20, 2008.
[135] R. Sothornvit and J. M. Krochta, "Plasticizer effect on mechanical properties of β-lactoglobulin films," *Journal of Food Engineering*, vol. 50, pp. 149-155, 2001.
[136] A. Al-Hassan and M. Norziah, "Starch–gelatin edible films: water vapor permeability and mechanical properties as affected by plasticizers," *Food Hydrocolloids*, vol. 26, pp. 108-117, 2012.
[137] K. Vimala, M. M. Yallapu, K. Varaprasad, N. N. Reddy, S. Ravindra, N. S. Naidu, and K. M. Raju, "Fabrication of curcumin encapsulated chitosan-PVA silver nanocomposite films for improved antimicrobial activity," *Journal of Biomaterials and Nanobiotechnology*, vol. 2, p. 55, 2011.
[138] K. Pal, A. K. Banthia, and D. K. Majumdar, "Preparation and characterization of polyvinyl alcohol-gelatin hydrogel membranes for biomedical applications," *Aaps Pharmscitech*, vol. 8, pp. E142-E146, 2007.
[139] S. I. Park, M. Daeschel, and Y. Zhao, "Functional properties of antimicrobial lysozyme-chitosan composite films," *Journal of Food Science*, vol. 69, pp. M215-M221, 2004.
[140] M. Ahmad, S. Benjakul, T. Prodpran, and T. W. Agustini, "Physico-mechanical and antimicrobial properties of gelatin film from the skin of unicorn leatherjacket incorporated with essential oils," *Food Hydrocolloids*, vol. 28, pp. 189-199, 2012.
[141] J. M. Manski, A. J. van der Goot, and R. M. Boom, "Advances in structure formation of anisotropic protein-rich foods through novel processing concepts," *Trends in Food Science & Technology*, vol. 18, pp. 546-557, 2007.
[142] T. Moschakis, B. S. Murray, and C. G. Biliaderis, "Modifications in stability and structure of whey protein-coated o/w emulsions by interacting chitosan and gum arabic mixed dispersions," *Food Hydrocolloids*, vol. 24, pp. 8-17, 2010.
[143] K. Varaprasad, E. R. Sadiku, K. Ramam, J. Jayaramudu, and G. S. M. Reddy, "Significances of Nanostructured Hydrogels for Valuable Applications," 2014.
[144] T. Miyazawa and E. Blout, "The infrared spectra of polypeptides in various conformations: amide I and II bands1," *Journal of the American Chemical Society*, vol. 83, pp. 712-719, 1961.
[145] A. Sionkowska, M. Wisniewski, J. Skopinska, C. Kennedy, and T. Wess, "Molecular interactions in collagen and chitosan blends," *Biomaterials*, vol. 25, pp. 795-801, 2004.
[146] S. Mao, C. Guo, Y. Shi, and L. C. Li, "Recent advances in polymeric microspheres for parenteral drug delivery-part 1," *Expert opinion on drug delivery*, vol. 9, pp. 1161-1176, 2012.
[147] M. N. Angles and A. Dufresne, "Plasticized starch/tunicin whiskers nanocomposites. 1. Structural analysis," *Macromolecules*, vol. 33, pp. 8344-8353, 2000.
[148] N. M. Sarbon, F. Badii, and N. K. Howell, "The effect of chicken skin gelatin and whey protein interactions on rheological and thermal properties," *Food Hydrocolloids*, vol. 45, pp. 83-92, 2015.
[149] J. Zhang, S. Xu, S. Zhang, and Z. Du, "Preparation and characterization of tamarind gum/sodium alginate composite gel beads," *Iranian Polymer Journal*, vol. 17, pp. 899-906, 2008.
[150] C. M. Yoshida, E. Oliveira, and T. T. Franco, "Chitosan tailor-made films: the effects of additives on barrier and mechanical properties," *Packaging Technology and Science*, vol. 22, pp. 161-170, 2009.

[151] P. Goyal, R. Dhar, S. S. Sagiri, K. Uvanesh, K. Senthilguru, G. Shankar, A. Samal, K. Pramanik, I. Banerjee, and S. S. Ray, "Synthesis and characterization of novel dual environment-responsive hydrogels of Hydroxyethyl methacrylate and Methyl cellulose," *Designed Monomers and Polymers*, vol. 18, pp. 367-377, 2015.
[152] M. James, D. Hughes, Z. Chen, H. Lombard, D. Hattingh, D. Asquith, J. Yates, and P. Webster, "Residual stresses and fatigue performance," *Engineering Failure Analysis*, vol. 14, pp. 384-395, 2007.
[153] H. J. Maria, N. Lyczko, A. Nzihou, K. Joseph, C. Mathew, and S. Thomas, "Stress relaxation behavior of organically modified montmorillonite filled natural rubber/nitrile rubber nanocomposites," *Applied Clay Science*, vol. 87, pp. 120-128, 2014.
[154] M. Berberan-Santos, E. Bodunov, and B. Valeur, "History of the Kohlrausch (stretched exponential) function: Focus on uncited pioneering work in luminescence," *arXiv preprint arXiv:0804.1814*, 2008.
[155] S. L. Shenoy, W. D. Bates, H. L. Frisch, and G. E. Wnek, "Role of chain entanglements on fiber formation during electrospinning of polymer solutions: good solvent, non-specific polymer–polymer interaction limit," *Polymer*, vol. 46, pp. 3372-3384, 2005.
[156] K. Pal, A. Banthia, and D. Majumdar, "Biomedical evaluation of polyvinyl alcohol–gelatin esterified hydrogel for wound dressing," *Journal of Materials Science: Materials in Medicine*, vol. 18, pp. 1889-1894, 2007.
[157] J. G. Ibrahim, M. H. Chen, and D. Sinha, *Bayesian survival analysis*: Wiley Online Library, 2005.

Dissemination

Journal Articles (From Thesis)

1. **G. S. Shaw**, K. Uvanesh, S.N. Gautham, Vinay Singh, Krishna Pramanik, Indranil

Banerjee, Naresh Kumar & Kunal Pal. Development and characterization of gelatin-tamarindgum/carboxymethyl tamarind gum based phase-separated hydrogels: a comparative study. Designed Monomers and Polymers, 2015. Published online. DOI: 10.1080/15685551.2015.1041075. (SCI, Impact factor: 2.78)

2. **G. S. Shaw**, Dibyajyoti Biswal, Anupriya B., Indranil Banerjee, Krishna Pramanik, Arfat Anis and Kunal Pal. Preparation, characterization and assessment of the novel gelatin-tamarind gum/carboxymethyl tamarind gum based phase-separated films for skin tissue engineering applications. Polymer-Plastics Technology and Engineering (In press). (SCI, Impact factor: 1.48).

Journal Articles (From other works)

1. Priyanka Goyal, Rik Dhar, Sai S. Sagiri, K. Uvanesh, K. Senthilguru, **G. S. Shaw**, Ajit Samal, Krishna Pramanik, Indranil Banerjee, Sirsendu Sekhar Ray & Kunal Pal. Synthesis and characterization of novel dual environment-responsive hydrogels of Hydroxyethyl methacrylate and Methyl cellulose. Designed Monomers and Polymers, 2015. Published online. DOI: 10.1080/15685551.2015.1012626. (SCI, Impact factor: 2.78)

2. Sai Sateesh Sagiri, Uvanesh Kasiviswanathan, **G. S. Shaw**, Meenakshi Singh, Arfat Anis, and Kunal Pal. Effect of sorbitan monostearate concentration on the thermal, mechanical and drug release properties of oleogels. Korean Journal of Chemical Engineering. Published online. DOI: 10.1007/s11814-015-0295-4. (SCI, Impact factor: 1.166).

3. S. P. Mallick, **G. S. Shaw**, Uvanesh K., D. Biswal, Suraj Nayak, S. S. Sagiri, V. K. Singh1, M. K. Bhattacharya, A. Anis and K. Pal. An in-depth analysis of the mechanical, electrical and drug release properties of gelatin-starch phase-separated hydrogels. Polymer-Plastics Technology and Engineering.published online. SCI, Impact factor: 1.48).